Summer 8-20-2021

Characterizing the Role of Prophages on WHIB7 Expression and Antibiotic Resistance in Mycobacterium Chelonae

Jaycee J. Cushman
University of Maine, jaycee.cushman@maine.edu

CHARACTERIZING THE ROLE OF PROPHAGES ON *WHI*B7 EXPRESSION AND ANTIBIOTIC RESISTANCE IN *MYCOBACTERIUM CHELONAE*

By

Jaycee J. Cushman

B.S. University of Maine, 2019

A THESIS

Submitted in Partial Fulfillment of the

Requirements for the Degree of

Master of Science

(in Microbiology)

The Graduate School

The University of Maine

August 2021

Advisory Committee:

Sally D. Molloy, Associate Professor of Genomics, Advisor

Keith W. Hutchison, Professor Emeritus of Molecular Biology

Melody N. Neely, Associate Professor of Microbiology

Joshua B. Kelley, Assistant Professor of Biochemistry

CHARACTERIZING THE ROLE OF PROPHAGES ON *WHI*B7 EXPRESSION AND ANTIBIOTIC RESISTANCE IN *MYCOBACTERIUM CHELONAE*

By Jaycee Cushman

Thesis Advisor: Dr. Sally Molloy

An Abstract of the Thesis Presented
In Partial Fulfillment of the Requirements for the
Degree of Master of Science
(in Microbiology).
August 2021

Mycobacterial pathogens are responsible for an ongoing public health crisis. *Mycobacterium abscessus* is the causative agent of lung infections that disproportionately affect immunocompromised individuals and is the most intrinsically antibiotic-resistant bacterial species known. These characteristics make *M. abscessus* infections difficult to treat, with a success rate of only 45%. While some extensively resistant isolates are caused by mutations in drug targets, others appear to be a result of increased intrinsic drug resistance. Common among these strains is the presence of integrated viral genomes (prophage) that are known to contribute to fitness and antibiotic resistance in other pathogens but whose roles are largely unknown in mycobacteria.

M. chelonae is an opprtunisitc pathogen that is closely related to *M. abscessus*. We have demonstrated that the presence of an *M. abscessus* cluster R prophage, McProf, in *M. chelonae,* increased resistance to antibiotics, such as amikacin, relative to strains lacking the

prophage. The presence of McProf also enhances amikacin resistance in response to sub-lethal concentrations of antibiotics, or other cellular stresses such as infection by a second phage, BPs. Relative to strains carrying only one of the prophages or no prophage, the strain carrying two prophages, BPs and McProf, had the highest amikacin resistance. This strain also showed increased expression of the transcriptional activator, *whi*B7, which promotes expression of intrinsic antibiotic resistance genes. We investigated the role of BPs lysogenic gene products in the presence of McProf and showed that individual expression of these genes does not contribute to *whi*B7 upregulation, indicating that McProf likely plays a larger role in mediating this intrinsic resistance. We identified a McProf-encoded polymorphic toxin system and evaluated its effect on *whi*B7 expression in *M. chelonae* carrying the BPs prophage. The polymorphic toxin system elevates *whi*B7 expression but does not fully account for the dramatic increase in expression observed in the *M. chelonae* strain carrying both prophages.

This work suggests that prophages play a role in increasing intrinsic antibiotic resistance and stress adaptation in pathogenic mycobacteria. Given that most pathogenic mycobacteria carry one or more prophages, characterizing how prophages regulate antibiotic resistance genes and adaptation to stresses will provide insight for developing more effective therapies for mycobacterial diseases.

ACKNOWLEDGEMENTS

First, I would like to thank the late Dr. John Singer for listening to my interests during my orientation weekend and enrolling me in the MBMS Department when I had no idea where to begin to reach my goals. I would like to extend a very special thank you to Dr. Keith Hutchison, my first MBMS professor, for seeing my potential before I even believed in myself. It was because of your support and guidance that I pursued research experiences and ended up in the position to be writing a master's thesis today. I will always cherish our conversations, scientific and otherwise. Of course, I'd like to thank Dr. Sally Molloy for taking me on as a research student at Keith's request and keeping me around for the last 5 years. She has helped me develop as both a scientist and a role model, teaching me compassion along the way. Thank you to my thesis committee, Drs. Sally Molloy, Keith Hutchison, Josh Kelley, and Melody Neely for your guidance in my work. Thank you to all of the Molloy Lab members I have had the pleasure of working with over the years for providing assistance, laughs, and the occasional snacks. Thank you to everyone else in the MBMS Department for always ensuring a positive learning environment. Thank you to my mom and sister for never knowing how I spend my days but being proud of me just the same. And finally, a huge thank you to Dylan, my best friend, for your unwavering support through all of my endeavors. Thank you for doing everything you can to make my life easier even when I worked too much to make time for our family. Your actions never went unnoticed.

TABLE OF CONTENTS

ACKNOWLEDGEMENTS..... iv

LIST OF TABLES..... x

LIST OF FIGURES..... xi

LIST OF ABBREVIATIONS xiii

CHAPTER

1. REVIEW OF THE LITERATURE..... 1

    1.1. Mycobacteria are a major public health threat..... 1

    1.2. Emergence of multidrug resistance in pathogenic mycobacteria..... 3

    1.3. Transcriptional activator, *whi*B7, mediates antibiotic resistance..... 7

    1.4. Bacteriophage are the most abundant biological entity..... 11

    1.5. Prophage impact host fitness and virulence..... 13

    1.6. *Mycobacterium chelonae* as a model for studying pathogenic mycobacteria..... 16

2. CHARACTERIZING THE ROLE OF PROPHAGE ON *WHI*B7 EXPRESSION AND ANTIBIOTIC RESISTANCE IN *MYCOBACTERIUM CHELONAE*..... 19

    2.1. Chapter Summary..... 19

    2.2. Introduction..... 20

    2.3. Materials and Methods..... 23

        2.3.1. Bacterial and viral strains..... 23

        2.3.2. Curing *M. chelonae* WT of its naturally occurring prophage..... 25

        2.3.3. McProf genome annotation..... 27

2.3.4. Isolation of lysogenic strains…….. 28

2.3.5. RNA isolations…… 29

2.3.6. RNAseq and reap mapping…….. 30

2.3.7. cDNA synthesis and qRT-PCR…… 31

2.3.8. Minimum inhibitory concentration assays…… 32

2.4. Results…… 33

2.4.1. Co-habitating prophage result in increased antibiotic resistance in *M. chelonae*…… 33

2.4.2. Isolations and characterization of BPs single lysogen and non-lysogen strains of *M. chelonae*…… 36

2.4.3. Strains of *M. chelonae* carrying McProf demonstrate increased resistance to aminoglycosides…… 38

2.4.4. Prophage McProf enhances AMK resistance in response to sub-inhibitory concentrations of antibiotics…….. 40

2.4.5. Transcriptional activator, *whi*B7, is upregulated in double lysogens of *M. chelonae*…… 42

2.4.6. Upregulation of *whi*B7 only occurs in *M. chelonae* (BPs, McProf)…… 47

2.4.7. Sub-inhibitory concentrations of ACI, but not AMK, increase *whi*B7 expression in *M. chelonae* (BPs, McProf)…… 49

2.4.8. Characterization of the McProf prophage…… 51

2.4.9. Lysogenic gene expression profiles from the BPs and McProf prophage genomes…… 54

2.5. Discussion…… 56

3. CHARACTERIZING THE ROLE OF PHAGE BPS ON *WHI*B7 EXPRESSION IN STRAINS OF *MYCOBACTERIUM CHELONAE* CARRYING MCPROF…… 61

3.1. Chapter Summary…… 61

3.2. Introduction…… 62

3.3. Materials and Methods…… 64

3.3.1. Bacterial and viral strains…… 64

3.3.2. Isolation of lysogenic strains…… 66

3.3.3. Construction of recombinant strains…… 69

3.3.4. RNA isolations…… 71

3.3.5. cDNA synthesis and qRT-PCR…… 72

3.4. Results…… 73

3.4.1. Organization of the BPs and CLED96 genomes and gene expression profile of BPs in the *M. chelonae* double lysogen (BPs, McProf)…… 73

3.4.2. BPs gp5 does not drive changes in *whi*B7 expression…… 78

3.4.3. BPs gp33 does not drive changes in *whi*B7 expression…… 80

3.4.4. Co-expression of BPs gp5 and gp33 does not drive changes in *whi*B7 expression…… 82

3.4.5. BPs gp58 does not drive changes in whiB7 expression…… 84

3.5. Discussion…… 85

4. DETERMINING THE ROLE OF THE MCPROF POLYMORPHIC TOXIN CASSETTE ON *WHI*B7 EXPRESSION AND ANTIBIOTIC RESISTANCE IN *MYCOBACTERIUM CHELONAE*…… 91

4.1. Chapter Summary…… 91

4.2. Introduction…… 92

4.3. Material and Methods…… 97

4.3.1. Bacterial and viral strains…… 97

4.3.2. RNA isolation…… 98

4.3.3. Construction of recombinant strains…… 99

4.3.4. Isolation of lysogenic strains…… 101

4.3.5. Phage particle release test…… 102

4.3.6. cDNA synthesis and qRT-PCR…… 102

4.3.7. Minimum inhibitory concentration assays…… 103

4.4. Results…… 104

4.4.1. Generation of recombinant *M. chelonae* strains…… 104

4.4.2. Expression of the McProf polymorphic toxin cassette stabilizes BPs single lysogens of *M. chelonae*…… 105

4.4.3. The McProf polymorphic toxin cassette triggers upregulation of *whi*B7 in the presence of phage BPs…… 106

4.4.4. The McProf polymorphic toxin cassette is downregulated in *M. chelonae* (BPs, McProf)…… 107

4.4.5. Expression of the McProf polymorphic toxin cassette does not alter amikacin resistance…… 111

4.5. Discussion…… 113

5. CONCLUDING REMARKS AND FUTURE DIRECTIONS…… 118

LITERATURE CITED…….. 124

BIOGRAPHY OF THE AUTHOR……. 140

LIST OF TABLES

Table 2.1 Bacterial and viral strains used in this study…… 24

Table 2.2 Plasmids used in this study…… 25

Table 2.3 Standard PCR primers used in this study…… 27

Table 2.4 qRT-PCR primers used in this study…… 32

Table 2.5 Minimum inhibitory concentrations of *M. chelonae* strains…… 34

Table 2.6 Top 20 upregulated and downregulated genes in *M. chelonae* (BPs, McProf) relative to *M. chelonae* (McProf)…… 46

Table 2.7 *whi*B7 regulon genes upregulated in *M. chelonae* (BPs, McProf) relative to *M. chelonae* (McProf)…… 47

Table 3.1 Bacterial and viral strains used in this study…… 65

Table 3.2 Plasmids used in this study…… 66

Table 3.3 Standard PCR primers used in this study…… 68

Table 3.4 qRT-PCR primers used in this study…… 73

Table 4.1 Bacterial and viral strains used in this study…… 98

Table 4.2 Plasmids used in this study…… 98

Table 4.3 Standard PCR primers used in this study…… 101

Table 4.4 qRT-PCR primers used in this study…… 103

LIST OF FIGURES

Figure 1.1 Intrinsic mechanisms of antibiotic resistance in pathogenic mycobacteria……. 5

Figure 1.2 Phage replication cycles……. 12

Figure 2.1 Percent viability of *M. chelonae* (McProf) and *M. chelonae* (BPs, McProf) upon aminoglycoside treatment…….. 36

Figure 2.2 Percent viability of *M. chelonae* strains upon aminoglycoside treatment…….. 40

Figure 2.3 Percent viability of *M. chelonae* strains upon AMK treatment in the presence and absence of ACI……. 41

Figure 2.4 MA plot of *M. chelonae* (BPs, McProf) gene expression……. 42

Figure 2.5 WhiB7 protein alignment…… 44

Figure 2.6 qRT-PCR verification of RNAseq data……. 45

Figure 2.7 qRT-PCR analysis of *whi*B7 expression in *M. chelonae* strains…… 48

Figure 2.8 qRT-PCR analysis of *whi*B7 expression in *M. chelonae* strains in the presence and absence of ACI treatment……. 50

Figure 2.9 qRT-PCR analysis of *whi*B7 expression in *M. chelonae* strains in the presence and absence of AMK treatment…….. 51

Figure 2.10 Phamerator map of the McProf genome…….. 53

Figure 2.11 McProf ESX-like polymorphic toxin cassette……. 54

Figure 2.12 Lysogenic gene expression profiles of BPs and McProf…… 56

Figure 3.1 Phamerator map of the BPs integration cassette……. 75

Figure 3.2 Phamerator map and gene expression profile of the BPs genome…….. 77

Figure 3.3 qRT-PCR analysis of recombinant *M. chelonae* (McProf) strains expressing BPs gp5…….. 80

Figure 3.4 qRT-PCR analysis of recombinant *M. chelonae* (McProf) strains expressing BPs gp33……. 82

Figure 3.5 qRT-PCR analysis of recombinant *M. chelonae* (McProf) strains co-expressing BPs gp5 and gp33…… 83

Figure 3.6 qRT-PCR analysis of recombinant *M. chelonae* (McProf) strains expressing BPs gp58…… 85

Figure 4.1 Phage particle release in recombinant *M. chelonae* (BPs)…….. 106

Figure 4.2 qRT-PCR analysis of *wh*iB7 in recombinant strains of *M. chelonae* expressing the McProf polymorphic toxin cassette…… 107

Figure 4.3 $2^{-\Delta\Delta Ct}$ qRT-PCR analysis of polymorphic toxin cassette genes in *recombinant M. chelonae* strains…….. 109

Figure 4.4 McProf polymorphic toxin cassette gene expression profile…….. 110

Figure 4.5 ΔCt qRT-PCR analysis of McProf polymorphic toxin cassette genes in *recombinant M. chelonae* strains …….. 111

Figure 4.6 Percent viability of recombinant *M. chelonae* strains upon AMK treatment in the presence and absence of ACI…… 113

LIST OF ABBREVIATIONS

Acivicin (ACI)

Amikacin (AMK)

Anhydrotetracycline (ATc)

Basic Local Alignment Search Tool (BLAST)

Bacteriophage Recombineering of Electroporated DNA (BRED)

Clarithromycin (CLA)

Clustered regularly interspaced short palindromic repeat interference (CRISPRi)

Control of repressor's operator gene (*cro*)

Cystic fibrosis (CF)

Deoxyribonucleic acid (DNA)

Dimethyl sulfoxide (DMSO)

Enterohemorrhagic *E. coli* (EHEC)

Erythromycin ribosome methylase gene (*erm*)

Excision gene (*xis*)

Extensive drug resistance (XDR)

False Discovery Rate (FDR)

Glycerol kinase (*glp*K)

Guide RNA (sgRNA)

Human immunodeficiency virus (HIV)

Hygromycin (HYG)

Kanamycin (KAN)

Latent tuberculosis infection (LTBI)

Log2 fold change (Log2FC)

Luria broth (LB)

Messenger RNA (mRNA)

Minimum inhibitory concentration (MIC)

Multidrug resistance (MDR)

Mycobacterium tuberculosis complex (MTBC)

Non-tuberculous mycobacteria (NTM)

Oleic acid, albumin, dextrose (OAD)

Optical density at 600 nm wavelength (OD_{600})

Phage Evidence Collection and Annotation Network (PECAAN)

Plaque forming unit (PFU)

Polymerase chain reaction (PCR)

Polymorphic toxin (PT)

Quantitative real-time polymerase chain reaction (qRT-PCR)

Ribonucleic acid (RNA)

Ribosomal RNA (rRNA)

Shiga toxin gene (*stx*)

Tetracycline/aminoglycoside efflux pump gene (*tap*)

Tetracycline (TET)

Tobramycin (TOB)

Toxin-antitoxin (TA)

Transfer RNA (tRNA)

Tris-ethylenediaminetetraacetic acid (TE)

Tuberculosis (TB)

Type 6 secretion system (T6SS)

Type 7 secretion system (T7SS)

CHAPTER 1

REVIEW OF THE LITERATURE

1.1 Mycobacteria are a major public health threat

Mycobacteria are Gram-positive, non-motile, non-spore forming bacilli (Percival et al., 2014). These species are characterized by their thick cell walls, including an outer layer studded with mycolic acid (Alderwick et al., 2015). Mycobacteria are ubiquitous in air, soil, and water (Percival et al., 2014). More than 170 species have been identified thus far, and can be characterized as obligate, opportunistic, or non-pathogens (Fedrizzi et al., 2017). Genetically, mycobacteria can be distinguished by 16S rRNA sequence homology and high GC content, as well as presence of mycolic acid biosynthesis markers (Fedrizzi et al., 2017).

Mycobacteria are further grouped based on growth rate. The slow growth group requires more than 7 days to form colonies on solid media, while the rapid growth group forms colonies in 2 – 5 days (Bachmann et al, 2020). Slow-growing mycobacteria include obligate intracellular pathogens, such as *M. tuberculosis*, *M. bovis*, and *M. leprae*. Fast-growing species include both opportunistic pathogens and non-pathogens and are ubiquitous in the environment. Examples include pathogenic species, *M. abscessus* and *M. chelonae*, and non-pathogens, *M. smegmatis* and *M. gilvum* (Bachmann et al., 2020; Prasanna et al., 2013). Mycobacteria are also commonly characterized as belonging to the *Mycobacterium tuberculosis* complex (MTBC) or as non-tuberculous mycobacteria (NTM). The MTBC consists of all strains capable of causing tuberculosis in humans (Fan et al. 2015). Tuberculosis continues to press a major economic and public health burden upon the globe (WHO, 2020).

Prior to the COVID-19 pandemic, tuberculosis (TB), caused by *Mycobacterium tuberculosis*, was the leading cause of death by an infectious agent and still ranks in the top ten causes of death worldwide (WHO, 2020). Responsible for 2 billion current infections, 10 million new infections, and 1.4 million deaths in 2019, *M. tuberculosis* continues to thrive as a global health threat (WHO, 2020). Immunocompromised individuals, including those with human immunodeficiency virus (HIV), are especially susceptible to contracting TB, which is the leading cause of death among HIV-positive patients (WHO, 2020). TB is primarily a pulmonary disease, although disseminated infection is possible and is lethal in 50% of cases without chemotherapeutic intervention (Pai et al., 2016). *M. tuberculosis* is contracted through airborne transmission of respiratory droplets. Once inside the body, *M. tuberculosis* infects alveolar macrophage in the lungs. A collection of immune cells moves to encase the bacteria, resulting in granuloma formation. When bacterial cells are contained within granulomas, infection remains asymptomatic. However, the ability of *M. tuberculosis* to survive in macrophage leads to a persistent infection known as latent tuberculosis infection, or LTBI (Pai et al., 2016). If the bacterial load becomes too great for a granuloma to contain, cells will escape and can disseminate throughout the body and/or be expelled by the lungs. At this point, the patient has an active TB infection which is both symptomatic and contagious (Pai et al., 2016). Symptoms of active infection include fever, fatigue, weight loss, cough, and in some cases, hemoptysis. These symptoms range in severity from mild to deadly (Pai, 2016). In addition to the health crisis caused by *M. tuberculosis*, incidence of disease caused by fast-growing opportunistic mycobacterial pathogens, especially *M. abscessus*, has been increasing (Bachmann et al., 2020; Johansen et al., 2020).

While not as prominent as *M. tuberculosis*, prevalence of NTM infections, especially *M. abscessus* infections, are on the rise, with a steep increase in the last decade (Johansen et al., 2020). This increase can be attributed to environmental presence of NTM, as well as growing prevalence of risk factors, such as old age, immunosuppression, and chronic lung conditions, including cystic fibrosis. In fact, 10 – 20% of cystic fibrosis patients will develop *M. abscessus* infections (Johansen et al., 2020). While chance of infection is heightened in those with predispositions, NTM are capable of causing disease in otherwise healthy individuals as well (Johansen et al., 2020). Similar to TB, *M. abscessus* infection also results in granuloma formation, allowing the infection to persist for as long as several decades (Johansen et al., 2020). In severe cases, *M. abscessus* may cross the blood-brain barrier and cause cerebral abscesses and meningitis (Hurst-Hess et al., 2017). Due to extensive antibiotic resistance, the incidence rate *of M. abscessus* infection is greater than that of *M. tuberculosis* in most developed countries, with a successful treatment rate of only 45% (Griffith, 2019; Johansen et al., 2020).

1.2 Emergence of multidrug resistance in pathogenic mycobacteria

Pathogenic mycobacteria are well known for intrinsic mechanisms of drug resistance that make effective treatment of infections difficult. In fact, *M. abscessus* is one of the most intrinsically resistant species known. While *M. tuberculosis* and *M. abscessus* share many features of intrinsic resistance, even frontline TB drugs are ineffective against this organism (Nessar et al., 2012). For this reason, the known mechanisms of drug resistance in *M. abscessus* will be covered in this review.

Intrinsic resistance refers to naturally occurring characteristics that organisms possess to nullify the impact of antibiotics. The first line of defense in mycobacteria is the cell envelope. It is characterized as thick and waxy, with 60% lipid content. The structure of this envelope results in low permeability, making it difficult for antibiotics and other extracellular compounds to enter the cell (Nessar et al., 2012). Notably, mycobacteria have fewer porins spanning the cell envelope than observed in Gram-negative bacteria, further limiting antibiotic uptake (van Ingen et al., 2012). The membrane also works cooperatively with intracellular signals to shuttle unwanted compounds out of the cell (Nessar et al., 2012). *M. abscessus* encodes numerous proteins that function to either modify antibiotics or alter the drug target itself to render the drugs inactive. Rifampicin resistance is conferred by an ADP-ribosyltransferase, *arr*, which modifies the drug by catalyzing the addition of an ADP-ribose group (Rominski et al., 2017). Acetylases and phosphotransferases, as well as the *tap* efflux pump are responsible for aminoglycoside resistance (Nessar et al., 2012; van Ingen et al., 2012). β-lactamases degrade β-lactam antibiotics (Nessar et al. 2012). Several efflux pumps, including *tap* and *tet*V result in tetracycline resistance (van Ingen et al., 2012). Quinolone resistance is conferred through acetylases and efflux pumps, including *lfr*A (van Ingen et al., 2012). The *erm* methylase methylates 23S rRNA to prevent macrolide binding (Nash et al., 2009). The extent of intrinsic drug resistance in mycobacteria leaves few effective treatment options.

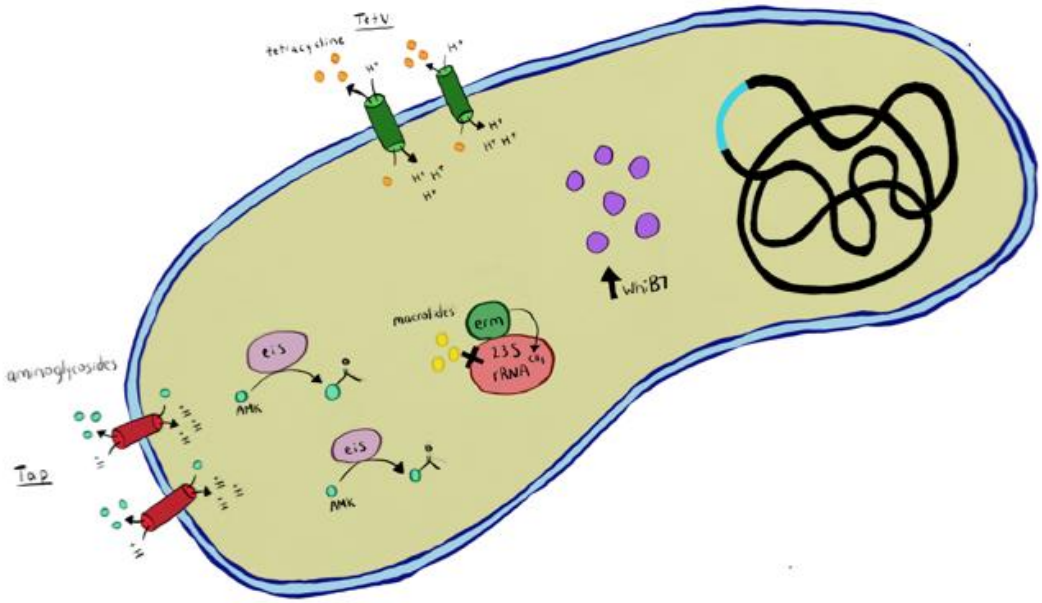

Figure 1.1 Intrinsic mechanisms of antibiotic resistance in pathogenic mycobacteria. This schematic represents many mechanisms of intrinsic resistance displayed by *M. abscessus*, including drug efflux pumps and drug-modifying enzymes. Many of the genes responsible for antibiotic resistance are positively regulated by *whi*B7.

Standard treatment for active TB infection includes a four-drug regimen consisting of isoniazid, rifampicin, pyrazinamide, and ethambutol for a minimum of six months (Pai et al., 2016; WHO, 2020). Treatment for *M. abscessus* infection involves a combination therapy of clarithromycin and amikacin, along with an injectable antimicrobial, such as cefoxitin. Treatment is long in duration, often 12 or more months, and can result in toxic side effects typical of amikacin treatment (Hurst-Hess et al., 2017). In severe cases, surgical intervention to remove infected tissue may be attempted (van Ingen et al., 2012). Treatment for both *M. tuberculosis* and *M. abscessus* infections has been further limited by emergence of multi-drug resistant (MDR) and extensively resistant (XDR) strains.

The definition and prevalence of MDR and XDR TB infections has been well characterized. MDR strains are resistant to both rifampicin and isoniazid. XDR strains are resistant to fluoroquinolones and at least one injectable aminoglycoside in addition to rifampicin and isoniazid (Pai et al., 2016). The WHO estimates that 3.3% of new cases and 18% of existing cases are MDR, with a 10% increase in treatment of MDR strains since 2017 (WHO, 2020). Additionally, 12,350 people developed XDR infections in 2019 (WHO, 2020). All acquired antibiotic resistance observed in *M. tuberculosis* thus far are a result of spontaneous point mutations within drug targets (Nasiri et al., 2017). Resistance to isoniazid, rifampicin, pyrazinamide, and ethambutol are caused by mutations in *kat*G, *rpo*B, *pnc*A, and *emb*CAB respectively (Nasiri et al., 2017).

The prevalence of *M. abscessus* infections is not as well quantified and are often misidentified. However, the incidence of new *M. abscessus* infections has been on the rise over the last decade (Johansen et al., 2020). While *M. abscessus* is already intrinsically resistant to most drug groups, strains have also acquired additional resistance to aminoglycosides, macrolides, or both. In fact, some strains have developed resistance to all known antibiotics (Johansen et al., 2020). Spontaneous point mutations in *rrs*, which encodes 16S rRNA, are associated with aminoglycoside resistance (Nessar et al., 2012; Guo et al., 2020; Johansen et al., 2020). To date, four possible point mutations have been identified that confer this resistance (Nessar et al., 2012). Point mutations within the 23S rRNA encoding-gene, *rrl*, leads to macrolide resistance (Guo et al., 2020; Johansen et al., 2020). However, not all extensively resistant phenotypes can be attributed to genetic mutations, suggesting that other unidentified mechanisms may play a role in antibiotic resistance (Nessar et al., 2012). Common among all

MDR strains is the upregulation of transcriptional activator, *whi*B7, which regulates genes that confer intrinsic antibiotic resistance (Guo et al., 2020).

1.3 Transcriptional activator, *whi*B7, mediates antibiotic resistance

The *whi*B family (*whi*B1 – 7) of genes are a group of transcriptional regulators found in the *Actinomyces* genus, which includes significant pathogenic species such as mycobacteria, streptomyces, and nocardia (Burian et al., 2015; Barka et al., 2016). These transcription factors are characterized by four conserved cysteine residues and a helix-turn-helix DNA binding motif (Larsson et al., 2012). Each of the seven genes of the *whi*B family contributes to virulence, and the majority have been assigned additional functions (Bush, 2018). *whi*B1, *whi*B3, *whi*B4, and *whi*B7 assist in maintaining redox balance. *whi*B2 plays a role in cell growth and septation. *whi*B7 plays an especially pivotal role in virulence by regulating genes involved in antibiotic resistance and survival in macrophage (Morris et al., 2005; Burian et al., 2015; Bush, 2018).

*whi*B7 is a transcriptional activator that mediates genes directly involved in antibiotic resistance, as well as antibiotic-induced stress response genes, including those involved in redox and metabolism (Morris et al., 2015; Burian et al., 2012). It has a signature structure that includes four conserved cysteine residues, a G(V/I)WGG turn, and a C-terminal AT-hook necessary for DNA binding (Burian et al., 2013). Expression of *whi*B7 occurs from an antibiotic-inducible promoter and is transcribed by a SigA-containing RNA polymerase (Burian et al., 2018). In addition, the *whi*B7 promoter contains an AT-rich motif that allows WhiB7 to bind and amplify its own expression, making it autoregulatory (Burian et al., 2013). Burian et al. (2015) identified 86 drugs capable of inducing the *whi*B7 promoter after screening 600 compounds, including every available antibiotic and other biological agents. The 86 inducing compounds

belong to a variety of structural and drug target groups. *whi*B7 is also upregulated 14-fold in *M. tuberculosis* when cells are introduced into murine macrophage (Larsson et al., 2012). It is predicted that this induction is caused by the reducing agent, glutathione, encountered in macrophage (Burian et al., 2015).

Interestingly, the *whi*B7 promoter is constitutively active at a low level in the absence of antibiotics, however the *whi*B7 open reading frame (ORF) itself is not transcribed due to the presence of a Rho-independent terminator upstream of the *whi*B7 ORF. An upstream ORF (uORF) located between the *whi*B7 promoter and terminator is predicted to act, in conjunction with the terminator, as a riboregulatory attenuation system (Burian et al., 2018). In these systems, the presence of a regulatory metabolite can affect translation of the uORF, which in turn alters the secondary structure of the terminator sequence. This results in anti-termination and subsequent transcription of the downstream gene (Dar et al., 2016). In the case of *whi*B7, anti-termination is achieved through exposure to sub-lethal concentrations of antibiotics and other biologically active compounds (Burian et al., 2018). Once translated, WhiB7 stimulates expression of other genes within its regulon, including *tap*, *tet*V, and *eis*, by binding to the SigA subunit of RNA polymerase and directing it to target genes (Burian et al., 2018).

While *whi*B7 homologs are conserved in mycobacteria, the number and function of genes within the regulon differs between species. *M. tuberculosis* encodes 12 genes belonging to the WhiB7 regulon, only four of which contribute to antibiotic resistance (*tap*, *eis*, *erm*, and *tet*V) (Morris et al., 2005; Shur et al., 2017). In contrast, *M. abscessus* encodes 128 genes belonging to the *whi*B7 regulon, including those identified in *M. tuberculosis*. Several have been identified

with direct roles in intrinsic antibiotic resistance that are upregulated upon *whi*B7 induction via drug exposure (Hurst-Hess et al., 2017).

WhiB7 regulates an erythromycin ribosome methylase (*erm*) that contributes to resistance to macrolides, a frontline ribosome-targeting drug family used to treat *M. abscessus* infections (Luthra et al., 2018). They cease protein synthesis by targeting the polypeptide exit tunnel and causing tRNA dissociation (Luthra et al., 2018). The erythromycin ribosome methylase, or *erm*, methylates 23S rRNA at the A2058 position to lower macrolide binding affinity (Luthra et al., 2018). An *erm* homolog, *erm*(41), is regulated by *whi*B7 and confers macrolide resistance in two of three *M. abscessus* subspecies (*M. massiliense* lacks this gene) (Nash et al., 2009).

Efflux pumps are energy-dependent membrane proteins that export compounds out of cells (Ramon-Garcia et al., 2012). A tetracycline/aminoglycoside efflux pump (*tap*) is regulated by *whi*B7 and, as the name suggests, confers resistance to tetracyclines and aminoglycosides by shuttling them out of the cell (Ramon-Garcia et al., 2012). Shur et al. (2017) have also provided evidence that Tap is capable of exporting macrolides and fluoroquinolones. In addition, Tap plays a role in stationary phase survival, and therefore latency, by shuttling toxic waste products out of the cell (Ramon-Garcia et al., 2012).

*whi*B7 controls the expression of several GCNS-related N-acetyltransferase (GNAT) family genes in *M. abscessus* (Luthra et al., 2018). This family includes the enhanced intracellular survival, or *eis*, gene known for its role in macrophage intracellular survival and kanamycin resistance in *M. tuberculosis* (Chen et al., 2012). N-acetyltransferases target aminoglycosides. Aminoglycosides, like macrolides, inhibit protein synthesis. However, they do so by binding 16S rRNA, although the binding site differs by drug within this class (Luthra et al., 2018). 2'-N-

acetyltransferases are conserved in mycobacteria and acetylate aminoglycosides with a 2' amino group, including gentamycin, tobramycin, and kanamycin (Luthra et al., 2018). The *whi*B7 regulon of *M. abscessus* encodes two *eis* genes. *eis*1 is a homolog of the *eis* gene in *M. tuberculosis*. *eis*2 is a homolog of the *eis* gene *in Anabaena variabilis* and is significant in that it confers resistance to amikacin, a frontline drug used to treat *M. abscessus* infection (Luthra et al., 2018). In terms of intracellular survival, *eis* acetylates, and therefore activates, phosphatase 16/mitogen-activated protein kinase phosphatase-7 (DUSP16/MPK-7). DUSP16/MPK-7 inhibits death of infected macrophage (Luthra et al., 2018).

Many MDR and XDR isolates of *M. abscessus* demonstrate a >10-fold increase in *whi*B7 expression, along with an increase in expression of associated antibiotic resistance genes, relative to drug-susceptible strains (Wu et al., 2019). The cause of this upregulation is not known; however, it is hypothesized that exposure to sub-inhibitory clarithromycin as a result of drug concentration gradients encountered in tissues during treatment of *M. abscessus* infection results in upregulation of *whi*B7 (Pryjma et al., 2017). Similarly, reduced drug penetration observed during treatment of *M. tuberculosis* infection is associated with acquired drug resistance, although whether *whi*B7 expression is impacted has not been measured (Dheda et al., 2018). There is also evidence that prophage can alter bacterial antibiotic resistance (Wang et al., 2010). While prophage-encoded virulence genes appear to be more abundant in mycobacteriophage identified in clinical isolates of pathogenic NTM compared to environmental mycobacteriophage, their impact on increased antibiotic resistance has not been explored (Glickman et al., 2020).

1.4 Bacteriophage are the most abundant biological entity

Bacteriophage (phage) are viruses that infect bacteria (Haq et al., 2011). They are the most abundant biological entity on Earth, quantified at approximately 10^{31} particles (Suttle, 2016). The majority of phage belong to the order *Caudovirales*, or tailed, double-stranded DNA phage, rather than the I*noviridae*, or filamentous phage group (Hatfull and Hendrix 2011; Knezevic et al., 2021). The structure of these phage particles consists of an icosahedral head that encapsulates genetic material, as well as a fibrous tail. Tailed phage are categorized into three different families based on tail structure: *myoviridae* (contractile tails), *siphoviridae* (long, non-contractile tails), and *podoviridae* (short non-contractile tails), and possess incredibly diverse genomes (Hatfull and Hendrix 2011). As of January 2021, 18,679 Actinobacteria phages have been isolated, and 3,698 of these have been fully sequenced and characterized (Russell and Hatfull, 2017). Of these phages, 11,468 are able to infect mycobacteria. Phage are categorized by cluster. Phage within the same cluster share at least 35% shared gene content (Pope et al., 2017; Dedrick et al., 2021). To date, there are 140 clusters and 157 subclusters. There are 63 phages with no known relatives which belong to the singleton cluster (Russell and Hatfull, 2017).

Phage replicate by two distinct pathways: the lytic and lysogenic cycle. Phage infection begins with attachment to the host cell via interactions with a specific host cell receptor, followed by transfer of genetic material into the bacterial host (Stone et al., 2019). Lytic phage strictly replicate through the lytic cycle and use host machinery to propagate within the cell, beginning with replication of genetic material, then expression of particle structural proteins. These products are used to assemble new viral particles. Once the host cell is filled to capacity

with viral particles, phage-encoded proteins (holins and lysins) facilitate cell lysis, releasing progeny into the extracellular environment (Haq et al., 2011). The progeny then moves on to infect other cells and repeat the process. Temperate phages are capable of carrying out both the lytic and lysogenic cycle. During lysogeny, the phage genome is inserted into the genome of the bacterial host via phage- and host-encoded proteins. The bacterium carrying the integrated phage genome is called a lysogen. Once a phage is integrated into its host, it is termed a prophage. The prophage genome remains latent, replicating along with the bacteria (Haq et al., 2011).

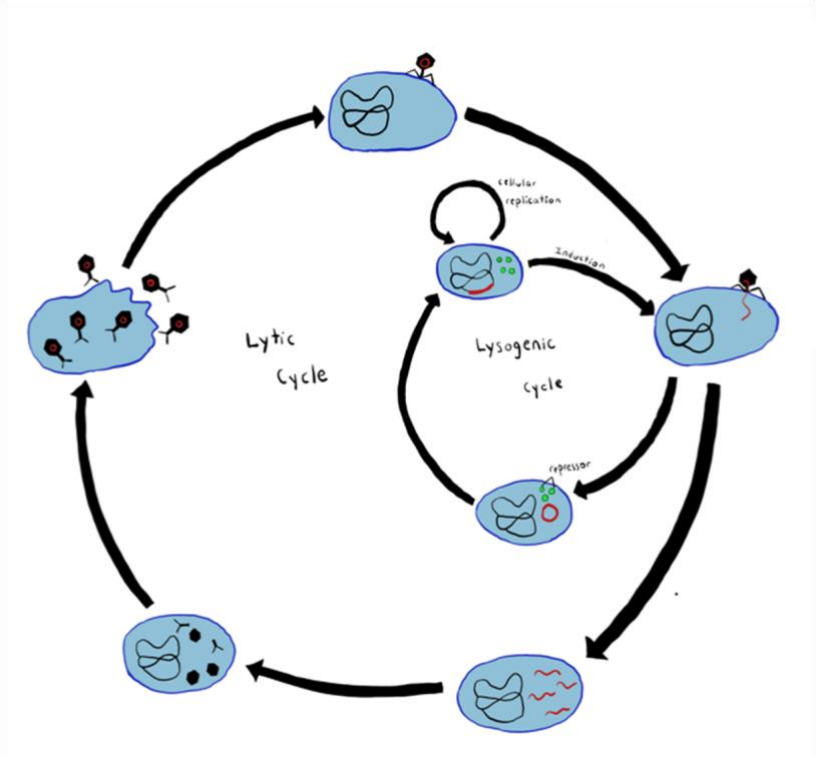

Figure 1.2 Phage replication cycles. Phage replicate by either lytic or lysogenic growth.

Temperate phage, those able to form lysogens, typically maintain lysogeny through expression of an immunity repressor gene which serves as a transcriptional regulator to inhibit expression of phage replication and structural elements typical of lytic growth. Repressors also confer immunity to infection by related phage. (Petrova et al., 2015). However, a process

known as induction may occur randomly in a small fraction of cells, or in response to stress in a large fraction of cells. During this process, concentrations of the immunity repressor decrease in the cell, allowing expression of lytic genes and the production of virions (Casjens, 2003). Some temperate phages additionally encode a repressor gene, control of repressor's operator (*cro*), which promotes lytic gene expression and replication by inhibiting expression of the immunity repressor (Gao et al., 2013). Lytic phages are now being harnessed for their ability to kill bacterial cells (Dedrick et al., 2019).

Lytic phages, and phages engineered to be lytic, have the potential to revolutionize medicine by providing an alternative to antibiotic treatment, specifically in regard to bacteria that have developed multi-drug resistance (Dedrick et al., 2019; Jault et al., 2018; Altamirano et al., 2019). Phage therapy utilizes the lytic aspect of viruses as means to target and destroy pathogenic bacteria (Hatfull, 2014). In fact, phage therapy was successfully employed recently to treat a CF patient with a lethal MDR *M. abscessus* infection following lung transplantation (Dedrick et al., 2019). A cocktail of three phages (Muddy, ZoeJ, and BPs) were given both intravenously and topically twice daily for 32 weeks to treat disseminated and wound infections. Two of the phages, ZoeJ and BPs, lytically infected *M. abscessus* at a poor efficiency. To remediate this, the phages were genetically engineered to remove their respective immunity repressor genes to force strictly lytic infections (Dedrick et al., 2019). Prior to this treatment regimen, the patient, only 15 years old, had been placed on palliative care as a result of the infection. Throughout treatment, the patient improved clinically, skin nodules resolved, and *M. abscessus* was no longer detectable in sputum. This is the first example where phage therapy was employed to successfully treat a mycobacterial infection (Dedrick et al., 2019).

The results of this study are promising for future treatment of XDR *M. abscessus* infections and has paved the way for development of phage therapies aiming to prevent and treat other mycobacterial infections, especially *M. tuberculosis*. Carrigy et al. (2019) has demonstrated that inhalation of nebulized mycobacteriophage, D29, is an effective prophylactic measure for *M. tuberculosis* infection in mice, modeling a potential preventative treatment option for high-risk individuals. Additionally, a five-phage cocktail has been developed to target the MTBC and was successful in killing *M. tuberculosis* strains *in vitro* (Guerro-Bustamante et al., 2021). While lytic phages may be harnessed to treat bacterial infections, prophage may enhance infections by increasing fitness and virulence of its host.

1.5 Prophage impact host fitness and virulence

The presence of prophage is extensive in bacterial pathogens and likely play a significant role in bacterial evolution (Brussow et al., 2004). Up to 20% of bacterial chromosomes consist of prophage or prophage-like elements (Fan et al., 2014). Interestingly, genes expressed from prophage may alter the host in a beneficial manner and phage-encoded genes have been shown to increase virulence, antibiotic resistance, and antibiotic tolerance in lysogen populations (Casjens, 2003; Kaper et al., 2004; Hyder and Streitfeld, 1978; Muniesa et al., 2013; Wang et al., 2016).

Prophage-encoded toxins are the most obvious mechanism of increasing pathogenesis (Wang et al., 2016). For example, Shiga toxin (*stx*)-encoding prophage are present in bacterial strains responsible for enterohemorrhagic *Escherichia coli* (EHEC) infections that result in bloody diarrhea and other complications (Kaper et al., 2004). The toxin is only expressed during late lytic infection. However, stress, including antibiotic treatment, triggers induction of *stx*-

encoding prophage into lytic replication, therefore resulting in toxin production (Kaper et al, 2004). Similarly, the filamentous phage, Pf4, that resides in *Pseudomonas aeruginosa* influences biofilm formation (Webb et al., 2004; Rice et al., 2009). This is not a result of a phage-encoded toxin but demonstrates a direct role in increasing virulence. The presence of Pf4 makes treatment of *P. aeruginosa* infection difficult and is especially detrimental to CF patients who often harbor persistent infections (Webb et al., 2004; Wang et al., 2016).

Prophages may serve as genetic switches to regulate bacterial gene expression under different conditions if integration disrupts gene function (Rabinovich et al., 2012). For example, *Listeria monocytogenes*, a human pathogen, encodes a competence system necessary for phagosomal escape and intracellular growth. This system is rendered nonfunctional due to the presence of prophage, A118, that integrates into the competence system activator, *com*K (Rabinovich et al., 2012). A118 serves as a genetic switch by excising from the host genome, but not entering lytic growth, upon encountering the intracellular environment of macrophage. Excision results in an intact *com*K, leading to activation of the competence system and establishment of intracellular infection (Rabinovich et al., 2012).

Prophage can also contribute to increased antibiotic resistance. Some cases are a result of direct introduction of a resistance gene. An example of this is found in *Streptococcus pyogenes*. MDR variants of *S. pyogenes* are predicted to be a result of acquired macrolide resistance through introduction of a prophage-encoded *erm* (Hyder and Streitfeld, 1978). Prophages influence antibiotic resistance in other models where the mechanisms of how they do so remain unknown. For example, a study done by Wang et al. (2010) on *E. coli* K12 carrying nine cryptic prophages (prophage unable to carry out a lytic infection) demonstrated that

prophage contribute to antibiotic resistance. They conducted a curing experiment and found that antibiotic sensitivity increased as the number of prophages decreased, with the strain lacking all prophages being the most sensitive (Wang et al., 2010).

Toxin-antitoxin (TA) systems are abundant in bacteria and are associated with increased virulence (Slayden et al., 2018; Harms et al., 2018). These genes may be encoded by the bacterial genome but are also frequently encoded on mobile elements, including prophages (Corray et al., 2017; Harms et al., 2018; Leplae et al., 2011; Dedrick et al., 2017; Harms et al., 2017). However, the mechanisms by which they may increase bacterial virulence is largely unexplored (Yao et al., 2018). TA systems consist of two genes that are typically adjacent and transcribed together. The toxin interrupts cellular processes, often by interfering with or degrading genetic material. The antitoxin binds and neutralizes the toxin (Wang et al., 2011). Several functions of prophage-encoded TA systems have been identified. First, TA systems can aid in bacterial persistence by altering the metabolic rate of the cell, allowing it to withstand antibiotic exposure and other stressors (Wood, 2016). Additionally, prophage-encoded TA systems have been shown to mediate biofilm formation in *E. coli* (Wang et al., 2011). TA systems are also known to stabilize mobile elements such as plasmids and prophages. This is the case with the ParE/CopA TA system encoded by the CP4So prophage found in *Shewanella oneidensis* (Yao et al., 2018). It has also been demonstrated that prophage encoded TA systems can confer abortive infection (Dedrick et al., 2017). Prophage-encoded TA systems are triggered upon infection by another phage. The antitoxin is degraded, and the toxin induces altruistic suicide of the cell. Sacrificing the cell prevents lytic phage proliferation, thereby protecting the remaining bacterial population (Fineran et al., 2009).

One or more prophage/prophage-like elements have been identified in sequenced pathogenic mycobacterial strains; however, their roles remain to be fully characterized (Fan et al., 2014). All strains of *M. tuberculosis* carry prophage φRv1, φRv2, or both (Fan et al., 2015). *M. bovis* BCG, the vaccination strain, lacks these prophages due to deletions, and interestingly, are unable to cause infections in humans. Work done by Fan et al. (2015) demonstrated that several prophage genes are upregulated in *M. tuberculosis* during both nutrient starvation and oxygen depletion. The mechanism of how these genes contribute to fitness has yet to be identified but it makes sense that they play a role in stress adaptation of mycobacterial intracellular pathogens (Fan et al., 2015).

1.6 *Mycobacterium chelonae* as a model for studying the role of prophage in pathogenic mycobacteria

M. chelonae, a member of the *M. abscessus*/*M. chelonae* complex, is a rapidly growing opportunistic human pathogen (Jaen-Luchoro et al., 2016). While it is primarily known as a cause of mycobacteriosis in marine organisms due to its high abundance in water systems, it is also a common cause of skin and soft tissue infections in humans (Jacobs et al., 2009). This is especially prevalent in healthcare settings, where *M. chelonae* is isolated from post-surgical wounds, implants, catheters, and dialysis ports (Jaen-Luchoro et al., 2016). It is also responsible for corneal infection (de Moura et al., 2014). *M. chelonae* rarely causes lung or disseminated disease, but it is possible in high-risk groups, including CF patients (Jaen-Luchoro et al., 2016).

The wild-type *M. chelonae* genome (CCUG 47445) spans 5,029,817 bp, contains 4,726 predicted coding sequences, and has a GC content of 64% (Jaen-Luchoro et al., 2016). It is a very close relative of the prevalent human pathogen, *M. abscessus*, sharing more than 80%

sequence identity at the protein-coding level. In fact, *M. abscessus* was previously misidentified as *M. chelonae* due to nearly identical biochemical and morphological features. *M. abscessus* was not recognized as a separate species until 1992 (de Moura et al., 2014).

Despite the homology and identical biosafety level (BSL-2) between the two species, *M. chelonae* is safer to work with, making it an ideal pathogenic mycobacterial model in a laboratory setting. The optimal growth temperature of *M. chelonae* is 30˚C, and it cannot grow at 37˚C (the internal temperature of the human body), providing an explanation as to why it is the causative agent of primarily superficial infections (Johansen et al., 2020). *M. chelonae* is a fast-growing model organism relative to other mycobacteria, with a generation time of approximately 5 hours. While it has a similar antibiotic resistance profile to *M. abscessus*, *M. chelonae* lacks *erm*, making it susceptible to macrolides and therefore providing an effective treatment option (Nash et al., 2009). In addition, *M. chelonae* is able to infect both murine and human macrophage cell lines, as well as zebrafish, making both *in vitro* and *in vivo* studies possible (Whipps et al., 2008).

M. chelonae is also an ideal model for studying the role of prophage in pathogenic mycobacteria. It carries a naturally occurring cluster MabR prophage named McProf that has been identified in clinical isolates of *M. abscessus* and is also susceptible to infection by mycobacteriophage that include both *M. abscessus* and *M. tuberculosis* in their host ranges (Dedrick et al., 2021).

CHAPTER 2

CHARACTERIZING THE ROLE OF PROPHAGE ON *WHI*B7 EXPRESSION AND ANTIBIOTIC RESISTANCE IN *MYCOBACTERIUM CHELONAE*

This chapter is a modified version of the following manuscript: Cushman J, Freeman E, McCallister S, Schumann A, Hutchison KW, Molloy SD. (2021) Increased *wh*iB7 expression and antibiotic resistance in *Mycobacterium chelonae* carrying two prophages. *BMC Microbiology*, *21*(176) doi: 10.1186/s12866-021-02224-z

2.1 Chapter Summary

Mycobacterium abscessus is the most intrinsically antibiotic-resistant species known. It is the causative agent of lung infections that disproportionately affect immunocompromised individuals. These characteristics make *M. abscessus* infections difficult to treat, with a success rate of only 45% (Griffith, 2019; Johansen et al., 2020). While some extensively resistant isolates are caused by mutations in drug targets, others appear to be a result of increased intrinsic drug resistance (Guo et al., 2020). Common among pathogenic mycobacteria is the presence of integrated viral genomes (prophage) that are known to contribute to fitness and antibiotic resistance in other pathogens but whose roles are largely unknown in mycobacteria (Fan et al., 2014; Fan et al., 2015; Bibb and Hatfull, 2002).

We have demonstrated that the presence of an *M. abscessus* cluster R prophage, McProf, in *M. chelonae* ATCC®35752 increased resistance to antibiotics such as amikacin, relative to strains lacking the prophage. The presence of McProf also enhances amikacin resistance in response to sub-lethal concentrations of antibiotics, or other cellular stresses such as infection by a second phage, BPs. Relative to strains carrying only one of the prophages or no prophage,

the strain carrying two prophages, BPs and McProf, had the highest amikacin resistance. This strain also showed increased expression of the transcriptional activator, *whi*B7, which promotes expression of intrinsic antibiotic resistance genes (Morris et al., 2005; Burian et al., 2012). This work suggests that prophages play a role in increasing intrinsic antibiotic resistance and stress adaptation in pathogenic mycobacteria. Given that most pathogenic mycobacteria carry one or more prophages and encounter drug gradients in tissues during infection, characterizing how prophages regulate antibiotic resistance genes and adaptation to stresses will provide insight for developing more effective therapies for mycobacterial diseases.

2.2 Introduction

Prophage (integrated viral genomes) are major drivers of bacterial virulence and antibiotic resistance in bacteria, yet the mechanisms of prophage-mediated antibiotic resistance are unknown (Wang et al, 2010; Wang et al., 2016). Prophages are common in mycobacteria, including clinical isolates of emerging non-tuberculosis pathogenic mycobacteria, *Mycobacterium avium* and *M. abscessus* (Fan et al., 2014; Glickman et al., 2020). *M. abscessus* is the causative agent of lung infections that disproportionately affects immunocompromised individuals and is one of the most intrinsically antibiotic-resistant species known (Griffith, 2019; Johansen et al., 2020). Extensively resistant isolates share increased expression of conserved mycobacterial intrinsic antibiotic resistance genes such as *whi*B7, making drug treatment challenging (Griffith, 2019; Guo et al., 2020). Understanding how intrinsic antibiotic resistance genes are regulated in pathogenic mycobacteria would provide opportunities to develop novel and more effective treatment approach (Burian et al., 2018; Guo et al., 2020).

Currently, the only effective treatment option is combination therapy of amikacin (AMK) and clarithromycin (CLA), along with an injectable antimicrobial such as cefoxitin, for as long as 2 years with harsh side effects (Hurst-Hess et al., 2017). Recent efforts in sequencing of clinical *M. abscessus* isolates determined that mutations in the 23S rRNA gene, *rrl,* and in the *erm* gene, which confers macrolide (e.g. clarithromycin) resistance, are typically associated with elevated CLA resistant phenotypes but did not account for all the clarithromycin resistant phenotypes (Guo et al., 2020). Consistent among all clarithromycin-resistant isolates was elevated expression of genes in the *whi*B7 regulon, including the transcription factor *whi*B7 and its target genes such as drug efflux pumps and antibiotic resistance genes, *erm* and *eis* (Burian et al., 2013; Hurst-Hess et al., 2017; Guo et al., 2020). These latter genes confer macrolide and aminoglycoside resistance, respectively. Likewise, in AMK-resistant isolates of *M. abscessus* there is typically a 10-fold increase in *whi*B7 expression relative to AMK susceptible strains (Wu et al., 2019).

*whi*B7 is conserved across all mycobacteria, including pathogenic and non-pathogenic species such as *M. tuberculosis*, *M. abscessus*, *M. chelonae* and *M. smegmatis* (Morris et al., 2005; Burian et al., 2012). *whi*B7 is upregulated in the presence of environmental stressors, including the intracellular environment of a macrophage and exposure to subinhibitory drug concentrations, but the cause of upregulation in extensively resistant *M. abscessus* is not well understood (Morris et al., 2005; Burian et al., 2012). Characterizing the pathways that lead to increased *whi*B7 expression and intrinsic drug resistance in pathogenic mycobacteria will be important for identifying new targets for novel drug development (Nessar et al., 2012; Dheda et al., 2018).

Prophages are present in most bacterial pathogens and contribute to virulence and antibiotic resistance (Brussow et al., 2004; Wang et al., 2016). In some models, the role and mechanism of prophage impact is clear. *E. coli* 0157:H7 causes enterohemorrhagic disease and is pathogenic due to a toxin encoded by the Stx prophage (Kaper et al., 2004). In other models, the role is of prophage clear, but the mechanism is not understood. *E. coli* K12 carries 9 cryptic prophages (transcriptionally active prophage that cannot carry out lytic infections) (Wang et al., 2010). Wang et al. (2010) showed that as the number of prophages decreased through a series of curing experiments, so did resistance to antibiotics. The strain lacking all prophages was most susceptible to drugs. Toxin/antitoxin (TA) systems encoded by prophage are also known to increase resistance and persistence in the presence of antibiotics. In *E. coli,* prophage-encoded TA pair RalR/RalA increases resistance to broad-spectrum fosfomycin and the RelE toxin of prophage Qin leads to persistence in the presence of ciprofloxacin, ampicillin and tobramycin (Christensen et al., 2001; Guo et al., 2014; Neubauer et al., 2009). The majority of mycobacterial pathogens also carry prophage, and they are hypothesized to play a role in virulence yet remain largely uninvestigated (Fan et al., 2014; Fan et al., 2015; Bibb and Hatfull, 2002). However, it has been shown that removal of prophage from *M. tuberculosis* renders it nonpathogenic (Fan et al., 2015). This suggests that mycobacterial prophages are necessary for the success of their pathogenic hosts.

In this study we examine the impact of two mycobacteriophages on intrinsic antibiotic resistance and *whi*B7 expression in the non-tuberculous mycobacterial pathogen, *M. chelonae,* a member of the *M. abscessus/chelonae* complex. The disease caused by *M. chelonae*, mainly soft tissue and disseminating infections, differs from that of *M. abscessus*; however, the *whi*B7-

dependent mechanisms of intrinsic resistance are conserved across all mycobacteria, including *M. chelonae* (Morris et al., 2005; van Ingen et al., 2009). Additionally, *M. chelonae* shares 103 of the 128 genes belonging to the *whi*B7 regulon in *M. abscessus* (Hurst-Hess et al., 2017). We identified a naturally occurring prophage in *M. chelonae* that also occurs in the sequenced genomes of at least 25 clinical isolates of *M. abscessus* (Molloy, Unpublished). We characterized the genome of the *M. chelonae* prophage, McProf, and created a cured strain that lacks prophage. Antibiotic resistance and gene expression of this strain was compared to that of *M. chelonae* carrying a single or multiple prophages.

2.3 Materials and Methods

2.3.1. Bacterial and viral strains

Mycobacterium chelonae (ATCC®35752, American Type Culture Collection, Manassas, VA) was grown in liquid Middlebrook 7H9 broth (BD, Sparks, MD) supplemented with 10% oleic acid, albumin, dextrose (OAD) and 0.05% Tween 80 at 30˚C with shaking at 230 RPM. Tween 80 was excluded from bacterial cultures used in minimum inhibitory concentration and phage infection assays. The wildtype strain of *M. chelonae* carries a naturally occurring prophage, McProf, and will be referred to as *M. chelonae* (McProf). Kanamycin was used as a selective measure for recombinant strains at a concentration of 250 μg mL^{-1} in liquid and solid media. Competent *E. coli* DH5 cells were prepared by New England Biolabs, (Ipswich, MA) and grown in Luria broth base, Miller (BD) supplemented with 50 μg mL^{-1} of kanamycin at 37˚C with shaking at 230 RPM for propagation of plasmids. Bacterial strains used in this study are listed in **Table 2.1.** Plasmids used in this study are listed in **Table 2.2**.

Mycobacteriophage BPs was obtained from the Hatfull Laboratory and cultivated by plaque assay using *M. chelonae* (McProf) or *M. smegmatis* MC^2155 (Sampson et al., 2009). Serially diluted phage samples were incubated for 15 min at room temperature in 0.5-mL aliquots of late log phase bacteria. Aliquots were plated in 4.5 mL of 0.45% 7H9 top agar onto 7H10 agar plates. High titer phage lysate stocks were generated by flooding bacterial lawns with nearly confluent lysis with phage buffer (10 mM Tris/HCl pH 7.5, 10 mM $MgSO_4$, 1 mM $CaCl_2$, 68.5 mM NaCl). Viral strains used in this study are listed in **Table 2.1**.

Table 2.1 Bacterial and viral strains used in this study.

Bacterial Strains	**Strain Description**	**Source**
Escherichia coli		
DH5α	Supercompetent cells	NEB
Mycobacterium chelonae		
Non-lysogen (ΔMcProf)	Mutant strain of *M. chelonae* ATCC 35752 lacking prophage McProf	This study
Single lysogen (BPs)	BPs lysogen of *M. chelonae* (ΔMcProf)	This study
Single lysogen (McProf)	*M. chelonae* ATCC 35752 with naturally-occurring prophage, McProf	ATCC
Double lysogen (BPs, McProf)	BPs lysogen of *M. chelonae* ATCC 35752	This study
Mycobacterium smegmatis		
MC^2155	*M. smegmatis* ATCC 700084	ATCC

Viral Strains	**Virus Description**	**Source**
BPs	Cluster G mycobacteriophage	Hatfull Laboratory

Table 2.2 Plasmids used in this study.

Plasmid Name	Vector	Phage Genes	Genome Coordinates	Description
pST-KT_*xis*	pST-KT	McProf gp5	3,169 – 3,405	Tetracycline-inducible mycobacterial expression vector carrying McProf gp5 (excise)

2.3.2 Curing *M. chelonae* WT of its naturally occurring prophage

Mycobacterial expression vector, pST-KT (Parikh et al., 2013) carries a tetracycline-inducible promoter and kanamycin resistance gene. Curing *M. chelonae* (McProf) of its naturally occurring prophage was achieved by overexpression of the McProf excision (*xis*) gene (McProf gp5). pST-KT was digested with BamHI and HindII to linearize the vector, removing a 67-bp fragment according to the manufacturer's recommendations (New England Biolabs, Ipswich, MA). Linearized vector was purified on a DNA clean-up column (NEB). An overexpression vector was constructed by cloning a 292-bp G-block (Integrated DNA Technologies, Coralville, IA) that included 27 bp and 24 bp of plasmid sequences that flank the 5' and 3' ends of digested vector respectively, and an internal sequence that corresponds to the McProf gp5 ORF (3,169 – 3,405 bp) into *M. chelonae* (McProf) via Gibson Assembly (NEB). Resulting plasmid was transformed into competent *E. coli* DH5 according to the manufacturer's recommendations and plated on selective L agar supplemented with 50 μg mL^{-1} of kanamycin (KAN). Recombinant plasmid, referred to as pST-KT_*xis* was propagated in *E. coli* DH5α and sequenced to ensure presence of *xis*.

pST-KT_*xis* was electroporated into competent *M. chelonae* (McProf) according to de Moura et al. (2014) and PCR screened for presence of the plasmid (**Table 2.3**). Briefly, electrocompetent *M. chelonae* cells were prepared by washing with ice-cold 10% glycerol four

times. Plasmid DNA in 500 ng quantities were electroporated with 100 µL of electrocompetent *M. chelonae* in 0.2-cm gap cuvettes. A sample of electrocompetent cells lacking plasmid DNA served as a negative control. Electroporation was carried out in a single pulse at 2.5 kV, 25 mF, 1,000 Ω. Cells were suspended in 900 µL of room-temperature 7H9-OAD and incubated at 30˚C with shaking for 4 h prior to plating on 7H10-OAD agar plates supplemented with 250 µg mL^{-1} of KAN. Transformant colonies were PCR screened for presence of the plasmid (**Table 2.3**).

The recombinant strain was grown for 48 h at 30˚C with shaking and sub-cultured to an optical density of 0.05 measured at a wavelength of 600 nm (OD_{600}). Cultures were then grown to an optical density of 0.6 and treated with 500 µg mL^{-1} of anhydrotetracycline (ATc) prepared in dimethyl sulfoxide (DMSO) or an equal volume of DMSO before incubating for an additional 72 h at 30˚C with shaking. A 0.5-mL sample from treated and mock-treated cultures was harvested, serially diluted, and plated in 100-µL volumes onto 7H10-OAD supplemented with 250 µg mL^{-1} of KAN. Plates were then incubated for 5 d at 30˚C. Bacterial colonies were lysed and PCR screened for loss of McProf using a set of four primers that amplify either *att*L and *att*R sites (indicating integrated prophage) or *att*B and *att*P sites (indicating excised prophage) (**Table 2.3**). PCR products showing intact an intact *att*B site were sequenced to confirm complete loss of prophage sequence. The resulting cured strain is referred to as *M. chelonae* (ΔMcProf) (**Table 2.1).**

Table 2.3 Standard PCR primers used in this study.

Target	Primers	Sequence (5' to 3')
McProf attL	Mc_attL_F	CGTCACGTTGGGGACTATCT
	Mc_attL_R	TTGAGCTGCGGATAACCTCT
McProf attR	Mc_attR_F	CGCTTGTAATCGTCGTA
	McProphageRR	ATAACTTTCGGCGGTTCCTT
McProf attP	Mc_attR_F	CGCTTGTAATCGTCGTA
	Mc_attL_R	TTGAGCTGCGGATAACCTCT
McProf attB	Mc_attL_F	CGTCACGTTGGGGACTATCT
	McProphageRR	ATAACTTTCGGCGGTTCCTT
BPs attL	BPs_attB_F	GTCTCGTTACTGGCGAGCTT
	BPs_attP_R	CGGGTAGTAGGCAGATGAGC
BPs attR	BPs_attP_F	GCTTTATCCAGGGTTGACCA
	BPs_attB_R	CGGTAGTAGGCAGATGAGC
BPs attP	BPs_attP_F	GCTTTATCCAGGGTTGACCA
	BPs_attP_R	CGGGTAGTAGGCAGATGAGC
BPs attB	BPs_attB_F	GTCTCGTTACTGGCGAGCTT
	BPs_attB_R	CGGTAGTAGGCAGATGAGC
pST-KT	pST-KT_cloning_F	AATATTGGATCGTCGGCAC
	pST-KT_cloning_R	GGAATTTAATCGCGGCCTC

2.3.3 McProf genome annotation

Phaster (Arndt et al., 2016) was used to identify the McProf prophage region within the *M. chelonae* genome. Phage attachment sites, *att*L and *att*R, were determined using DNA Master (http://cobamide2.bio.pitt.edu) to yield genome end sequences. The phage genome was annotated using DNA Master and the Phage Evidence Collection and Annotation Network (PECAAN) (https://pecaan.kbrinsgd.org/index.html). An initial auto-annotation was performed using GeneMark and Glimmer to identify ORFs and gene start coordinates (Borodovsky et al.,

2003; Delcher et al., 1999). Annotation results were validated by manual inspection. Predicted gene functions were determined by Basic Local Alignment Search Tool (BLASTand HHpred analysis (Altschul et al., 1990; Soding et al., 2005). A genome map was generated in Phamerator using the McProf_DB database (Cresawn et al., 2011).

2.3.4 Isolation of lysogenic strains

To generate BPs lysogen strains (Sampson et al., 2009), either *M. chelonae* (McProf) or *M. chelonae* (ΔMcProf) was serially diluted and plated in 4.5 mL of 7H9 top agar onto 7H10-OAD agar plates. Plates were treated or not treated with 10^9 plaque forming units (PFUs) of BPs. Plates were then incubated for 6 d at 30˚C. Resulting colonies were grown in liquid culture to test for phage particle release and superinfection immunity. Efficiency of lysogeny was calculated by dividing the number of colonies on virus-treated plates by the number of colonies on non-treated plates and multiplying by 100 to yield a percentage.

Genomic DNA was extracted from the *M. chelonae* (BPs, McProf) double lysogen and sent to Jackson Laboratory for sequencing (Genome Technologies at Jackson Laboratory, Bar Harbor, ME). Whole genome libraries were prepared and sequenced on a 2x150-bp MiSeq run. The presence of the BPs prophage was confirmed through reads that did not align to the bacterial reference genome. Primers were designed to PCR amplify BPs attachment sites, *att*L and *att*R, to confirm prophage integration for continued cultivation of lysogen strains (**Table 2.3**). Lysogen strains carrying the BPs prophage or BPs and McProf prophages are referred to as *M. chelonae* (BPs) and *M. chelonae* (BPs, McProf) respectively (**Table 2.1**).

2.3.5 RNA isolations

Total RNA was extracted from four replicates of 4-mL samples of *M. chelonae* strains at an OD_{600} of 1.0. Samples were harvested into 6-mL of RNAProtect Bacteria Reagent (Qiagen, Germantown, MD) and centrifuged at 5,000 x *g* for 10 min. Cell pellets were resuspended in 100 μL of Tris-ethylenediaminetetraacetic acid (TE) with 20 mg mL^{-1} of lysozyme and incubated at room temperature for 40 min. Cells were treated with 700 μL of RLT buffer (Qiagen) and transferred to 2-mL Lysing Matrix B tubes (MP Biomedicals, Irvine, CA). Samples were homogenized for 8 min at 50 Hz in a TissueLyser LT (Qiagen). RNA was isolated from cell lysates using the RNeasy Mini Kit (Qiagen) according to the manufacturer's instructions. A first DNase (Qiagen) treatment was performed on the columns. RNA was eluted in 50 μL of hot nuclease-free water before undergoing a second DNase treatment using the Turbo DNA-Free Kit (Thermo Scientific, Waltham, MA) according to the manufacturer's recommendations. RNA concentrations were measured using a NanoDrop ND-1000 spectrophotometer (NanoDrop Technologies, Montchanin, DE). RNA quality was assessed through gel electrophoresis using the RNA FlashGel System (Lonza, Rockland, ME) according to the manufacturer's instructions.

Experiments involving acivicin (ACI) or amikacin (AMK) treatment prior to harvest were completed with the following modifications to the previously described procedure. ACI-treated samples were grown to an OD_{600} of 0.7 and treated with 75 μM of drug for 3 h prior to harvest. AMK-treated samples were grown to an OD_{600} of 0.9 and treated with 16.7 μM of drug for 1 h prior to harvest. Untreated control samples were incubated for an equal amount of time prior to harvest for both experiments. In addition, 2-mL PowerBead Pro tubes (Qiagen) were used for homogenization.

2.3.6 RNAseq and read mapping

RNA underwent quality control analysis, library preparation, and paired end sequencing on an Illumina HiSeq 2500 at the Delaware Sequencing and Genotyping Center (Newark, DE). Samples were run on two lanes with 51-bp read lengths. Raw data files were uploaded the Galaxy server at usegalaxy.org (Afgan et al., 2018). Read files were concatenated, FastQC was used to assess quality, and reads were trimmed using Trim Galore! according to FastQC output (Andrew, 2010; Kreuger, 2019). Trim Galore! parameters allowed for reads with a minimum quality score of 30, 9-bp 5' end trim, and 1-bp 3' end trim to be kept. Due to incomplete rRNA depletion prior to sequencing, rRNA reads were computationally removed through alignment to the *M. chelonae* rRNA operon using Bowtie2 and unaligned reads were retained (Longmead et al., 2012). This left an average of 2,280,954 reads per sample for *M. chelonae* (McProf) and 2,484,260 reads per sample for *M. chelonae* (BPs, McProf). The average read depth for both strains was 40. Reads were then quantified and aligned to the *M. chelonae* transcriptome (coding transcript fasta file obtained from GenBank) using Salmon (Patro et al., 2017). Alignment parameters were set to correct for the high GC content of mycobacterial genomes and strand specificity, with mate pair 1 coming from the reverse strand.

Salmon outputs were used to determine differential gene expression using the R statistical package, DESeq2 (Love et al., 2014). Significant regulation was identified by a Log2 fold change (Log2FC) greater than 1 and a maximum False Discovery Rate (FDR) of 0.05. Genes with low expression were defined as those with less than 10 reads mapped and were subsequently removed. *M. chelonae* gene functions are poorly characterized. To overcome this, an ortholog table was generated based on genes in the *M. smegmatis*, *M. abscessus*, and *M.*

tuberculosis genomes using the OrthoDB pipeline (Zdobnov et al., 2014). This, in combination with blastP via MyocBrowser and HHpred, allowed for significantly upregulated predicted virulence genes in *M. chelonae* to be identified (Kapopoulou et al., 2011; Zimmerman et al., 2018).

2.3.7 cDNA synthesis and qRT-PCR

cDNA was synthesized in 20-μL reactions containing 500 ng of total RNA using the qScript cDNA Supermix (Quantabio, Beverly, MA) according to the manufacturer's recommendations. Reactions were run under the following thermal cycle: 5 min at 25˚C, 20 min at 42˚C, and 5 min at 85˚C for inactivation. Working stocks of cDNA were prepared by diluting samples 1:6 in 10 mM Tris.

Primers for quantitative real-time PCR (qRT-PCR) assays were designed to amplify a 100-bp region with the gene of interest using Primer3 (**Table 2.4**). qRT-PCR assays were carried out in triplicate reactions in 25-μL volumes containing 200 nM of each primer, 1 μL of cDNA (diluted 1:6), and PerfeCTa SYBR Green Supermix (Quantabio) according to the manufacturer's instructions. Positive and no-template controls were included in each assay. Reactions were run using the Bio-Rad CFX96 Real-Time system (Bio-Rad Laboratories, Hercules, CA). Reactions were initially incubated for 3 min at 95˚C, followed by 40 cycles of 10 s at 95˚C and 30 s at 60˚C, and lastly a melt curve to confirm a single amplicon per target gene. Change in RNA abundance was normalized to *M. chelonae* 16S rRNA, and relative expression determined using the $2^{-\Delta\Delta CT}$ method (Livak et al., 2001).

Table 2.4 qRT-PCR primers used in this study.

Target	Primers	Sequence (5' to 3')
16S	16S_qPCR_F1	CCGGATAGGACCACACACTT
	16S_qPCR_R1	ATTACCCCACCAACAAGCTG
whi B7	whiB7_qPCR_F4	ACTTTCCGCGAACCACAG
	whiB7_qPCR_R1a	ATGATGACCGTCGAAGTGG
tap	Mc_tap_F1	GGGATTGAAGTTCGTCTGGA
	Mc_tap_R1	GCTTGGGCAGCAATACACTT
glp K	Mc_glykin_F5	AGCTGCTGTCGTTCTTTTCC
	Mc_glykin_R1	TCACACCAAAGGGCTCTACC

2.3.8 Minimum inhibitory concentration assays

Minimum inhibitory concentration assays were performed according to Burian et al. (2012) and Ramon-Garcia et al. (2013). Cultures were grown in 7H9-OAD supplemented with 0.05% Tween 80 at 30˚C with shaking and sub-cultured such that overnight incubation resulted in an OD_{600} of 0.1 – 0.3. Cultures were diluted to a density of 10^5 cells ml^{-1} and applied in 50-μL volumes to wells of a 96-well plate containing 50 μl of 7H9 media with antibiotic concentrations that varied by 2-fold dilutions across the plate. Amikacin (AMK) assays involving an acivicin (ACI) pre-treatment were carried out by diluting cultures to a density of 10^5 cells mL^{-1}, treating with 75 μM of ACI, and incubating for 3 h. Media containing varying 2-fold concentrations of antibiotics were applied to plates in 50-μL volumes. AMK assays were performed at concentrations ranging from 512 – 4 μg mL^{-1}. Tobramycin (TOB) assays were performed at concentrations ranging from 64 – 0.5 μg mL^{-1}. Tetracycline (TET) and clarithromycin (CLA) assays were performed using 2-fold dilutions of antibiotic concentrations ranging from 64 – 0.5 and 3 – 0.02 μg mL^{-1} respectively. Clarithromycin was prepared in DMSO, and therefore DMSO was included in all wells of CLA assays. Each strain was applied in replicates of six at each drug

concentration. Bacteria was applied in the absence of drugs in replicates of 16 as a control. Additionally, wells containing only media plus drug at each concentration were included to serve as an absorbance blank. Inoculated plates were sealed with porous adhesive culture plate films (VWR International, Radnor, PA), wrapped with parafilm and incubated at 30°C for 2 d. A solution of 25% Tween 80 and AlamarBlue (Bio-Rad) was added to each well in 25- and 1-μL volumes respectively, incubated at 30˚C for 1 d, and OD measured at 570- and 600 nm. Percent viability of cells was calculated as the percent difference in reduction between antibiotic-treated cells and untreated cells according to the manufacturer's instructions. Each assay was replicated in a minimum of two independent experiments.

2.4 Results

2.4.1 Co-habitating prophages result in increased aminoglycoside antibiotic resistance in *M. chelonae*

The wildtype *M. chelonae* (ATCC® 35752) carries a naturally occurring 67,657-bp prophage that we have named McProf. To determine how prophages impact gene expression and the antibiotic resistance phenotype of *M. chelonae* we added a second prophage. We identified three mycobacteriophages capable of infecting *M. chelonae*, Muddy, WildCat and BPs, of which only BPs is known to be temperate (Hatfull et al., 2010; Hatfull, 2013; Sampson et al., 2009). A double lysogen of *M. chelonae* was created from the WT *M. chelonae* strain using the cluster G mycobacteriophage, BPs (Sampson et al., 2009). BPs integrates into an *attB* site located within the 3' end of the host tRNA-Arg gene (BB28_RS01100), that is similar to the BPs *attB* site in *M. smegmatis* (Msmeg_6349) (Sampson et al., 2009). BPs lysogens of the *M. chelonae* WT strain (BPs, McProf) appear to be more stable than BPs lysogens of *M. smegmatis*.

Lysogens form at a higher efficiency in *M. chelonae* WT (25%) compared to that in *M. smegmatis* (5%) and release fewer particles into cell culture supernatant (10^4 – 10^5 PFUs mL^{-1} compared to 10^{10} PFUs mL^{-1}) (Sampson et al., 2009; Broussard et al., 2013).

We tested susceptibility of *M. chelonae* (BPs, McProf) to aminoglycosides, AMK and TOB, as well as TET and CLA compared to *M. chelonae* (McProf) by minimum inhibitory concentration (MIC) assay to identify whether presence of an additional prophage alters the antibiotic resistance phenotype. The presence of the second prophage, BPs, significantly increased resistance to both aminoglycosides (**Table 2.5**). There was not a consistent significant difference in resistance to TET. As a positive control, we exposed the *M. chelonae* (McProf) strain to sub-inhibitory concentrations of acivicin (ACI), a known inducer of intrinsic resistance in mycobacteria (Hurst-Hess et al., 2017). As expected, ACI significantly increased the resistance of *M. chelonae* (McProf) in both the AMK and TOB assays (**Table 2.5**). ACI treatment did not significantly alter TET or CLA resistance of *M. chelonae* (McProf).

Table 2.5. Minimum inhibitory concentrations for each *M. chelonae* strain as determined by the lowest drug concentration that completely inhibited cell growth.

	MIC (µg mL^{-1})							
Antibiotic:	**AMK**		**TOB**		**TET**		**CLA**	
ACI Treatment:	**-**	**+**	**-**	**+**	**-**	**+**	**-**	**+**
Strain								
M. chelonae (McProf)	64	128	8	16	16	16	3	6
M. chelonae (BPs, McProf)	128	128	16	ND*	16	16	3	ND*
M. chelonae (BPs)	32	64	8	8	16	16	3	6
M. chelonae (ΔMcProf)	32	64	8	ND*	16	16	3	ND*

ND* = Not Determined

We also determined the viability of the strains after antibiotic treatment by adding AlamarBlue to the wells to detect metabolic activity (**Figure 2.1**). There was a statistically

significant difference in viability between the double lysogen and WT strains treated with 64 μg mL^{-1} AMK and 8 μg mL^{-1} TOB. We noted a slight increase in viability of the WT strain at 8 μg mL^{-1} of TOB; however, there was no evidence of growth at this concentration of TOB. The WT strain treated with ACI in both the AMK and TOB assay had the highest viability at these drug concentrations. Some background reduction of AlamarBlue was observed for both strains at doses higher than the observed MIC; however, there was no growth detected in those wells.

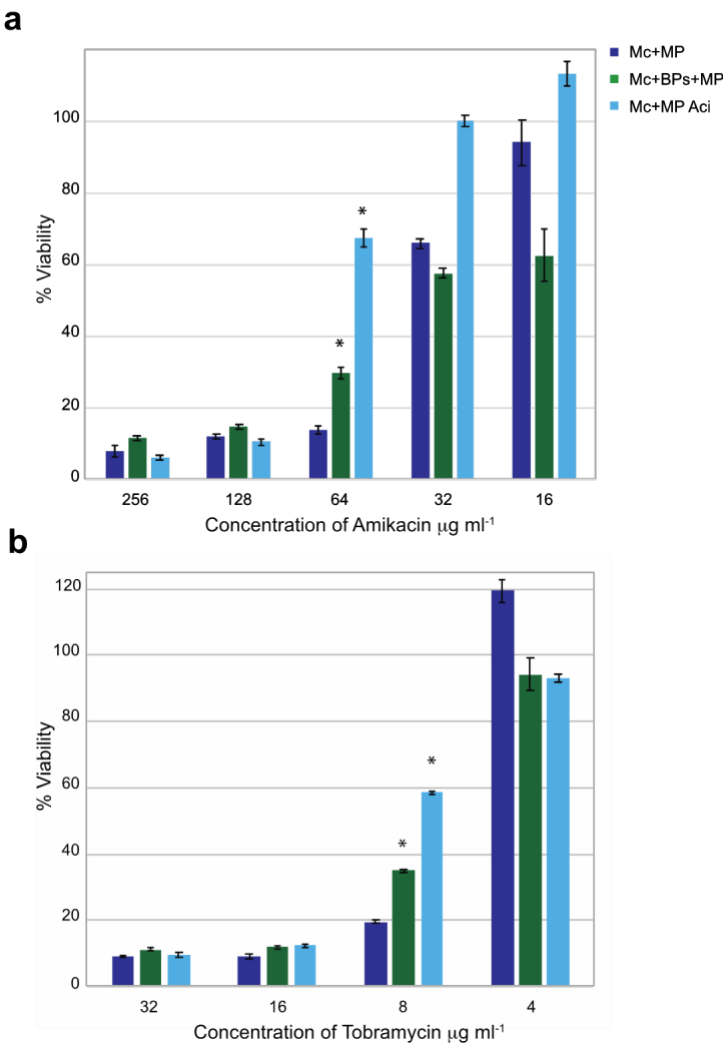

Figure 2.1 Percent viability of M. chelonae (McProf) and *M. chelonae* (BPs, McProf) upon aminoglycosde treatment. Percent viability of *M. chelonae* carrying single prophage McProf (MP) and two prophages, BPs and McProf, in the presence of varying concentrations of **a.** AMK and **b.** TOB. As a positive control, single McProf lysogens were treated with 75 µM acivicin (Aci) a known inducer of *whi*B7. Graphs represent average values ± SE of the mean with n=6. The optical density was measured at 570- and 600 nm after addition of 1 µL of AlamarBlue and the percent difference in reduction between antibiotic-treated cells and untreated cells was calculated. Mean percent reduction by *M. chelonae* that are statistically significant are indicated by an Asterix (Wilcoxon rank sum, $p<0.05$). Data is representative of three independent experiments.

2.4.2 Isolation and characterization of BPs single lysogen and non-lysogen strains of *M. chelonae*

To better understand how the presence of the second prophage increases antibiotic resistance, we generated a strain of *M. chelonae* that contains no prophage (*M. chelonae* (ΔMcProf)) and from that, a single BPs lysogen of *M. chelonae* (**Table 2.1**). We removed the McProf prophage by creating a recombinant strain of *M. chelonae* (McProf) that overexpresses the McProf excise gene (gp5) from an inducible mycobacterial expression plasmid (**Table 2.2**)

(Parikh et al., 2013). We identified ATc-induced bacterial colonies that had an intact *attB* site by PCR amplification and sequencing (**Table 2.3**), indicating loss of the prophage and an active integrase system. To determine if McProf phage particles are released from *M. chelonae* (McProf) cells through spontaneous induction, concentrated culture supernatants were plated onto lawns of the newly acquired non-lysogen strain (ΔMcProf), but we were unable to detect plaques. PCR analysis of *M. chelonae* (McProf) culture supernatants also failed to detect the McProf *attP* sequence, which would have indicated the presence of either excised McProf genome or linear McProf genome in phage particles. It is possible that there is a mutation that we were not able to identify that prevents McProf from carrying out a successful lytic infection. Alternatively, *M. chelonae* may not be the natural host and McProf is capable of lytically infecting other mycobacterial hosts.

The non-lysogen strain of *M. chelonae* (ΔMcProf) was used to isolate single lysogens of BPs. Although we were able to isolate BPs lysogens in the non-lysogen strain of *M. chelonae*, they are less stable than BPs lysogens formed in the WT strain (McProf) and comparable to lysogens formed in *M. smegmatis* (Sampson et al., 2009; Broussard et al., 2013). We determined efficiency of lysogeny to be 5% and particle release from lysogen culture supernatant was 10^{10} PFU mL^{-1}. This contrasts an efficiency of 25% and particle release of 10^{5} PFU mL^{-1} observed in *M. chelonae* (BPs, McProf), suggesting that McProf may play a role in lysogen stabilization

2.4.3 Strains of *M. chelonae* carrying McProf demonstrate increased resistance to aminoglycosides

To determine the roles of prophages BPs and McProf in the increased resistance observed in the double lysogen, we determined the MIC and viability of double (BPs, McProf) and single (BPs or McProf) *M. chelonae* lysogens relative to non-lysogen cells (ΔMcProf) in the presence of varying levels of AMK, TOB, TET and CLA (**Table 2.5** and **Figure 2.2**). The presence of the naturally occurring prophage, McProf, significantly contributes to AMK resistance in *M. chelonae* in the presence and absence of ACI treatment (**Table 2.5**). The WT strain carrying McProf alone had a higher MIC for AMK (64 μg mL^{-1}) relative to the non-lysogen strain (ΔMcProf) (MIC of 32 μg mL^{-1}) (Burian et al., 2012; Hurst-Hess et al., 2017). Treatment of these two strains with ACI increased the MIC for both strains; however, the MIC for ACI-treated WT (McProf) strain was two-fold higher than that of the ACI-treated non-lysogen (ΔMcProf) strain (**Table 2.5**) The presence of a second prophage, BPs, also increases resistance to AMK, with bacterial growth at doses as high as 64 μg mL^{-1}. Although the double lysogen had the same MIC as the ACI-treated WT strain (128 μg mL^{-1}) (**Table 2.5**), the cell viability of the ACI-treated WT strain was statistically higher than that of the double lysogen (**Figure 2.2a**). BPs alone had no effect on AMK resistance suggesting that BPs only increases AMK resistance through an interaction with the naturally occurring prophage, McProf.

The presence of the prophages McProf and BPs also altered TOB resistance in *M. chelonae* (**Table 2.5** and **Figure 2.2b**). The WT (McProf) strain did not have a higher TOB MIC than the non-lysogen strain (8 μg mL^{-1}), but in the presence of ACI, the MIC for WT (McProf) strain increased two-fold (16 μg mL^{-1}), whereas the MIC for the non-lysogen (ΔMcProf) strain

remained 8 μg mL^{-1}. It is possible a difference would be detected at TOB doses between 4- and 8 μg mL^{-1}. The TOB MIC for the double lysogen (BPs, McProf) was the same as that for the ACI-treated WT (McProf) strain; however, the viability for ACI-treated WT (McProf) strain was significantly higher than that of the double lysogen at 8 μg mL^{-1} (**Table 2.5** and **Figure 2.2b**).

Since *M. chelonae* lacks *erm*, which confers intrinsic macrolide resistance (Nash et al., 2009), we anticipated that there would be minimal change in CLA resistance regardless of prophage treatment. We observed that prophages had little effect on CLA resistance, although ACI treatment did increase resistance in *M. chelonae* (McProf) and *M. chelonae* (ΔMcProf). Additionally, TET resistance was largely unaltered by the presence of prophages nor by ACI treatment (**Table 2.5**).

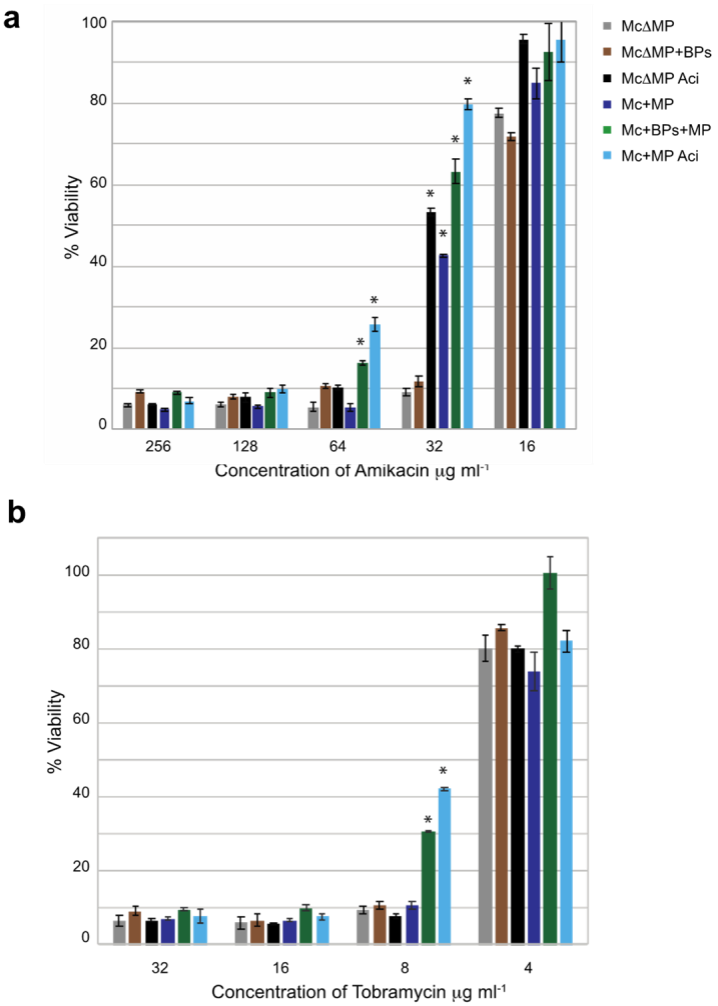

Figure 2.2 Percent viability of M. chelonae strains upon aminoglycoside treatment. Percent viability of *M. chelonae* carrying single prophage McProf, two prophage, BPs and McProf, no prophage, or single BPs prophage in the presence of varying concentrations of **a.** AMK and **b**. TOB. As a positive control, single McProf lysogens and non-lysogen cultures were treated with 75 µM acivicin (Aci), a known inducer of *whi*B7. Graphs represent average values ± SE of the mean with n=6. The optical density of was measured at 570- and 600 nm after addition of 1 µL of AlamarBlue and the percent difference in reduction between antibiotic-treated cells and untreated cells was calculated. Mean percent reduction by *M. chelonae* that are statistically significant are indicated by an Asterix (Wilcoxon rank sum, $p<0.05$). Data is representative of three independent experiments.

2.4.4 Prophage McProf enhances AMK resistance in response to sub-inhibitory concentrations of antibiotics.

Because the *M. chelonae* (McProf) strain treated with ACI had higher AMK resistance than the non-lysogen strain treated with ACI, we wondered if the presence of prophage McProf enhances the effect of sub-inhibitory concentrations of antibiotics on AMK resistance. To determine the interaction between ACI and the presence of one or both prophages, we treated all four lysogen and non-lysogen strains with sub-inhibitory concentrations of ACI and repeated the AMK resistance assay. The presence of McProf increases the effect of ACI on AMK

resistance compared to the non-lysogen whereas the BPs prophage alone does not (**Table 2.5** and **Figure 2.3**). The double lysogen treated with ACI did not have a higher MIC than the WT (McProf) strain treated with ACI; however, cultures of the ACI-treated double lysogen (BPs, McProf) did consistently have a statistically higher viability than that of ACI-treated WT (McProf) strain at AMK doses of 64 μg mL^{-1}. The presence of BPs and ACI appear to interact with McProf to increase AMK resistance.

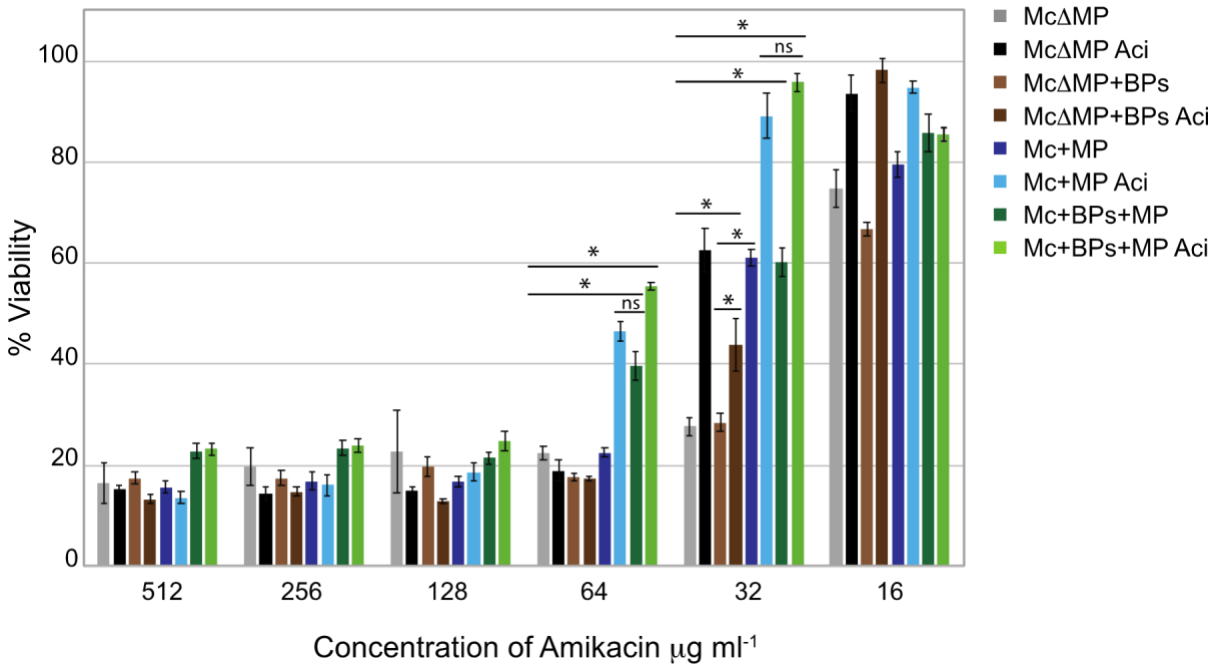

Figure 2.3 Percent viability of *M. chelonae* strains upon AMK treatment in the presence and absence of ACI. Percent viability of *M. chelonae* carrying no prophage ΔMcProf (McΔMP), BPs prophage (Mc+BPsΔMP), prophage McProf (Mc+MP) or both prophage BPs and McProf (Mc+BPs+MP) in the presence of varying concentrations of amikacin. To determine if the presence of each prophage interacts with sub-inhibitory concentrations of antibiotics, each strain was treated or not treated with 75 μM acivicin (Aci). Graphs represent average values ± SE of the mean with n=3. The optical density of was measured at 570- and 600 nm after the addition of 2 μL of AlamarBlue and the percent difference in reduction between antibiotic-treated cells and untreated cells was calculated. Data is representative of two independent experiments.

2.4.5 Transcriptional activator, *whi*B7, is upregulated in double lysogens of *M. chelonae*

RNA was isolated from *M. chelonae* (McProf) and *M. chelonae* (BPs, McProf), and RNAseq analysis performed to determine whether the presence of a second prophage (BPs) influenced gene expression that could explain the increased antibiotic resistance observed in the double lysogen strain. Strikingly, the presence of BPs in the wildtype strain altered expression of 417 of 4,867 genes relative to *M. chelonae* (McProf). This indicated that 8.5% of *M. chelonae* genes were differentially expressed in the presence of a second prophage, including a variety of predicted virulence genes (**Figure 2.4**).

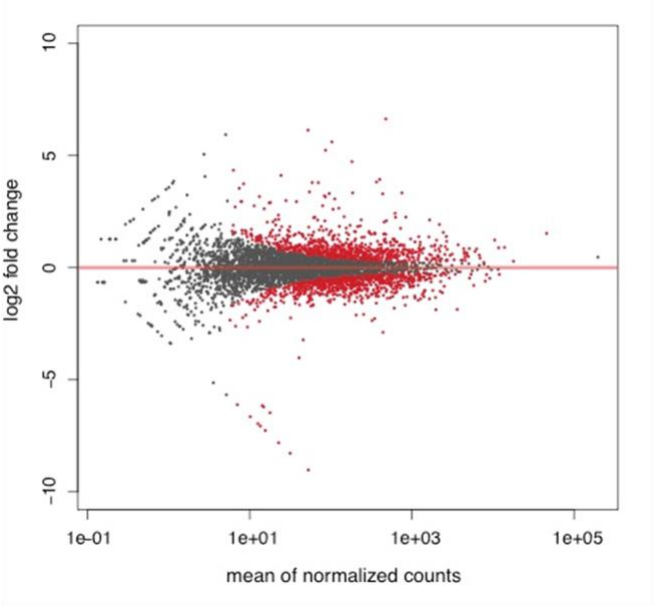

Figure 2.4 MA plot of *M. chelonae* (BPs, McProf) gene expression. MA Plot presenting the relationship between average expression level (mean of normalized counts) of *M. chelonae* genes and their fold change (log2fold change) in the double *M. chelonae* lysogen (BPs, McProf) relative to the WT strain (McProf). Red indicates genes identified as differentially expressed at an FDR of 0.05 or smaller.

The majority of the top-ranked genes in the double lysogen belonged to the *whi*B7 regulon, genes in *M. tuberculosis* with functions related to antibiotic resistance and increased survival in macrophage (**Tables 2.6** and **2.7**) (Morris et al., 2005). Notably, the fifth most upregulated gene was identified as transcriptional activator, *whi*B7 (BB28_RS17590), at a fold-change of 26.5. Analysis of the *M. chelonae* Whib7 peptide sequence showed characteristics of *whi*B7 genes in mycobacteria, including a conserved iron sulfur cluster binding domain and C-

terminal AT-hook DNA binding domain (Burian et al., 2013; Hurst-Hess et al., 2017) (**Figure 2.5**). Additionally, *M. chelonae* WhiB7 shares 95% peptide sequence identity with its *M. abscessus* ortholog (MAB_3508c). *M. chelonae* contains 103 of the 128 genes belonging to the *whi*B7 regulon in *M. abscessus*, 30 of which are significantly upregulated in *M. chelonae* (BPs, McProf) (Hurst-Hess et al., 2017). Multiple genes from the *whi*B7 regulon that were upregulated have known roles in intrinsic antibiotic resistance, including GNAT acetyltransferases, *eis*1 and *eis*2 (BB28_RS05390 and BB28_RS22650 respectively), multi-drug efflux transporter, *tap* (BB28_RS06750), and efflux pump, *tet*V (BB28_RS13560) (**Table 2.7**). Also included in this regulon are additional GNAT acetyltransferases (BB28_RS23100 and BB28_RS01940) and ABC transporters with ATP binding domains that likely function in drug resistance (**Tables 2.6** and **2.7**). In *M. abscessus* and *M. tuberculosis, erm* is part of the *whi*B7 regulon and provides macrolide resistance but the gene is not present in the *M. chelonae* genome (Nash et al., 2009). *M. chelonae* lacks this *whi*B7 regulon gene, but it does encode a newly discovered gene in the *whi*B7 regulon*,* the ribosome splitting factor *hflX* (MAB_3042c)*,* which is reported to contribute to macrolide resistance in *M. abscessus* (Nash et al., 2009; Rudra et al., 2020). Expression of the *M. chelonae hflX* was slightly elevated in double lysogens relative to the WT strain (McProf) (BB28_RS14985; LogFC=2.8, FDR=8.4^{-33}) but this did not result in significant changes in CLA resistance in the double lysogen (**Table 2.7**). An additional 25 *whi*B7 regulon genes were upregulated but had fold changes of less than 2.

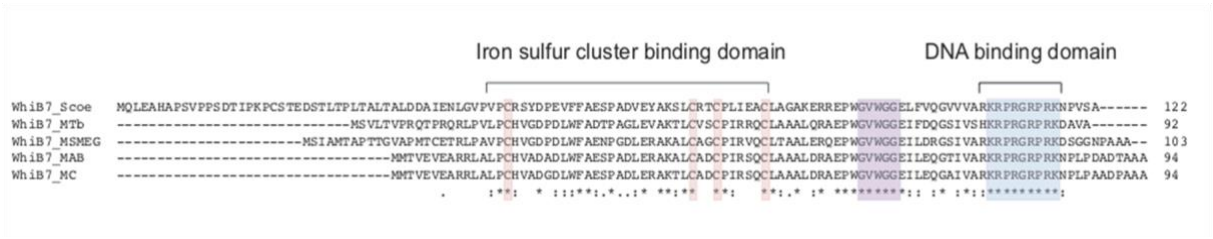

Figure 2.5 WhiB7 protein alignment. Clustal Omega alignment of the protein coding sequence for WhiB7 in *M. tuberculosis* (MTb), *M. smegmatis* (MSMEG), *M. abscessus* (MAB), and *M. chelonae* (MC). Highlighted regions represent conserved sequences typical of *whi*B7 genes.

The most highly regulated gene, with a 99-fold increase in expression, was annotated as a flotillin protein with no known function (BB28_RS01845) (log2FC = 6.6, FDR = 6.4^{-124}) (**Table 2.6**). Several of the most down regulated genes in the lysogen include a *pad*R-family transcription factor (BB28_RS01835, Log2FC= -8.3, FDR = 1.4^{-10}) and genes involved in glycerol uptake (*glp*F, BB28_RS01835, Log2FC= -6.2, FDR = 4.5^{-06}) and metabolism (*glp*K, BB28_RS01840, Log2FC= -9.0, FDR = 1.1^{-12}) (**Table 2.6**) (Ehrt et al., 2005). RNAseq data were validated by performing qRT-PCR on two independent sets of RNA measuring relative expression of upregulated (*whi*B7 and *tap*) and downregulated (glycerol kinase (*glp*K)) genes as indicated by the RNAseq data (**Figure 2.6**).

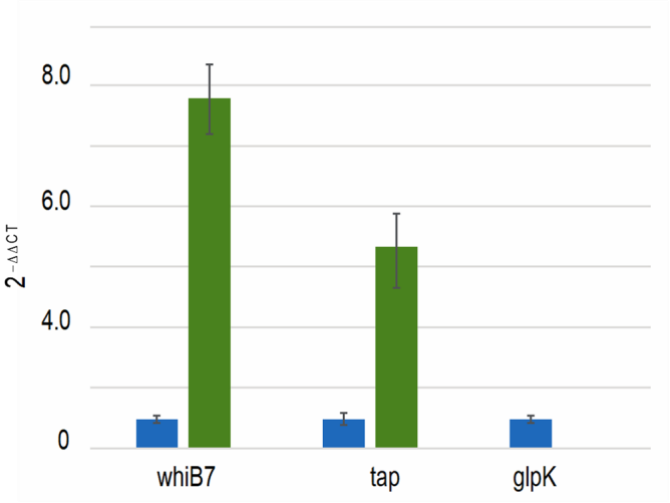

Figure 2.6 qRT-PCR verification of RNAseq data. The average relative expression levels of *whi*B7, *tap*, and *glp*K in *M. chelonae* (BPs, McProf) (green bars) relative to *M. chelonae* (McProf) (blue bars) measured by SYBR Green qRT-PCR. Genes were selected based on up- or downregulation in RNAseq data to validate results. RNA was isolated in triplicate from cells at an OD_{600} of 1.0. Graphs represent average values ± standard error of the mean with n=3 and are representative of two independent trials. Means with different letters are significantly different (Tukey's HSD, α=0.05).

Table 2.6 Top 20 upregulated and downregulated genes in *M. chelonae* (BPs, McProf) relative to *M. chelonae* (McProf).

MCH[a] gene ID	Predicted function[b]	log2FC[c]	FDR[d]	MAB[e] Gene ID	MAB Gene Description	MTB[f] Gene ID	MTB Gene Description
BB28_RS04255	**flotillin protein**	6.6	6.4E-124	NA	NA	NA	NA
BB28_RS19005	**hypothetical protein**	6.1	9.1E-18	MAB_3786c	Hypothetical protein	NA	NA
BB28_RS23100	**N-acetyltransferase**	5.6	4.4E-38	MAB_4621c	Putative acetyltransferase	NA	NA
BB28_RS23095	**hypothetical protein**	5.3	2.8E-35	MAB_4620c	Hypothetical protein	NA	NA
BB28_RS17590	**WhiB7 transcriptional regulator**	4.7	1.3E-73	MAB_3508c	Putative transcriptional regulator	Rv3197A	transcriptional regulator WhiB7
BB28_RS05390	**GNAT family N-acetyltransferase (eis1)**	4.1	5.8E-12	MAB_1125c	Hypothetical acetyltransferase, GNAT family	Rv1947	hypothetical protein
BB28_RS04260	**class I SAM-dependent methyltransferase**	3.9	1.0E-120	MAB_0963c	Putative polyketide synthase protein	NA	NA
BB28_RS03915	**hypothetical protein**	3.8	2.8E-116	MAB_0857	Putative monooxygenase	NA	NA
BB28_RS20465	**KR domain-containing protein**	3.8	3.4E-26	MAB_4053c	dehydrogenase/reductase	NA	NA
BB28_RS16665	**iron ABC transporter permease**	3.8	4.5E-31	MAB_2262c	Hypothetical ABC transporter ATP-binding protein	Rv1348	iron ABC transporter ATP-binding protein/permease IrtA
BB28_RS06460	**NAD(P)-dependent oxidoreductase**	3.4	1.2E-21	MAB_1344c	Putative DTDP-glucose-4,6-dehydratase-related protein	Rv3468c	dTDP-glucose 4,6-dehydratase
BB28_RS11540	**ABC transporter ATP-binding protein**	3.3	3.5E-64	MAB_2355c	protein	NA	NA
BB28_RS22650	**GNAT family N-acetyltransferase (eis2)**	3.3	1.4E-176	MAB_4532c	hypothetical protein	NA	NA
BB28_RS06750	**tap multidrug efflux transporter**	3.3	7.3E-35	MAB_1409c	Putative drug antiporter protein precursor	Rv1258c	multidrug-efflux transporter
BB28_RS13560	**TetV Efflux Pump**	3.3	9.8E-94	MAB_2780c	Putative transporter	NA	NA
BB28_RS20470	**pyridoxamine 5'-phosphate oxidase family protein**	3.2	4.1E-29	MAB_4054c	hypothetical protein	NA	NA
BB28_RS03190	**EamA family transporter**	3.2	3.5E-06	MAB_0677c	Conserved hypothetical protein	NA	NA
BB28_RS17050	**hypothetical protein**	3.2	5.1E-32	MAB_3424c	hypothetical protein	NA	NA
BB28_RS06235	**acyltransferase**	3.1	2.7E-39	MAB_1297c	hypothetical protein	NA	NA
BB28_RS01940	**N-acetyltransferase**	3.0	2.9E-11	MAB_0404c	Putative acetyltransferase	NA	NA
BB28_RS13285	**ferrochelatase**	-2.1	4.5E-40	MAB_2721c	Ferrochelatase (Protoheme ferro-lyase)	Rv1485	ferrochelatase
BB28_RS19235	**alpha-hydroxy-acid oxidizing enzyme**	-2.1	2.9E-35	MAB_3834c	Possible L-lactate dehydrogenase (cytochrome) LldD1	Rv0694	mycofactocin system heme/flavin oxidoreductase MftD
BB28_RS08645	**epoxide hydrolase**	-2.2	2.4E-07	MAB_1628c	hypothetical protein	NA	NA
BB28_RS13295	**beta-ketoacyl-ACP reductase**	-2.3	3.4E-56	MAB_2723c	3-oxoacyl-	Rv1483	3-oxoacyl-ACP reductase FabG
BB28_RS13290	**enoyl-acyl-carrier-protein reductase FabI**	-2.4	2.0E-60	MAB_2722c	(NADH)	Rv1484	NADH-dependent enoyl-ACP reductase
BB28_RS08640	**hypothetical protein**	-2.4	2.6E-04	NA	NA	NA	NA
BB28_RS19655	**universal stress protein**	-2.7	1.2E-03	MAB_3904	hypothetical protein	Rv2028c	universal stress protein
BB28_RS16545	**acyl-ACP desaturase**	-2.9	1.3E-75	MAB_3354	Probable acyl-	NA	NA
BB28_RS05070	**cytochrome c oxidase subunit I**	-3.2	2.8E-16	MAB_1042c	I	NA	NA
BB28_RS11065	**iron ABC transporter permease**	-4.0	3.8E-16	NA	NA	NA	NA
BB28_RS01880	**DUF58 domain-containing protein**	-6.2	5.8E-06	MAB_0388c	hypothetical protein	Rv3693	membrane protein
BB28_RS01835	**glycerol uptake glpF**	-6.2	4.5E-06	MAB_0381	Glycerol uptake facilitator protein (GlpF)	NA	NA
BB28_RS01885	**MoxR family ATPase**	-6.5	1.2E-06	MAB_0389c	Putative regulatory protein	Rv3692	methanol dehydrogenase transcriptional regulator MoxR
BB28_RS01875	**stage II sporulation protein M**	-6.6	1.2E-06	MAB_0387	hypothetical protein	Rv3694c	transmembrane protein
BB28_RS24340	**RDD family protein**	-7.0	2.4E-07	MAB_0386c	hypothetical protein	Rv3695	membrane protein
BB28_RS01830	**KR domain-containing protein**	-7.1	1.5E-07	MAB_0380	dehydrogenase/reductase	NA	NA
BB28_RS01890	**DUF4350 domain-containing protein**	-7.3	4.6E-08	MAB_0390c	hypothetical protein	Rv3691	hypothetical protein
BB28_RS01900	**membrane protein**	-7.8	2.0E-09	MAB_0392c	hypothetical protein	Rv3689	transmembrane protein
BB28_RS01845	**PadR family transcriptional regulator**	-8.3	1.4E-10	MAB_0383c	Putative transcriptional regulator, PadR-like	NA	NA
BB28_RS01840	**glycerol kinase**	-9.0	1.1E-12	MAB_0382	Glycerol kinase (GlpK)	Rv3696c	glycerol kinase

[a]MCH = *Mycobacterium chlelonae*

[b]Genes that belong to the WhiB7 regulon are in bold

[c]Log2 Fold Change for the double lysogen (+BPs+McProf) of *M. chelonae*

[d]FDR = False Discovery Rate

[e]MAB = *Mycobacterium abscessus*

[f]MTB = *Mycobacterium tuberculosis*

Table 2.7 *whi*B7 regulon genes upregulated in *M. chelonae* (BPs, McProf) relative to *M. chelonae* (McProf).

MCH[a] gene ID	Predicted function	log2 FC[b]	FDR[c]	MAB[d] gene ID	Predicted Function
BB28_RS19005	hypothetical protein	6.1	9.1E-18	MAB_3786c	Hypothetical protein
BB28_RS23100	N-acetyltransferase	5.6	4.4E-38	MAB_4621c	Putative acetyltransferase
BB28_RS23095	hypothetical protein	5.2	2.8E-35	MAB_4620c	Hypothetical protein
BB28_RS17590	WhiB7 transcriptional regulator	4.7	1.3E-73	MAB_3508c	Putative transcriptional regulator
BB28_RS05390	GNAT family N-acetyltransferase (eis1)	4.1	5.8E-12	MAB_1125c	Hypothetical acetyltransferase, GNAT family
BB28_RS06460	NAD(P)-dependent oxidoreductase	3.4	1.2E-21	MAB_1344c	Putative DTDP-glucose-4,6-dehydratase-related protein
BB28_RS11540	ABC transporter ATP-binding protein	3.3	3.5E-64	MAB_2355c	Putative ABC transporter ATP-binding protein
BB28_RS22650	GNAT family N-acetyltransferase (eis2)	3.3	1E-176	MAB_4532c	N- acetyltransferase(eis2)
BB28_RS06750	*tap* multidrig efflux transporter	3.3	7.3E-35	MAB_1409c	Putative drug antiporter protein precursor
BB28_RS13560	TetV Efflux Pump	3.3	9.8E-94	MAB_2780c	TetV Efflux Pump
BB28_RS20470	pyridoxamine 5'-phosphate oxidase family protein	3.2	4.0E-29	MAB_4054c	Hypothetical protein
BB28_RS17050	hypothetical protein	3.2	5.1E-32	MAB_3424c	hypothetical protein
BB28_RS01940	N-acetyltransferase	3.0	2.9E-11	MAB_0404c	Putative acetyltransferase
BB28_RS09285	ABC transporter ATP-binding protein	2.9	2.7E-07	MAB_1846	Putative ABC transporter ATP-binding protein
BB28_RS12530	18 kDa antigen (HSP 16.7)	2.3	2.5E-31	MAB_3467c	18 kDa antigen (HSP 16.7)
BB28_RS03635	EamA/RhaT family transporter	2.0	1.4E-04	MAB_0766	Hypothetical conserved integral membrane protein
BB28_RS18890	membrane protein	1.8	1.9E-17	MAB_3762	hypothetical protein
BB28_RS17595	hypothetical protein	1.8	3.6E-41	MAB_3509c	Hypothetical protein
BB28_RS06440	TIGR00730 family Rossman fold protein	1.6	2.7E-08	MAB_1340	hypothetical protein
BB28_RS13900	methyltransferase domain-containing protein	1.6	1.6E-13	MAB_2845	Probable trans-aconitate methyltransferase
BB28_RS05350	hypothetical protein	1.6	2.2E-27	MAB_1117c	Hypothetical protein
BB28_RS14985	GTPase HflX	1.5	8.4E-33	MAB_3042c	Probable GTP-binding protein HflX
BB28_RS20665	isocitrate lyase (AceA)	1.5	3.9E-12	MAB_4095c	Isocitrate lyase (AceA)
BB28_RS06230	hypothetical protein	1.5	2.7E-03	MAB_1296	hypothetical protein
BB28_RS06840	hypothetical protein	1.5	1.1E-05	MAB_1413	hypothetical protein
BB28_RS00915	cation transporter	1.5	4.6E-29	MAB_0183c	Putative cation transporter
BB28_RS19745	LysE family translocator	1.5	3.7E-07	MAB_3913	Putative translocator
BB28_RS06445	TIGR00730 family Rossman fold protein	1.4	2.1E-06	MAB_1341	hypothetical protein
BB28_RS12685	aminoglycoside phosphotransferase	1.1	1.6E-02	MAB_4837c	Possible phosphotransferase
BB28_RS14560	GNAT family N-acetyltransferase	1.0	2.7E-17	MAB_2959	Putative acetyltransferase

[a]MCH = *Mycobacterium chlelonae*

[b]Log2 Fold Change for the double lysogen (+BPs+McProf) of *M. chelonae*

[c]FDR = False Discovery Rate

[d]MAB = *Mycobacterium abscessus*

2.4.6 Upregulation of *whi*B7 only occurs in *M. chelonae* (BPs, McProf)

To determine how the presence and absence of each prophage impacts *whi*B7 expression, RNA was isolated from each strain at an OD_{600} of 1.0 and *whi*B7 mRNA levels were measured by qRT-PCR in the BPs single lysogen, double lysogen (BPs, McProf), and non-lysogen

(ΔMcProf) and compared to that of the WT strain (McProf) (**Figure 2.7)**. Although *whi*B7 expression was slightly elevated in the non-lysogen (2-fold) and BPs single lysogen (4-fold) strains relative to the WT strain (McProf), the dramatic increase in *whi*B7 expression (~40-fold) only occurred in *M. chelonae* carrying both prophages (BPs, McProf). The elevated *whi*B7 expression occurred in the absence of known inducers of *whi*B7, such as ACI, which suggests BPs-encoded gene products interact with prophage McProf, resulting in *whi*B7 induction. The elevated expression of *whi*B7 in the double lysogen likely explains the increased resistance to AMK and TOB in the absence of ACI treatment (**Table 2.5** and **Figure 2.4**).

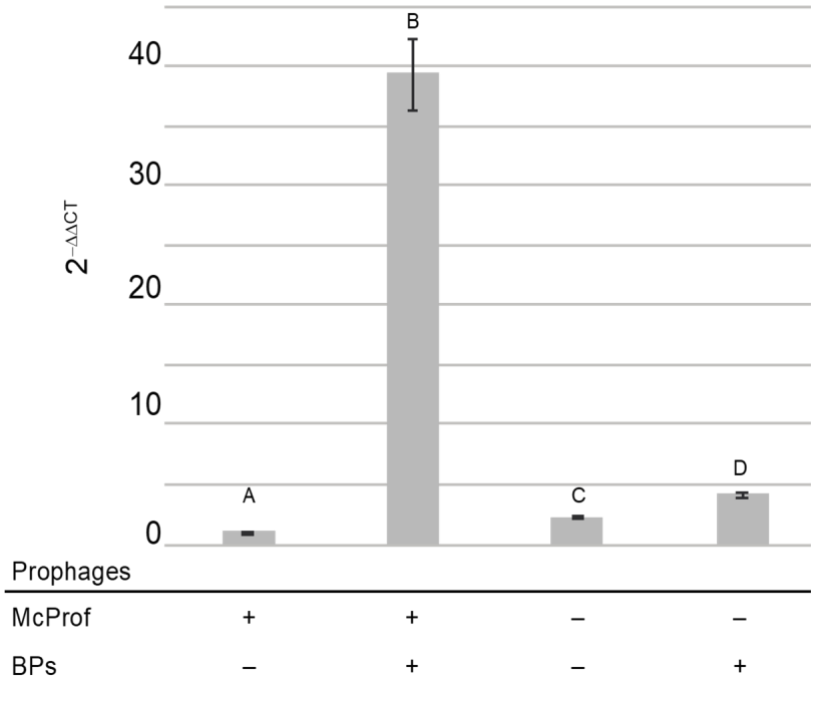

Figure 2.7 qRT-PCR analysis of *whi*B7 expression in *M. chelonae* strains. The average relative expression levels of *whi*B7 in *M. chelonae* carrying McProf alone, BPs and McProf, no prophage, and BPs alone as measured with SYBR Green qRT-PCR. Cultures were grown to an OD_{600} of 1.0 before harvesting RNA in triplicate. Graphs represent average values ± standard error of the mean with n=3 and are representative of two independent trials. Means with different letters are significantly different (Tukey's HSD, α=0.05).

2.4.7 Sub-inhibitory concentrations of ACI, but not AMK, increase *whi*B7 expression in *M. chelonae* (BPs, McProf)

We were surprised that the *M. chelonae* (McProf) strain had the lowest expression of *whi*B7 expression among the four strains given that it had higher AMK resistance, both in the presence and absence of ACI, than the two strains that lack McProf. We reasoned this may be due to *whi*B7-independent intrinsic resistance, such as cell wall permeability, and/or *whi*B7 induction in the presence of AMK, which is a more potent inducer of *whi*B7 than ACI (Hurst-Hess et al., 2017). Likewise, we wondered if the heightened viability observed in the single and double McProf lysogen strains in the presence of AMK and ACI was due to increased *whi*B7 expression. To assess this, we measured *whiB*7 expression in double, single, and non-lysogen strains following a 3-h treatment with 75 μM ACI or 1-h treatment with 16.7 μM AMK (**Figures 2.8** and **2.9**).

ACI treatment resulted in increased *whi*B7 expression in all four strains relative to untreated strains (**Figure 2.8**). Expression of *whi*B7 was highest in the double lysogen strain (BPs, McProf) treated with ACI which correlates with the observed AMK resistance of this strain. *whi*B7 expression in the single and non-lysogen strain increased with ACI treatment; however, the relative levels of *whi*B7 expression did not correlate with AMK resistance (**Figure 2.3a**). Although the fold-increase of *whi*B7 in ACI-treated strains relative to control strains was highest in the WT strain (McProf) (9.5-fold) *whi*B7 was lower than that of the ACI-treated BPs single lysogen, which demonstrated lower AMK resistance.

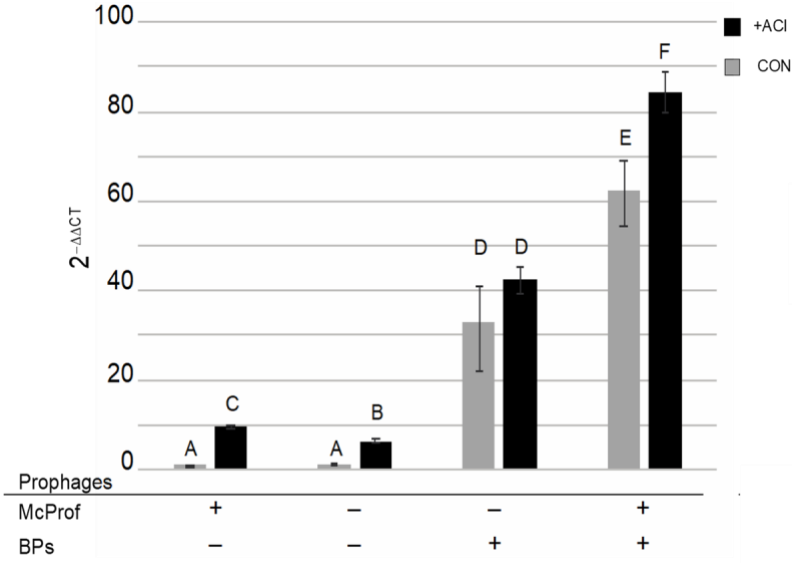

Figure 2.8 qRT-PCR analysis of *whi*B7 expression in *M. chelonae* strains in the presence and absence of ACI treatment. The average relative expression levels of *whi*B7 in *M. chelonae* carrying McProf alone, no prophage, BPs alone, or BPs and McProf as measured with SYBR Green qRT-PCR. RNA was harvested in triplicate from strains grown to an OD_{600} of 0.7 before treating or not treating with 75 µM ACI and incubating for an additional 3 h. The culture OD_{600} at time of harvest was close to 1 but differed slightly for each strain and treatment. Graphs represent mean ± SE with n=3. Letters represent statistically significant differences (Tukey's HSD, α =0.05).

Strains that lack the McProf prophage had the greatest increase in *whi*B7 expression in response to AMK treatment. The non-lysogen and BPs single lysogen had 28- and 7-fold increases in *whi*B7 expression in response to AMK treatment, respectively (**Figure 2.9**). AMK had less of an effect on *whi*B7 expression in strains carrying McProf. AMK treatment resulted in a 3.5-fold increase in *whi*B7 expression in the single McProf lysogen and no significant increase in *whi*B7 expression in the double lysogen. It's possible that AMK doesn't result in strong induction of *whi*B7 expression in the McProf-carrying strains due to cell wall permeability

and/or efflux, and if so, this could also explain the AMK-resistant phenotypes observed in the single McProf and double lysogen strains.

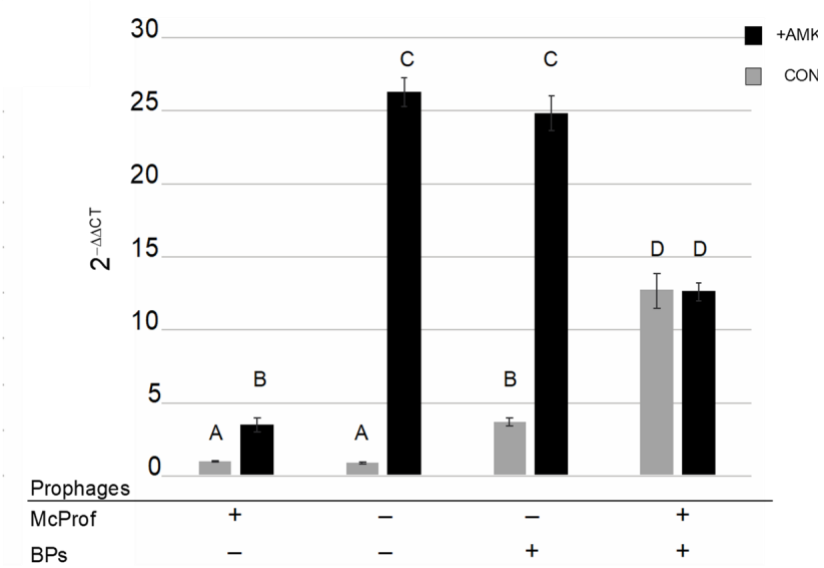

Figure 2.9 qRT-PCR analysis of *whi*B7 expression in *M. chelonae* strains in the presence and absence of AMK treatment. The average relative expression levels of *whi*B7 in *M. chelonae* carrying McProf alone, no prophage, BPs alone, or BPs and McProf as measured with SYBR Green qRT-PCR. RNA was harvested in triplicate from strains grown to an OD_{600} of 0.9 before treating or not treating with 16.7 µM AMK and incubated for an additional 1 h. Graphs represent mean ± SE with n=3. Letters represent statistically significant differences (Tukey's HSD, α =0.05).

2.4.8 Characterization of the McProf prophage

The McProf genome was characterized to uncover potential interactions between the naturally occurring prophage and BPs in *M. chelonae* to increase whiB7 expression and antibiotic resistance. McProf is 67,657 bp in length, spanning coordinates 1,521,426 – 1,589,648 in *M. chelonae* CCUG 47445. The genome encodes 98 putative genes, no tRNAs, and has been annotated in its prophage format with the first gene located immediately adjacent to *att*L (**Figure 2.10**). The McProf prophage is integrated into a leftward oriented tRNA-Lys

(BB28_RS07905) and is flanked by 45-bp attachment sites, *att*L and *att*R (5'-TGCGCCGTCAGGGGCTCGAACCCCGGACCCGCTGATTAAGAGTCA-3').

Gp1 encodes a rightward transcribed tyrosine integrase, followed by a gene of unknown function (gp2) and the predicted immunity repressor (gp3). Gp3 shares high sequence similarity with immunity repressors identified in other mycobacteriophages, such as singleton DS6A, and cluster K12 phages, DismalFunk, DismalStressor, Findley, Milly, and Marcoliusprime (Russel and Hatfull, 2016). Gp4 and gp5 encode Cro (control of repressor's operator) and excise respectively and contain helix-turn-helix (HTH) DNA binding motifs characteristic of these genes. The McProf genome follows the typical synteny of bacteriophage with genes involved in DNA replication and metabolism oriented downstream of the integration cassette. Structural genes span gp51 – 82 and include a lysis cassette encoding lysin A, lysin B, and holin (gp76 -78 respectively). Between the structural genes and the *att*R site is a region of genes that are typically expressed during lysogeny, although many of these genes do not have a predicted function in McProf (Dedrick et al., 2017). Genes within this region with predicted functions include an ADP-ribosyl glycosylhydrolase (gp86), a HTH DNA binding protein (gp89), a membrane protein (gp90), an AAA-ATPase (gp91), and a polymorphic toxin cassette (gp96 – 98).

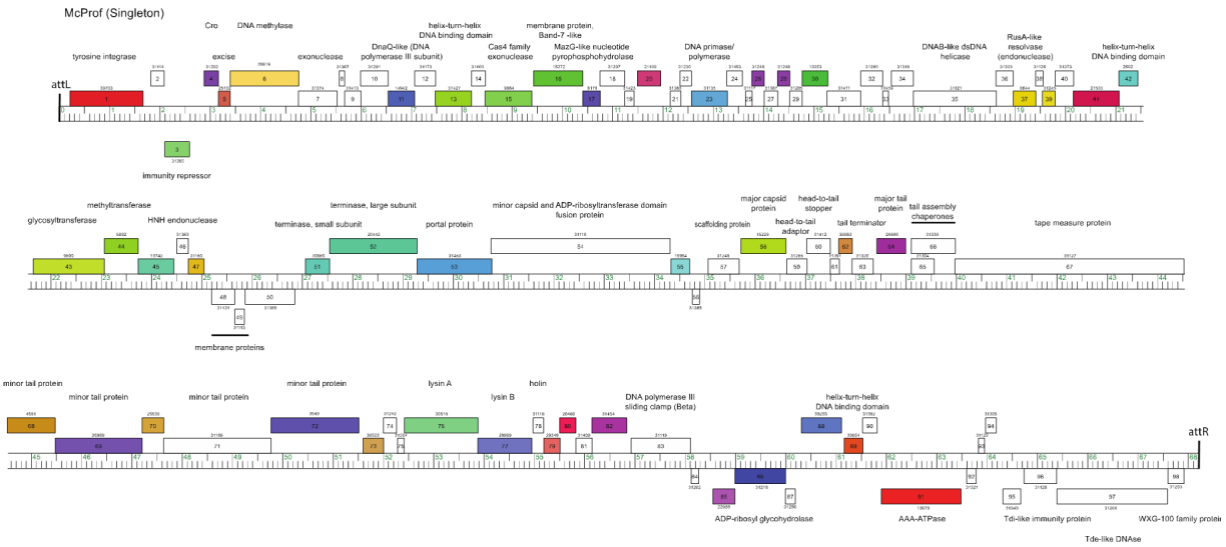

Figure 2.10 Phamerator map of the McProf genome. The coordinates of the McProf genome are represented by the ruler. Genes are shown as colored boxes above (transcribed rightwards) or below (transcribed leftward) the ruler. The map was generated using Phamerator (Cresawn et al., 2011).

Of interest is the polymorphic toxin (PT) cassette on the rightmost arm of the McProf genome, as it encodes proteins that are likely secreted by a mycobacterial Type 7 secretion system (T7SS) expressed by *M. chelonae* (Esx3 or Esx4). HHpred analysis of gp98 suggests that it encodes a 105-amino acid product consistent with T7SS proteins based on helical domains with high similarity to characteristic WXG-100 motifs (Pallen, 2002). However, gp98 includes a SAG motif that is slightly different from the conserved WXG motif. Gp97 appears to encode a 732-amino acid polymorphic toxin. The C-terminus includes a toxin_43 motif (PF15604.6) with high sequence similarity to Type 6 secretion system (T6SS) polymorphic toxin, TdeI. This toxin was identified in *Agrobacterium tumefaciens* (Atu4350) and belongs to a family of proteins exhibiting DNase activity characterized by a conserved HxxD catalytic domain in the C-terminus (Ma et al., 2014). In addition, gp97 contains a WXG-100 motif in the N-terminus and a likely

T7SS secretion signal, YxxxD/E, in the C-terminus (Daleke et al., 2012). Gp96 encodes a predicted 216-amino acid Tdi-like immunity protein, which are known to be paired with Tdi toxins to neutralize its activity. Gp96 includes the conserved domains characteristic of Tdi proteins, GAD and DUF1851 (**Figure 2.11**) (Ma et al., 2014).

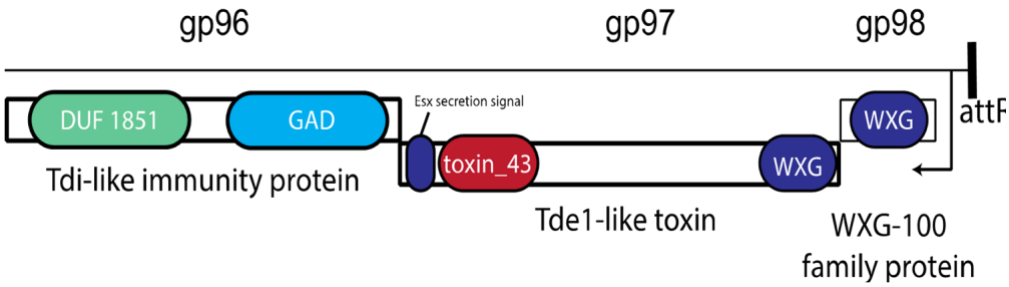

Figure 2.11 McProf ESX-like polymorphic toxin cassette. Graphical domain organization of the McProf-encoded polymorphic toxin cassette (gp96 – 98).

2.4.9 Lysogenic gene expression profiles from the BPs and McProf prophage genomes.

To determine if the presence of BPs alters gene expression from the McProf prophage genome, differential expression of McProf genes was examined between the WT strain (McProf) and the double lysogen (BPs, McProf). None of the expressed McProf genes were significantly differentially expressed in the presence of the BPs prophage (FC>1.99 and FDR<0.05). Because there was no difference in expression profiles, we present below the expression profile of only the McProf prophage from the *M. chelonae* WT (McProf) strain (**Figure 2.12b**).

The immunity repressors from both the BPs (gp33) and McProf (gp3) genomes are highly expressed during lysogeny of *M. chelonae* (**Figure 2.12**). The BPs genome also expresses, gp58, a gene of unknown function that is part of a mycobacteriophage mobile element

(MPME1) (**Figure 2.12a**) (Sampson et al., 2009). There are an additional 15 genes expressed at varying levels from the McProf genome (**Figure 2.12b**). The integrase (gp1) is expressed at low levels and is adjacent to a moderately expressed gene of no known function (gp2). There are three reverse oriented genes, gp48 – 50, located between the HNH endonuclease (gp47) and the small subunit terminase (gp51) and a small reverse oriented gene (gp56) adjacent to the scaffolding protein with moderately and low expression, respectively. We were not able to determine functions for these genes; however, gp46 and gp47 do have predicted membrane domains. The remaining genes expressed from the McProf prophage genome are located between the structural genes and *att*R and many do not have predicted gene functions, including the most highly expressed McProf gene, gp84. There is also strong expression from the gene cassette containing the putative WXG-100 family polymorphic toxin and immunity protein (gp96 – 98). None of the expressed McProf genes were significantly differentially expressed in the presence of the BPs prophage (FC>1.99 and FDR<0.05).

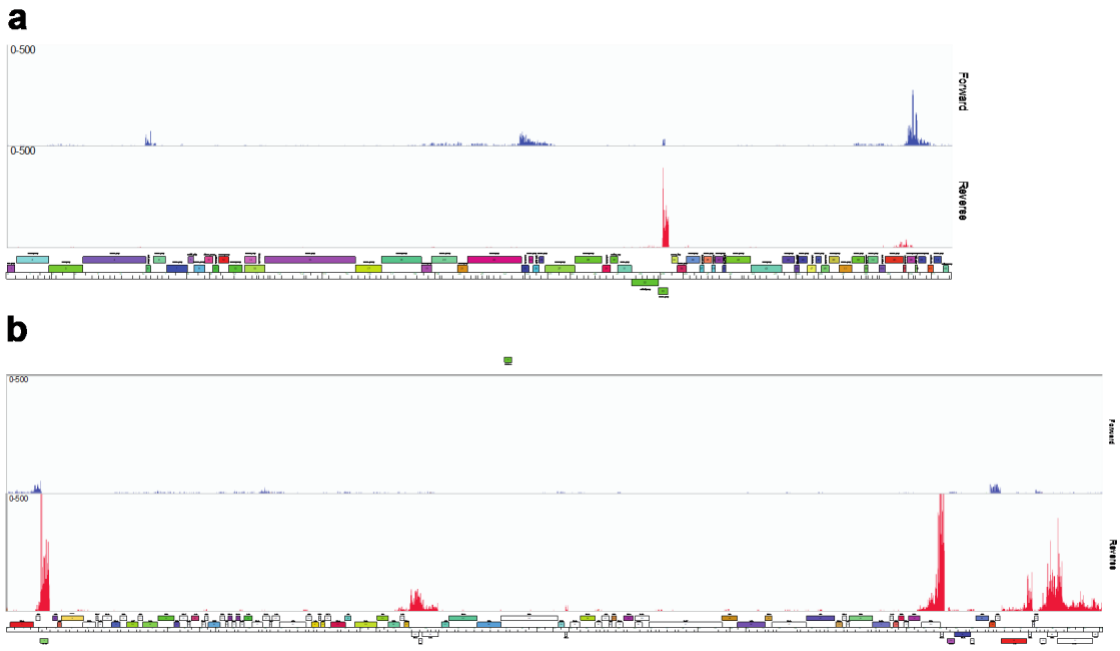

Figure 2.12 Lysogenic gene expression profiles of BPs and McProf. Lysogenic gene expression profiles of prophages **a.** BPs and **b.** McProf from the *M. chelonae* WT strain. RNAseq profiles are shown for forward (blue) and reverse (red) DNA strands. Note that in **a.** the sequence reads are mapped to the viral BPs genome rather than prophage genome whereas in **b.** the sequence reads are mapped to the McProf prophage genome. The number of reads mapped are on the y-axis and the genome maps are shown below. Genes expressed from the McProf prophage genome in the double lysogen were not significantly different from the WT strain and therefore the expression profile was not included.

2.5 Discussion

Cases of NTM infections have been on the rise in recent decades (Johansen et al., 2020). *M. abscessus*, a causative agent of pulmonary infections, has become a major health concern, especially for immunocompromised individuals, due to extreme antibiotic resistance (Johansen et al., 2020). Frontline antibiotics used to treat *M. abscessus* infections include CLA and AMK. However, the bacteria encounter a drug gradient in tissues and often develop resistance during the course of treatment (Guo et al., 2020). In many cases, resistance is caused by mutations in

16S or 23S rRNA which confer resistance to AMK and CLA respectively, but do not account for extensively resistant phenotypes in all isolates (Nessar et al., 2012). Additionally, induction of the *whi*B7 regulon contributes to increased resistance and *whi*B7 expression is elevated in extensively resistant strains of *M. abscessus* compared to those susceptible to treatment (Guo et al., 2020). Elucidating the mechanisms that trigger upregulation of *whi*B7 could lead to more effective therapies for extensively resistant mycobacterial infections.

We have demonstrated that the presence of prophages in mycobacteria contribute to increased AMK and TOB resistance (**Table 2.5** and **Figure 2.4**). This is similar to the effect previously described in *E. coli* where strains lacking prophages were more sensitive to □-lactam (Wang et al., 2010). Interestingly, the McProf prophage alone appears to play a more significant role, but addition of second prophage (BPs) amplifies the effect of McProf on antibiotic resistance. Strains of *M. chelonae* carrying BPs only or no prophage were more susceptible to AMK relative to those carrying McProf. Additionally, ACI treatment increased AMK and TOB resistance in all strains, which makes sense because ribosome-targeting antibiotics induce *whi*B7 expression and therefore increase intrinsic antibiotic resistance (**Table 2.5** and **Figure 2.5**) (Morris et al., 2005; Burian et al., 2012). However, this effect was elevated in *M. chelonae* (McProf) in AMK assays and further enhanced by presence of BPs compared to *M. chelonae* (ΔMcProf), indicating that McProf plays a substantial role in mediating AMK resistance.

The dramatically higher *whi*B7 expression in the strain carrying both prophages (BPs, McProf) likely contributes to the heightened AMK and TOB resistance observed in the double lysogen (**Figures 2.7** and **2.9; Tables 2.6** and **2.7**). We observed high *whi*B7 expression in the double lysogen in the absence of antibiotics or other conditions known to induce *whi*B7,

revealing prophage as a novel mechanism of inducing *whi*B7 expression and intrinsic antibiotic resistance. Also upregulated in the double lysogen are *whi*B7 regulon genes that can explain the increased resistance to aminoglycosides AMK and TOB (Pryjma et al, 2017). The GNAT acetyltransferase, *eis2,* and *tap,* a multidrug efflux pump, were each upregulated ~10-fold in the double lysogen and confer resistance to aminoglycosides (Hurst-Hess et al., 2017; Ainsa et al., 1998; Chen et al., 2012). 2′-N-acetyltransferase AAC(2′) also contributes to resistance to TOB and AMK, however this gene (BB28_RS22055) was not significantly upregulated in our data set (Luthra et al., 2018). It is possible that other N-acetyltransferases (BB28_RS23100, BB28_RS01940, BB28_RS14560), aminoglycoside phosphotransferases (BB28_RS12685), or potential efflux pumps (BB28_11540) upregulated in our dataset contributed to AMK and TOB resistance of the double lysogen (**Table 2.7**). Tap, along with TetV (BB28_RS13560) target tetracycline efflux, however, we did not consistently see an increase in TET resistance across all our MIC trials (De Rossi et al., 2002; De Rossi et al., 1998). Although *M. chelonae* lacks an *erm* gene, there was a slight elevation in the *whi*B7 regulon gene, *hflx,* but this did not result in a significant change in CLA resistance (Rudra et al., 2020).

There are likely other mechanisms of intrinsic resistance at play that contribute to increased aminoglycoside resistance in McProf-carrying strains. Although *whi*B7 expression was highest in the double lysogen (BPs, McProf) treated with ACI among the four strains, *whi*B7 expression levels in the single McProf strain did not correlate with its relative AMK resistance among the four strains. AMK is also a potent inducer of *whi*B7 expression in mycobacteria, but surprisingly, AMK had little to no effect on *whi*B7 expression in strains carrying McProf (Hurst-Hess et al., 2017). Conversely, *whi*B7 expression was significantly upregulated in strains lacking

McProf. It is possible that McProf somehow alters cell wall permeability. A decrease in permeability would likely contribute to the observed AMK resistance in these strains, and further investigating this potential effect will be important to understanding the impact of prophage on drug resistance.

We do not yet know how phage-encoded proteins from the two prophages, BPs and McProf, interact to alter *whi*B7 expression in the double lysogen strain. The McProf genome appears to only express genes through lysogenic infection of *M. chelonae*, whereas BPs can carry out lysogenic and lytic infection (via induction) in a population of double lysogen cells. It's therefore possible that either lytic or lysogenic gene expression from BPs interacts with McProf through an unknown mechanism to alter *whi*B7 expression. Alternately, the McProf-encoded ESX-like polymorphic toxin cassette should be investigated for contributions to altering *whi*B7 expression. Activated toxin systems could potentially act as a trigger to the WhiB7 stress response. Sub-inhibitory concentrations of antibiotics and BPs phage infection both enhanced antibiotic resistance in *M. chelonae* in the presence of prophage McProf (**Figures 2.1** and **2.3**), conditions also known to activate toxin systems (Kumar et al., 2019; LeRoux et al., 2015; Slayden et al., 2018; Wang et al., 2011). Toxin/antitoxin (TA) systems are also known to function as stress response modules and regulators of adaptive responses to stresses associated with host environment and drug treatment (Slayden et al., 2018). TA systems also stabilize replicative elements (e.g. plasmids and prophage) and defend against phage lytic infection (Yao et al., 2018; Fraikin et al., 2020; Wozniak et al., 2009). The increased stability of the BPs prophage in the presence of McProf compared to BPs lysogens in the cured *M. chelonae*

(ΔMcProf) and its reported instability in *M. smegmatis* strains suggests that the polymorphic toxin system encoded by McProf is active (Sampson et al., 2009; Broussard et al., 2013).

Our novel research findings indicate that prophage could be drivers of important intrinsic antibiotic resistance genes in response to stresses. To determine the mechanism by which phage alter intrinsic antibiotic resistance in mycobacteria, we are exploring the function and impact of specific phage genes on expression of *whi*B7.

CHAPTER 3

CHARACTERIZING THE ROLE OF PHAGE BPS GENE PRODUCTS IN INCREASED *WHI*B7 EXPRESSION IN STRAINS OF *MYCOBACTERIUM CHELONAE* CARRYING MCPROF

3.1 Chapter Summary

Mycobacterium abscessus is a nontuberculous pathogen associated with lung and disseminated infection and is becoming a major public health concern (Griffith, 2019). Emergence of extensively drug resistant strains has hindered effective treatment (Griffith, 2019). Common among these strains are integrated bacteriophage genomes (prophage) that are hypothesized to contribute to mycobacterial fitness and virulence (Fan et al., 2015). How prophage impact bacterial fitness, particularly when they don't encode an obvious virulence factor, is not understood.

We are investigating the role of prophage in mycobacterial fitness and antibiotic resistance in *M. chelonae*, a member of the *M. abscessus*/*M. chelonae* complex which carries a naturally occurring prophage, McProf. Previous RNAseq analysis of *M. chelonae* (McProf) carrying a second prophage, BPs, showed drastic changes in bacterial gene expression relative to the wildtype strain, as well as BPs single lysogen and non-lysogen strains. This included significant upregulation of *whi*B7, a conserved mycobacterial transcriptional activator that regulates genes associated with antibiotic resistance and stress adaptation (Morris et al. 2005; Burian et al., 2012). To investigate the role of BPs on *whi*B7 expression in double lysogens (*M. chelonae* (BPs, McProf)), we constructed recombinant strains of *M. chelonae* (McProf) to express lysogenic BPs genes, gp5, gp33, and gp58. qRT-PCR analysis of these strains

demonstrated no significant impact on *whi*B7 expression, indicating that BPs lysogenic gene products alone do not contribute to increased *wh*iB7 expression observed in *M. chelonae* (BPs, McProf). Taken together, these data suggest that altered expression of *whi*B7 may be caused by an alternative interaction between BPs and the naturally occurring prophage, McProf. Identifying prophage-encoded factors that contribute to fitness will be important in developing alternative treatment strategies for mycobacterial infections.

3.2 Introduction

Non-tuberculous mycobacterial infections are becoming increasingly prevalent and are difficult to treat due to high levels of intrinsic antibiotic resistance (Nessar et al., 2012). Emergence of extensively resistant strains presents a new challenge where infections are essentially impossible to eradicate, especially in the case of *Mycobacterium abscessus* (Johansen et al., 2020). While mutations in drug targets have explained extensive resistance in some *M. abscessus* isolates, it does not account for all of these phenotypes (Guo et al., 2020). All extensively resistant isolates, however, have elevated expression of the conserved mycobacterial transcriptional activator, *whi*B7 (Griffith, 2019; Guo et al., 2020).

*whi*B7 regulates genes involved in intrinsic antibiotic resistance and stress adaptation and is typically upregulated under stress conditions such as drug treatment and the intracellular environment of macrophage (Morris et al., 2005; Burian et al., 2012). However, the cause of this increased expression in extensively resistant strains in the absence of environmental triggers remains unknown. Recently, we demonstrated that integrated viral genomes (prophage) play a role in upregulation of *whi*B7 (Cushman et al., 2021).

Most pathogenic bacteria carry prophage that are known to contribute to fitness and antibiotic resistance. For example, the Pf4 prophage in *Pseudomonas aeruginosa* influences biofilm formation which allows for drug tolerance (Rice et al., 2009; Wang et al., 2016). Macrolide resistance is observed in multi-drug resistant strains of *Streptococcus pyogenes* that is conferred by a prophage-encoded erythromycin resistance, or *erm* gene (Hyder and Streitfeld, 1978; Wang et al., 2016). The majority of sequenced pathogenic mycobacteria to date carry at least one prophage or prophage-like element (Bibb and Hatfull, 2002; Fan et al., 2014; Dedrick et al., 2021). Recent efforts in sequencing clinical *M. abscessus* isolates showed that 85% of strains carry at least one prophage (Dedrick et al., 2021). Dedrick et al. (2021) identified 67 novel prophage sequences that have been assigned to 17 Mab clusters (A – Q) based on >35% shared gene content. However, their role on fitness and virulence has not been explored.

M. chelonae, an opportunistic pathogen belonging to the *M. abscessus*/*M. chelonae* complex, serves as an ideal model for studying the impact of prophage and mechanisms of antibiotic resistance in pathogenic mycobacteria. In addition to sharing >80% sequence identity with *M. abscessus*, *M. chelonae* also encodes a *whi*B7 regulon that shares 103 of the 128 genes identified in the *M. abscessus* regulon (Hurst-Hess et al., 2017). Additionally, it carries a novel cluster MabR prophage (McProf) that is closely related to prophages identified in the genomes of clinical *M. abscessus* strains (Molloy, Unpublished). Our previous work demonstrated that the addition of a second prophage, BPs, to wildtype *M. chelonae* (BPs, McProf) to form a double lysogen increased both *whi*B7 expression and resistance to aminoglycosides, amikacin and tobramycin. This phenotype was not observed in strains lacking the McProf prophage (BPs

single lysogen and non-lysogen strains of *M. chelonae*) suggesting an interaction between the two prophages occurs to increase *wh*iB7 expression (Cushman et al., 2021). How the two prophages interact to alter gene expression is not understood. It appears that McProf is unable to carry out a successful lytic infection in *M. chelonae*, and therefore only exists in its prophage form. Conversely, there is evidence of both lytic and lysogenic BPs growth in cultures of double lysogen cells. It is possible that either lytic or lysogenic BPs gene expression in the presence of McProf is responsible for changes in gene expression. However, the BPs prophage is extremely stable in the presence of the prophage McProf, and the majority of cells carry BPs in its prophage form in a double lysogen culture.

Here we explore the role of the BPs lysogenic gene products on *whi*B7 expression in the presence of prophage McProf. We have identified the lysogenic gene expression profile for BPs in double lysogens of *M. chelonae* (BPs, McProf) and generated recombinant strains of *M. chelonae* (McProf) to determine the impact of individual BPs lysogenic gene products on *whi*B7 expression.

3.3 Materials and Methods

3.3.1 Bacterial and viral strains

Mycobacterium chelonae (ATCC®35752, American Type Culture Collection, Manassas, VA) was grown in liquid Middlebrook 7H9 broth (BD, Sparks, MD) supplemented with 10% oleic acid, albumin, dextrose (OAD) and 0.05% Tween 80 at 30˚C with shaking at 230 RPM. The wildtype strain of *M. chelonae* carries a naturally occurring prophage, McProf, and will be referred to as *M. chelonae* (McProf). *M. smegmatis* MC^2155 (ATCC®700084, American Type Culture Collection) was cultivated in the same media in the absence of Tween 80 and grown at

37˚C with shaking. Kanamycin (KAN) was used as a selective measure for recombinant strains at a concentration of 250 µg mL^{-1} in liquid and solid media. Competent *E. coli* DH5 cells were prepared by New England Biolabs, (Ipswich, MA) and grown in Luria broth base, Miller (BD) supplemented with 50 µg mL^{-1} of KAN at 37˚C with shaking at 230 RPM for propagation of plasmids. Bacterial strains used in this work are listed in **Table 3.1.** Plasmids used in this study are listed in **Table 3.2**.

Mycobacteriophages BPs and CLED96 were obtained from the Hatfull Laboratory (Sampson et al., 2009) and cultivated by plaque assay using *M. chelonae* (McProf) or *M. smegmatis* MC^2155. Serially diluted phage samples were incubated for 15 min at room temperature in 0.5-ml aliquots of late log phase bacteria. Aliquots were plated in 4.5 ml of 0.45% 7H9 top agar onto 7H10 agar plates. High titer phage lysate stocks were generated by flooding bacterial lawns with nearly confluent lysis with phage buffer (10 mM Tris/HCl pH 7.5, 10 mM $MgSO_4$, 1 mM $CaCl_2$, 68.5 mM NaCl). Viral strains used in this study are listed in **Table 3.1**.

Table 3.1 Bacterial and viral strains used in this study.

Bacterial Strains	**Strain Description**	**Source**
Escherichia coli		
DH5α	Supercompetent cells	NEB
Mycobacterium chelonae		
Single lysogen (McProf)	*M. chelonae* ATCC 35752 with naturally-occurring prophage, McProf	ATCC
Double lysogen (BPs, McProf)	BPs lysogen of *M. chelonae* ATCC 35752	This study
Mycobacterium smegmatis		
MC^2155	*M. smegmatis* ATCC 700084	ATCC

Viral Strains	**Virus Description**	**Source**
BPs	Cluster G mycobacteriophage	Hatfull Laboratory
CLED96	Cluster G mycobacteriophage	Hatfull Laboratory

Table 3.2 Plasmids used in this study.

Plasmid Name	Vector	Phage Genes	Genome Coordinates	Description
pMHIR	pMH94	BPs gp32 and gp33	29,521 – 27,696	Integration-dependent pMH94 subclone carrying BPs gp32 (integrase), *attP*, and gp33 (immunity repressor) in place of the L5 integration cassette
pMHIattP	pMH94	BPs gp32 and gp33	29,270 – 27,696	Integration-dependent pMH94 subclone carrying BPs gp32 (integrase), *attP*, and a truncated form of gp33 (immunity repressor) in place of the L5 integration cassette
pMOHsp	pMO21	N/A	N/A	Bacterial partitioning vector, pMO21, subclone carrying a constiuitive Hsp60 promoter
pMOgp5	pMO21	BPs gp5	6,189 – 6,395	Bacterial partitioning vector, pMO21, subclone carrying a constiuitive Hsp60 promoter and BPs gp5
pMOgp58	pMO21	BPs gp58	39,973 – 40,308	Bacterial partitioning vector, pMO21, subclone carrying a constiuitive Hsp60 promoter and BPs gp58
pMOgp57-58	pMO21	BPs gp57 and gp58	39,824 – 40,308	Bacterial partitioning vector, pMO21, subclone carrying a constiuitive Hsp60 promoter and BPs MPME1 (gp57 and gp58)

3.3.2 Isolation of lysogenic strains

To generate BPs and CLED96 lysogen strains, *M. chelonae* (McProf) was serially diluted and plated in 4.5 mL of 7H9 top agar onto 7H10-OAD agar plates. One set of plates was treated with 10^9 plaque forming units (PFUs) of BPs or CLED96, while the second set was untreated. Plates were then incubated for 6 d at 30˚C. Resulting colonies were grown in liquid culture to test for phage particle release and superinfection immunity. Efficiency of lysogeny was calculated by dividing the number of colonies on virus-treated plates by the number of colonies on non-treated plates and multiplying by 100 to yield a percentage.

Genomic DNA was extracted from the *M. chelonae* (BPs, McProf) double lysogen and sent to Jackson Laboratory for sequencing (Genome Technologies at Jackson Laboratory, Bar Harbor, ME). Whole genome libraries were prepared and sequenced on a 2x150-bp MiSeq run. The presence of the BPs prophage was confirmed through reads that did not align to the bacterial reference genome. Primers were designed to PCR amplify BPs attachment sites, *att*L and *att*R, to confirm prophage integration for continued cultivation of lysogen strains (**Table 3.3**). This same PCR assay confirmed presence of the CLED96 prophage as well. The lysogen strains carrying the BPs and McProf or CLED96 and McProf prophages are referred to as *M. chelonae* (BPs, McProf) *and M. chelonae* (CLED96, McProf) respectively (**Table 3.1**).

Table 3.3 Standard PCR primers used in this study.

Target	Primers	Sequence (5' to 3')
pMOHsp	pMOHsp_seq_F	GTGGCGAACTCCGTTGTAGT
	pMOHsp_seq_R	GAGGGTGCCGTAGAAATGAC
L5 attL	L5_attB_L	GGTGGAGGGAAGTTCAGGTC
	L5_attP_R	AGTCTTCAGCGATCCCCATC
L5 attR	L5_attP_L	GAATGCCCCTCGTCTGTTC
	L5_attB_R	ACCTGCGTCCATACTTCGTC
L5 attP	L5_attP_L	GAATGCCCCTCGTCTGTTC
	L5_attP_R	AGTCTTCAGCGATCCCCATC
L5 attB	L5_attB_L	GAATGCCCCTCGTCTGTTC
	L5_attB_R	ACCTGCGTCCATACTTCGTC
BPs gp5	BPs_gp5_F	ATGACATTCCGAGAAGAAGCCGAAGCCGCA
	BPs_gp5_R	CTACGTTTCGCCGGCCGGATCCTGCCGGCC
pMOgp5	pMOHsp_BPsgp5_F	CGGACGGCGGAAGAAAGGAGAAAGCCAGCGATGA CATTCCGAGAAGAAGCCGAAGCCGCA
	pMOHsp_BPsgp5_R	CTGCAGCTGGATCCTAGATTTAAAGATCTGCTAC GTTTCGCCGGCCGGATCCTGCCGGCC
BPs gp33	gp32attP+221_F	CGCTGCCAGACCCCAATTGCGGAAC
	gp32attPgp33IG_R	CGGTTGGGGTCATGTGCACCAACATAG
	gp32attP+221_R	CTACTGATCGCGCGCCTTGAAGCTG
pMHIR	pMH94gp32attPgp33IG_F	CGAGCTCGGTACCCGGGGATCCTCTAGAGCGCTG CCAGACCCCAATTGCGGAAC
	pMH94gp32attPgp33IG_R	CGGCCAAGCTTGCATGCCTGCAGGTCGACGGTTG GGGTCATGTGCACCAACATAG
pMHIattP	pMH94gp32attPgp33IG_F	CGAGCTCGGTACCCGGGGATCCTCTAGAGCGCTG CCAGACCCCAATTGCGGAAC
	pMH94gp32attP+221_R	CCCGGCCAAGCTTGCATGCCTGCAGGTCGACTAC TGATCGCGCGCCTT
McProf attL	Mc_attL_F	CGTCACGTTGGGGACTATCT
	Mc_attL_R	TTGAGCTGCGGATAACCTCT
McProf attR	Mc_attR_F	CGCTTGTAATCGTCGTA
	McProphageRR	ATAACTTTCGGCGGTTCCTT
McProf attP	Mc_attR_F	CGCTTGTAATCGTCGTA
	Mc_attL_R	TTGAGCTGCGGATAACCTCT
McProf attB	Mc_attL_F	CGTCACGTTGGGGACTATCT
	McProphageRR	ATAACTTTCGGCGGTTCCTT
BPs attL	BPs_attB_F	GTCTCGTTACTGGCGAGCTT
	BPs_attP_R	CGGGTAGTAGGCAGATGAGC
BPs attR	BPs_attP_F	GCTTTATCCAGGGTTGACCA
	BPs_attB_R	CGGTAGTAGGCAGATGAGC
BPs attP	BPs_attP_F	GCTTTATCCAGGGTTGACCA
	BPs_attP_R	CGGGTAGTAGGCAGATGAGC
BPs attB	BPs_attB_F	GTCTCGTTACTGGCGAGCTT
	BPs_attB_R	CGGTAGTAGGCAGATGAGC

3.3.3 Construction of recombinant strains

Mycobacterial expression vector, pMO21, provided by the Hatfull Laboratory, carries a phage encoded ParABS system and kanamycin resistance gene, but lacks a promoter region. The plasmid was modified to include a constitutive Hsp60 promoter and is referred to as pMOHsp. pMO21 was digested with *Not*I per the manufacturer's recommendations (NEB) to linearize the vector. Linearized vector was purified on a DNA clean-up column (NEB). Digested pMO21 underwent a Gibson Assembly (NEB) reaction with a 445-bp G-block (Integrated DNA Technologies, Coralville, IA) carrying an *hsp*60 promoter region and flanking regions complementary to the plasmid ends to generate a vector with a constitutive promoter. Products were transformed into competent *E. coli* cells (NEB) and plated onto L agar supplemented with 50 μg mL^{-1} kanamycin (KAN). pMOHsp was linearized with *Kpn*I according to the manufacturer's recommendations (NEB). Expression vectors were constructed using 432-bp and 499-bp G-blocks (IDT) that each included 30 bp of plasmid backbone sequence that flank the *Kpn*I insertion site at the 5' and 3' end of the G-blocks and an internal sequence that corresponds to the BPs gp58 ORF (39,973 − 40,308 bp) or the entire MPME1 sequence (39,824 − 40,308 bp) (**Table 3.3**). The BPs gp58 ORF G-block was inserted into pMOHsp to generate an overexpression vector, while the MPME1 sequence was inserted into pMO21 and expressed from its native promoter. Similarly, gp5 was PCR amplified to include extensions that correspond to 30 bp of flanking sequence to the pMOHsp *Kpn*I insertion site. Fragments were assembled into the vector via Gibson Assembly (NEB) and transformed into competent *E. coli* DH5 according to the manufacturer's recommendations. Successful recombinant plasmids

harvested from transformants were confirmed by PCR (**Table 3.3**) and are referred to as pMOgp5, pMOgp57-58, and pMOgp58.

Bacterial expression vector, pMH94 (Lee et al., 1991) is integration-dependent and includes an L5 integration cassette and kanamycin resistance gene. The vector was digested with *Sal*I per the manufacturer's recommendation (NEB) in order to linearize the vector and remove the L5 integrase cassette. Fragments were separated on a FlashGel Recovery Cassette according to the manufacturer's instructions (Lonza, Rockland, ME) and a 4,136 bp fragment was recovered. The BPs integrase (gp32), *att*P site, immunity repressor (gp33) and upstream intergenic region including the native promoter (29,521 − 27,696 bp) were PCR amplified with primers that include 30-bp 5' extensions that correspond to the ends of *Sal*I-digested pMH94. Similarly, a control vector was constructed by PCR amplifying the BPs integrase, the *att*P site, and the 3' end of gp33 (29,270 − 27,696 bp) to prevent a functional immunity repressor from being expressed. Each insert was cloned into *Sal*I-digested pMH94 by Gibson cloning, as described above, to generate pMHIR and pMHIattP (**Table 3.2**).

All vectors were electroporated into competent *M. chelonae* strains according to de Moura et al. (2014). Briefly, electrocompetent *M. chelonae* cells were prepared by washing with ice-cold 10% glycerol four times. Plasmid DNA in 500 ng quantities were electroporated with 100 µL of electrocompetent *M. chelonae* in 0.2-cm gap cuvettes. A sample of electrocompetent cells lacking plasmid DNA served as a negative control. Electroporation was carried out in a single pulse at 2.5 kV, 25 mF, 1,000 Ω. Cells were suspended in 900 µL of room-temperature 7H9-OAD and incubated at 30˚C with shaking for 4 h prior to plating on 7H10-OAD agar plates supplemented with 250 µg mL^{-1} of KAN. Transformant colonies were PCR screened for presence

of the plasmid (**Table 3.3**). Because our work involved analysis of gene expression, specifically *whi*B7, plasmids were not maintained with antibiotic selection following generation of recombinant strains. pMOHsp, pMO21, and their respective subclones were maintained by a bacterial partitioning system encoded by the vector. pMH94 was maintained by integration into the L5 attachment site and pMHIR and pMHIattP were maintained by integration into the BPs attachment site. Successful expression of target genes in recombinant strains was confirmed by qRT-PCR.

3.3.4 RNA isolations

Total RNA was extracted from four replicates of 4-mL samples of *M. chelonae* strains at an OD_{600} of 1.0. Samples were harvested into 6-mL of RNAProtect Bacteria Reagent (Qiagen, Germantown, MD) and centrifuged at 5,000 x *g* for 10 min. Cell pellets were resuspended in 100 μL of Tris-ethylenediaminetetraacetic acid (TE) with 20 mg mL^{-1} of lysozyme and incubated at room temperature for 40 min. Cells were treated with 700 μL of RLT buffer (Qiagen) and transferred to 2-mL Lysing Matrix B tubes (MP Biomedicals, Irvine, CA). Samples were homogenized for 8 min at 50 Hz in a TissueLyser LT (Qiagen). RNA was isolated from cell lysates using the RNeasy Mini Kit (Qiagen) according to the manufacturer's instructions. A first DNase (Qiagen) treatment was performed on the columns. RNA was eluted in 50 μL of hot nuclease-free water before undergoing a second DNase treatment using the Turbo DNA-Free Kit (Thermo Scientific, Waltham, MA) according to the manufacturer's recommendations. RNA concentrations were measured using a NanoDrop ND-1000 spectrophotometer (NanoDrop Technologies, Montchanin, DE). RNA quality was assessed through gel electrophoresis using the RNA FlashGel System (Lonza, Rockland, ME) according to the manufacturer's instructions.

3.3.5 cDNA synthesis and qRT-PCR

cDNA was synthesized in 20-μL reactions containing 500 ng of total RNA using the qScript cDNA Supermix (Quantabio, Beverly, MA) according to the manufacturer's recommendations. Reactions were run under the following thermal cycle: 5 min at 25˚C, 20 min at 42˚C, and 5 min at 85˚C for inactivation. Working stocks of cDNA were prepared by diluting samples 1:6 in 10 mM Tris.

Primers for quantitative real-time PCR (qRT-PCR) assays were designed to amplify a 100-bp region with the gene of interest using Primer3 (**Table 3.4**). qRT-PCR assays were carried out in triplicate reactions in 25-μL volumes containing 200 nM of each primer, 1 μL of cDNA (diluted 1:6), and PerfeCTa SYBR Green Supermix (Quantabio) according to the manufacturer's instructions. Positive and no-template controls were included in each assay. Reactions were run using the Bio-Rad CFX96 Real-Time system (Bio-Rad Laboratories, Hercules, CA). Reactions were initially incubated for 3 min at 95˚C, followed by 40 cycles of 10 s at 95˚C and 30 s at 60˚C, and lastly a melt curve to confirm a single amplicon per target gene. Change in RNA abundance was normalized to *M. chelonae* 16S rRNA, and relative expression determined using the $2^{-\Delta\Delta CT}$ method (Livak et al., 2001).

Table 3.4 qRT-PCR primers used in this study.

Target	Primers	Sequence (5' to 3')
16S	16S_qPCR_F1	CCGGATAGGACCACACACTT
	16S_qPCR_R1	ATTACCCCACCAACAAGCTG
whiB7	whiB7_qPCR_F4	ACTTTCCGCGAACCACAG
	whiB7_qPCR_R1a	ATGATGACCGTCGAAGTGG
BPs gp5	gp5_qPCR_F1	GGTCAGAACGCCGAAATC
	gp5_qPCR_R1	CGTGAGCATCGTCTTGTACC
BPs gp33	gp33_qPCR_L (2)	GGCCCTTTTCCTTTTTCG
	gp33_qPCR_R (2)	TTCGTACCGCCTACTGATCG
BPs gp58	gp58_qPCR_F2	CCCGGTGGCACTATGACTAC
	gp58_qPCR_R2	GGTCCGTAGTGTTTGGTTGG

3.4 Results

3.4.1 Organization of the BPs and CLED96 genomes and gene expression profile of BPs in the *M. chelonae* double lysogen (BPs, McProf)

BPs is a temperate mycobacteriophage belonging to subcluster G1. Its genome spans 41,901 bp with a GC content of 66.6%, and it encodes 63 putative genes (Sampson et al., 2009). BPs is closely related to G1 phage, CLED96, which is nearly identical in sequence to BPs (a four-nucleotide difference) aside from lacking mycobacteriophage mobile element 1 (MPME1) (Sampson et al., 2009). BPs has a broad host range and is able to infect multiple mycobacterial species including *M. smegmatis*, *M. tuberculosis*, *M. abscessus*, and *M. chelonae* (Jacobs-Sera et al., 2012).

Genome organization follows the typical synteny of bacteriophage in linear orientation with structural and assembly components on the left arm followed by lysis and integration cassettes, and replication and recombination components on the right arm (Sampson et al.,

2009) (**Figure 3.2**). The lysis cassette includes gp27, gp28, and gp29, and encodes lysin A, lysin B, and holin, respectively. The integration cassette is downstream of this region, separated by two genes of unknown function. Gp32, gp33, and gp34 encode a tyrosine integrase, immunity repressor, and Cro, respectively. Lysogeny maintenance and the stability of cluster G immunity repressors is dependent upon phage genome integration into the bacterial genome (Broussard et al., 2013). The phage attachment site (*att*P) is located on the 3' end of the immunity repressor (Broussard et al., 2013; Villanueva et al., 2015) (**Figure 3.1**). Therefore, integration of the BPs genome into its host truncates the immunity repressor at the 3' end (Villanueva et al., 2015). This truncation results in translation of a functional repressor protein lacking the ssrA-like tag encoded on the C-terminus of gp33 that targets the protein for degradation (Villanueva et al., 2015). The BPs prophage integrates into a tRNA-Arg (BB28_RS01100) in *M. chelonae.* (McProf).

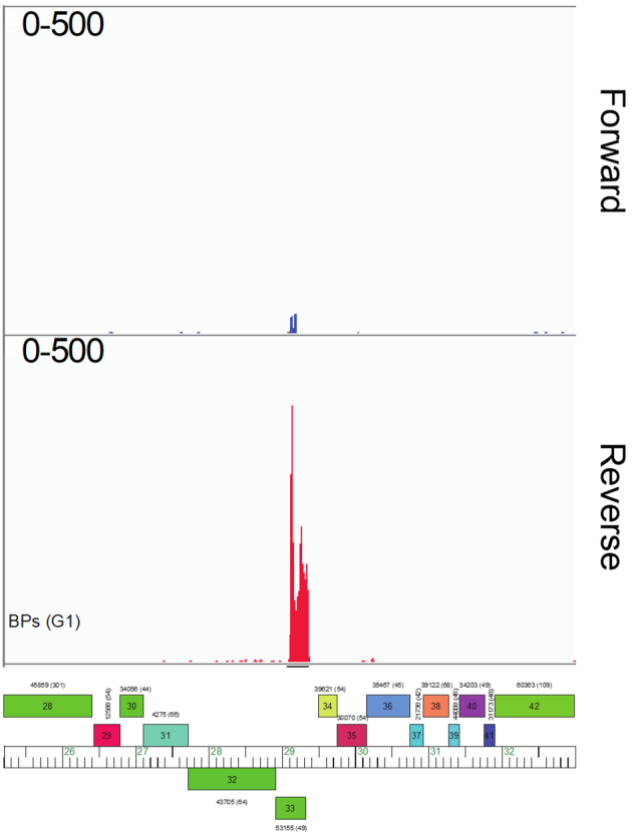

Figure 3.1 Phamerator map of the BPs integration cassette. The coordinates of the BPs genome are represented by the ruler. Genes are shown as colored boxes above (transcribed rightwards) or below (transcribed leftward) the ruler. RNAseq profiles are shown for forward (blue) and reverse (red) DNA strands. Note that the sequence reads are mapped to the viral BPs genome rather than prophage The map was generated using Phamerator (Cresawn et al., 2011).

Both BPs and CLED96 are able to form stable lysogens in *M. chelonae* WT. The efficiency of lysogeny was 25%, a significant increase compared to lysogens of *M. smegmatis* where efficiency is closer to 5% (Broussard et al., 2013). In addition, particle release from BPs lysogens of *M. chelonae* is low relative to BPs lysogens of *M. smegmatis*, measured at approximately 10^5 PFU mL^{-1} in *M. chelonae* lysogens compared to about 10^{10} PFU mL^{-1} in *M. smegmatis* lysogens.

RNAseq analysis of the BPs prophage in *M. chelonae* (McProf) showed that only two genes are highly expressed. As expected, the immunity repressor (gp33) was highly expressed. There was moderate expression from gp58, a gene of unknown function within a mycobacteriophage mobile element 1 (MPME1) (Sampson et al., 2009). Left arm genes, including gp5 and gp23 – 26 had low-level expression. Gp5 has no predicted function, although

HHpred analysis resulted in strong hits to a ribosome modulation factor (Zimmerman et al., 2018). Due to its location within an operon encoding structural genes, it is also likely functions in particle assembly and structure. Gp23 – 26 also do not have predicted functions, but their positioning between minor tail proteins and the lysis cassette suggests that they are also lytic genes. It is likely that the low number of reads mapping to gp5 and gp23 – 26 are a result of background lytic infection due to spontaneous induction in lysogen cultures.

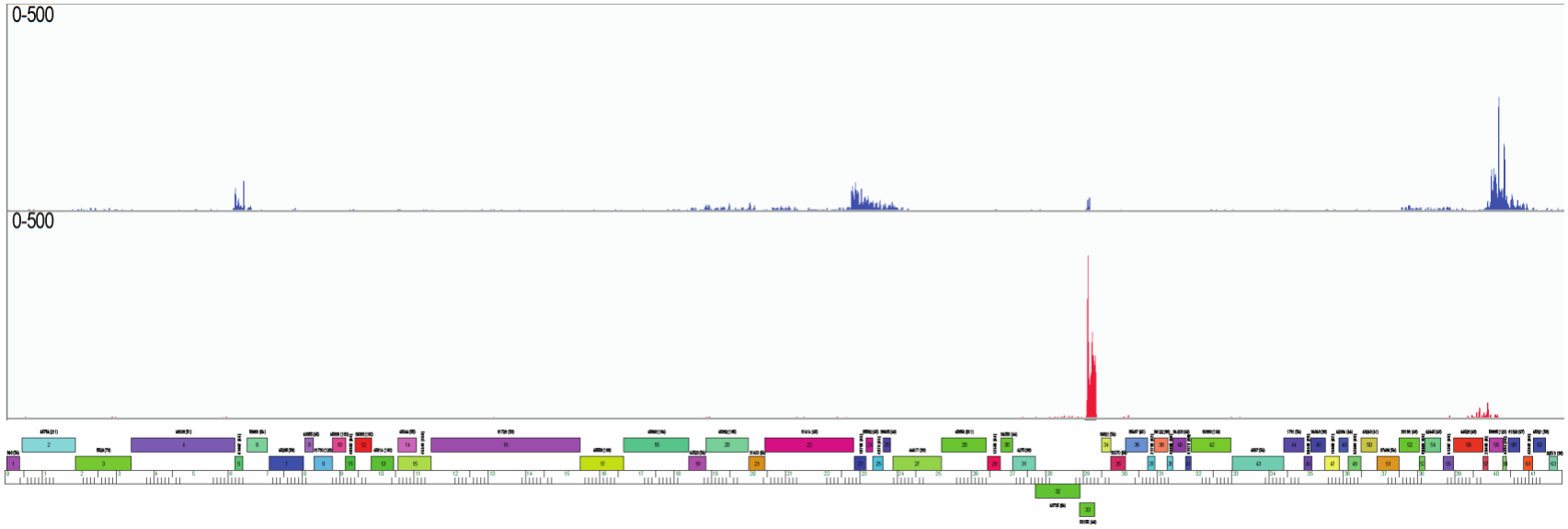

Figure 3.2 Phamerator map of the BPs genome. The coordinates of the genome are indicated by the ruler (kb). Colored boxes represent genes. Boxes above the ruler are rightward transcribed and those below the ruler are leftward transcribed. RNAseq reads are mapped to the viral genome of BPs. The number of reads mapped are indicated on the y-axis. The lysogenic gene expression profile, as determined by RNAseq is represented by blue (rightward transcribed genes) and red bars (leftward transcribed genes). The map was generated using Phamerator (Cresawn et al., 2011).

3.4.2 BPs gp5 does not drive changes in *whi*B7 expression

Since we observed a significant increase in *whi*B7 expression in *M. chelonae* (BPs, McProf) relative to the wildtype strain carrying McProf only, we decided to explore the impact of BPs lysogenic genes expressed in the double lysogen on *whi*B7 expression in the presence of prophage McProf, beginning with gp5.

BPs gp5 is located on the left arm of the phage genome within a region that encodes structural genes that are typically only expressed during lytic growth. However, there is no known function associated with this gene. Analysis of the protein coding sequence by blastP indicated relation to a ribosome modulation factor identified in *E. coli* and *T. thermophilus* with 69% coverage. Ribosome modulation factors can promote translation of leaderless transcripts (Beck and Moll, 2018). Leaderless transcripts are translated by pre-formed 70S ribosomes that bind directly to AUG start codons, protecting the transcripts from degradation (Sawyer et al., 2018; Beck and Moll, 2018). Nearly one quarter of mycobacterial transcriptomes are leaderless, meaning ribosome binding does not occur at a ribosome binding site upstream of the transcript start site (Canestrari et al., 2020). Since mycobacteria regularly translate leaderless mRNAs and therefore carry pre-formed 70S ribosomes, it is possible that expression of gp5 aids in stabilization of leaderless transcripts. This may alter mRNA levels of bacterial genes that could leads to an increase in expression of *whi*B7 and its associated antibiotic resistance genes.

To investigate the role of gp5 on *whi*B7 expression, we constructed an overexpression vector, pMOgp5, and isolated RNA from recombinant strains of *M. chelonae* carrying the overexpression and control vectors. The gp5 ORF was cloned into pMO21 subclone vector carrying a constitutive Hsp60 promoter (pMOHsp). This vector encodes a phage parABS system

that allows for maintenance of the plasmid in the absence of antibiotic selection (Dedrick et al., 2016). Recombinant and control strains were generated by introducing pMOgp5 and pMOHsp respectively into *M. chelonae* (McProf).

To ensure that gp5 was being expressed from our recombinant strains, we used qRT-PCR to measure levels of gp5 transcript in recombinant strains and compared this to gp5 expression levels in the double lysogen. *M. chelonae* carrying pMOgp5 expressed gp5 at a level more than 20,000-fold higher than *M. chelonae* (BPs, McProf) (**Figure 3.3a**). Overexpression of gp5 however did not affect *whi*B7 expression in the recombinant strain. *M. chelonae* overexpressing BPs gp5 demonstrated no significant difference in *whi*B7 expression compared to the empty vector control strain, and approximately 60-fold lower expression relative to *M. chelonae* (BPs, McProf) (**Figure 3.3b**).

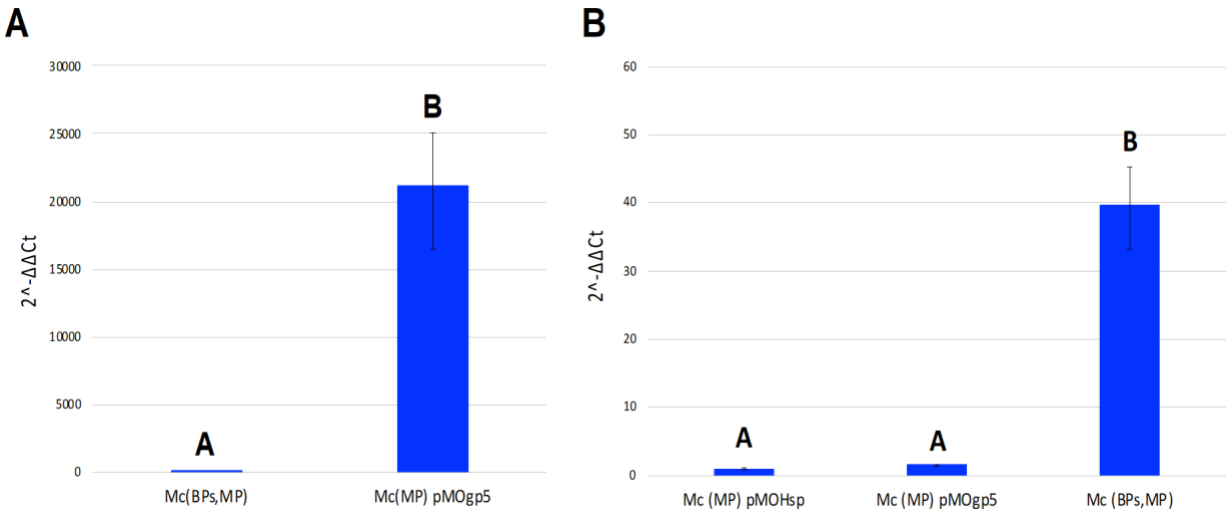

Figure 3.3 qRT-PCR analysis of recombinant *M. chelonae* (McProf) strains expressing BPs gp5. The average relative expression levels of BPs gp5 in *M. chelonae* (BPs, McProf) and *M. chelonae* (McProf) (pMOgp5) (**A**) and *whi*B7 in *M. chelonae* (McProf) (pMOHsp), *M. chelonae* (McProf) (pMOgp5), and *M. chelonae* (BPs, McProf) (**B**) as measured with SYBR Green qRT-PCR. Cultures were grown to an OD_{600} of 1.0 before harvesting RNA in triplicate. Graphs represent average values ± standard error of the mean with n=3 and are representative of two independent trials. Means with different letters are significantly different (Tukey's HSD, α=0.05).

3.4.3 BPs gp33 does not drive changes in *whi*B7 expression

The immunity repressor, gp33, is the most highly expressed gene in the BPs prophage. This is expected since phage repressors inhibit expression of genes associated with lytic replication while in a lysogenic state (Dedrick et al., 2013; Petrova et al., 2015). Given that repressors possess DNA binding capabilities, we wondered whether gp33 could modulate bacterial gene expression as well, resulting in upregulation of *whi*B7. To investigate this, we generated a recombinant strain of *M. chelonae* (McProf) (pMHIR) that encodes the BPs immunity repressor (**Table 3.2**).

We modified the integrative vector, pMH94, by removing the L5 integration cassette and replacing it with the BPs integration cassette (Lee et al., 1991). Plasmid pMHIR encodes the BPs integrase (gp32), the *att*P site, the entire immunity repressor (gp33) and the upstream region including the native promoter. As a control, we constructed an additional vector, pMHIattP, which encodes the integrase and attP site, but lacks the 5' end of the immunity repressor. pMHIR and pMHIattP were electroporated into *M. chelonae* (McProf). Vector integration allowed for plasmid maintenance in the absence of antibiotics.

Expression of gp33 in recombinant *M. chelonae* (McProf) carrying pMHIR was confirmed by qRT-PCR and did not differ from that of the double lysogen (BPs, McProf) (**Figure 3.4a**). *whi*B7 expression was then assessed by qRT-PCR (**Figure 3.4b**). BPs gp33 did not significantly alter *whi*B7, with near identical expression between the pMHIR strain and pMHIattP control strain. Additionally, *whi*B7 expression was approximately 50 times greater in *M. chelonae* (BPs, McProf), suggesting that the BPs repressor alone does not contribute to upregulation of *whi*B7 observed in the double lysogen strain.

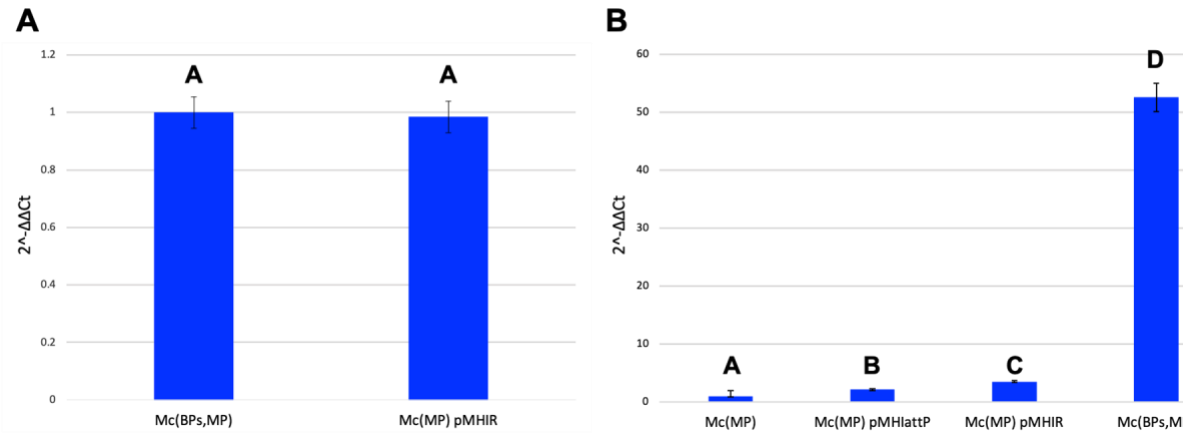

Figure 3.4 qRT-PCR analysis of recombinant *M. chelonae* (McProf) strains expressing BPs gp33. The average relative expression levels of BPs gp33 in *M. chelonae* (BPs, McProf) and *M. chelonae* (McProf) (pMHIR) (**A**) and *whi*B7 in *M. chelonae* (McProf), *M. chelonae* (McProf) (pMHIattP), *M. chelonae* (McProf) (pMHIR), and *M. chelonae* (BPs, McProf) (**B**) as measured with SYBR Green qRT-PCR. Cultures were grown to an OD_{600} of 1.0 before harvesting RNA in triplicate. Graphs represent average values ± standard error of the mean with n=3 and are representative of two independent trials. Means with different letters are significantly different (Tukey's HSD, α=0.05).

3.4.4 Co-expression of BPs gp5 and gp33 does not drive changes in *whi*B7 expression

Since BPs gp5 and gp33 did not impact *whi*B7 when expressed individually, we explored whether co-expression of these genes have an effect on *whi*B7 expression. The gp33 transcript appears to be leaderless, so we wondered if gp5 enhances production of repressor protein (Broussard et al., 2013).

The pMOgp5 overexpression vector was transformed into the recombinant strain o*f M. chelonae* (McProf) expressing gp33 from pMHIR. RNA was isolated from *M. chelonae* (McProf) (pMHIR, pMOgp5) and gp33 expression was compared to that of *M. chelonae* (BPs, McProf) and *M. chelonae* (McProf) (pMHIR) by qRT-PCR (**Figure 3.5a**). Interestingly, gp33 expression was slightly higher in the strain carrying both pMHIR and pMOgp5 relative to *M. chelonae* (BPs,

McProf) and the strain carrying pMHIR alone. We then determined relative *whi*B7 expression in these strains and found that expression was not significantly upregulated in the co-expression strain compared *to M. chelonae* (BPs, McProf) (**Figure 3.5b**). *whi*B7 expression was approximately 35-fold higher in the double lysogen. There was not a discernable difference in *whi*B7 expression between *M. chelonae* (McProf) (pMHIR, pMOgp5) and *M. chelonae* (McProf) (pMHIR). Overexpression of gp5 increased expression of gp33. However, this did not lead to altered *whi*B7 expression, indicating that gp33 does not play a role in the regulation of *whi*B7.

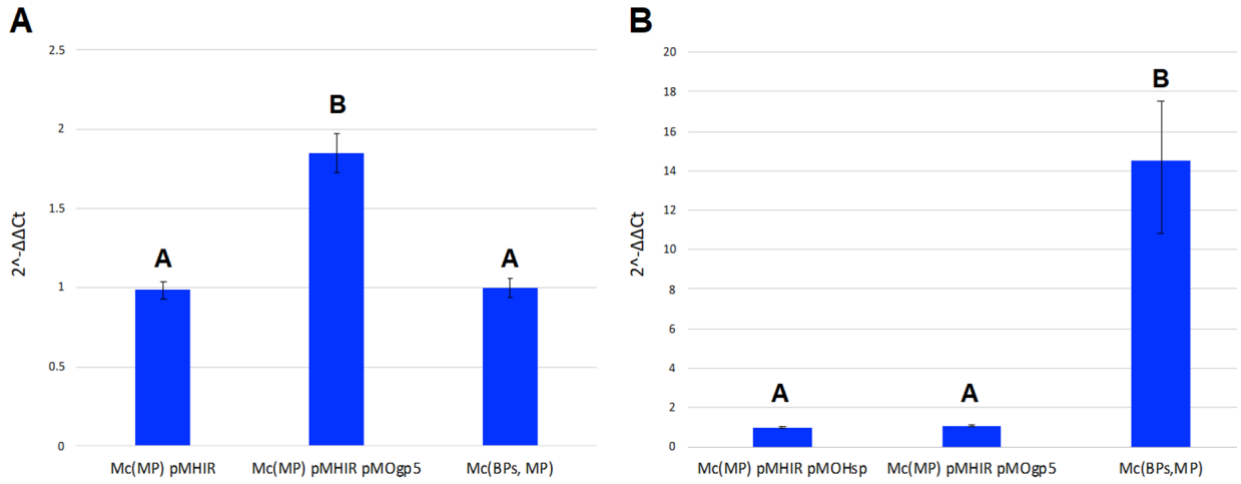

Figure 3.5 qRT-PCR analysis of recombinant *M. chelonae* (McProf) strains co-expressing BPs gp5 and gp33. The average relative expression levels of BPs gp33 in *M. chelonae* (McProf) (pMHIR), *M. chelonae* (McProf) (pMHIR, pMOgp5), and *M. chelonae* (McProf, BPs) (**A**) and *whi*B7 in *M. chelonae* (McProf) (pMHIR, pMOHsp), *M. chelonae* (McProf) (pMHIR, pMOgp5), and *M. chelonae* (BPs, McProf) (**B**) as measured with SYBR Green qRT-PCR. Cultures were grown to an OD_{600} of 1.0 before harvesting RNA in triplicate. Graphs represent average values ± standard error of the mean with n=3 and are representative of two independent trials. Means with different letters are significantly different (Tukey's HSD, α=0.05).

3.4.5 BPs gp58 does not drive changes in *whi*B7 expression

While the role of BPs gp58, encoded by MPME1, is unknown, its significant expression and potential to be a DNA binding protein made it worth investigating as a potential mediator of bacterial gene expression. Similar to gp5, we developed a recombinant strain of *M. chelonae* (McProf) expressing the gp58 ORF from the plasmid pMO21 to generate *M. chelonae* (McProf) (pMOgp58). We also generated a strain carrying the plasmid, pMOgp57 – 58, which lacks the Hsp60 promoter but encodes the entire MPME1 sequence to include its native promoter (**Table 3.2**). To determine if increased *whi*B7 expression occurs in double lysogens that lack gp58, we created a lysogen of *M. chelonae* (McProf) using cluster G1 phage, CLED96, which is nearly identical in sequence to BPs but lacks MPME1.

RNA was isolated from each strain and gp58 expression was confirmed by qRT-PCR (**Figure 3.6a**). Expression of gp58 from pMOgp58 was over 2,000-fold higher relative to *M. chelonae* (BPs, McProf) and expression of gp58 from pMOgp57 – 58 was comparable to the double lysogen. Relative expression of *whi*B7 was then measured (**Figure 3.6b**). *whi*B7 expression did not significantly differ between the control strain *M. chelonae* (McProf) (pMOHsp) and *M. chelonae* (McProf) strains expressing gp58 from the Hsp60 promoter (pMOgp58) or from the MPME1 promoter (pMOgp57 – 58). Expression of *whi*B7 was approximately 40-fold higher in *M. chelonae* (BPs, McProf) compared to gp58 expression strains. Interestingly, *M. chelonae* (CLED96, McProf) demonstrated a 10-fold increase in *whi*B7 expression relative to the gp58 expression and control strains but was still significantly lower compared to *M. chelonae* (BPs, McProf).

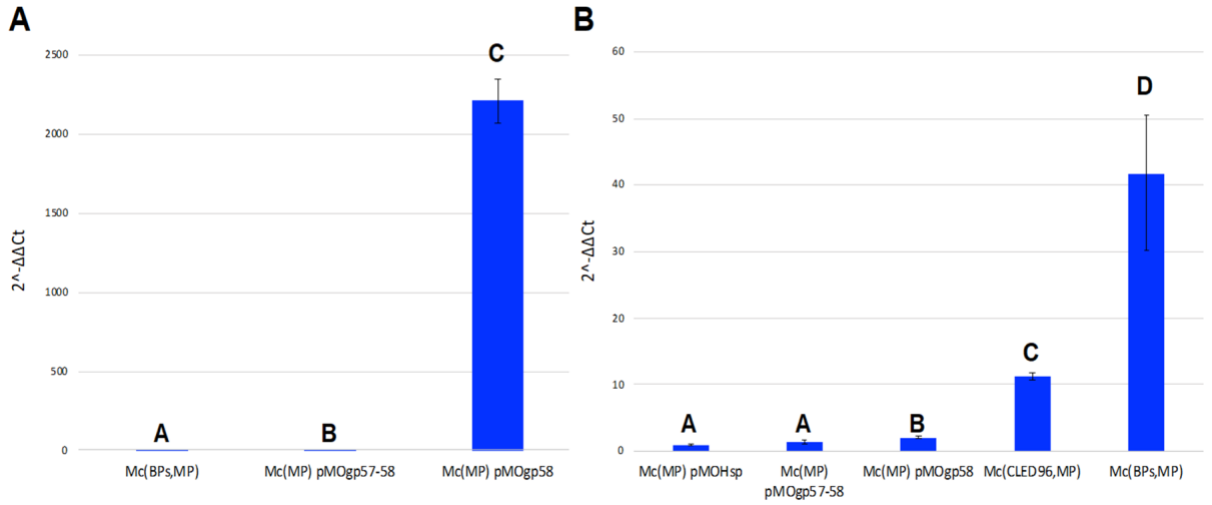

Figure 3.6 qRT-PCR analysis of recombinant *M. chelonae* (McProf) strains expressing BPs gp58. The average relative expression levels of BPs gp58 in *M. chelonae* (BPs, McProf) *M. chelonae* (McProf) (pMOgp57 – 58), and *M. chelonae* (McProf) (pMOgp58) (**A**) and *whi*B7 in *M. chelonae* (McProf) (pMOHsp), *M. chelonae* (McProf) (pMOgp57 – 58), *M. chelonae* (McProf) (pMOgp58), *M. chelonae* (CLED96, McProf), and *M. chelonae* (BPs, McProf) (**B**) as measured with SYBR Green qRT-PCR. Cultures were grown to an OD_{600} of 1.0 before harvesting RNA in triplicate. Graphs represent average values ± standard error of the mean with n=3 and are representative of two independent trials. Means with different letters are significantly different (Tukey's HSD, α=0.05).

3.5 Discussion

The prevalence of non-tuberculous mycobacterial disease has been steadily increasing in recent years. Treatment of these diseases, specifically *M. abscessus* infections, is difficult to manage due to extreme intrinsic drug resistance, posing a major health threat (Johansen et al., 2020). Further, emergence of extensively antibiotic resistant isolates of *M. abscessus* has rendered successful clearance of disease nearly impossible (Johansen et al., 2020). Extensive resistance in some *M. abscessus* strains can be attributed to mutations in 16S or 23S rRNA, the targets for aminoglycosides and macrolides respectively. However, mutations do not account for extensive resistance observed in all clinical isolates (Guo et al., 2020). Common among

extensively resistant *M. abscessus* strains is upregulation of transcriptional activator, *whi*B7, which regulates many genes associated with antibiotic resistance and stress adaptation (Guo et al., 2020; Morris et al., 2005; Burian et al., 2012). While *whi*B7 expression is known to be induced by stress conditions such as sub-lethal drug exposure, phage infection, and the intracellular environment of macrophages, the cause of upregulation in extensively resistant *M. abscessus* remains unknown (Cushman et al., 2021; Burian et al., 2012). Better understanding mechanisms of drug resistance in pathogenic mycobacteria is essential for developing more effective treatments.

We recently reported on the novel observation that phage infection impacts *whi*B7 expression in mycobacteria. The presence of prophage BPs increases expression of *whi*B7 in *M. chelonae*, but only in strains carrying the naturally occurring prophage, McProf. This suggests that an interaction between BPs and McProf triggers an upregulation of *whi*B7 (Cushman et al., 2021). McProf is only able to carry out lysogenic infection in *M. chelonae*. However, it appears that BPs carries out both lytic infection and lysogenic infection in a population of *M. chelonae* (BPs, McProf) cells (Cushman et al., 2021). It is unclear whether lytic or lysogenic BPs gene expression alters *whi*B7 expression in the presence of McProf. Here we describe the role of BPs lysogenic gene products on *whi*B7 expression in strains of *M. chelonae* carrying the McProf prophage.

The function of gp5 is unknown, but HHpred analysis showed strong hits to a ribosome modulation factor (Zimmerman et al., 2018). Ribosome modulation factors have the potential to alter ribosome populations and subsequently alter gene expression at the translational level.

Regardless of its true function, gp5 does not appear to contribute to increased *whi*B7 expression (**Figure 3.3b**).

The immunity repressor, gp33, is the most highly expressed gene from BPs and as a DNA binding protein, was a likely candidate for altering bacterial gene expression. High expression of the immunity repressor is expected given its role in preventing expression of lytic genes (Petrova et al., 2015). We attempted to overexpress gp33 in *M. chelonae* (McProf) using a pMOHsp backbone, which allows for maintenance of the plasmid through a ParABS system in the absence of antibiotic selection (Dedrick et al., 2016). However, the gp33 recombinant pMOHsp vector proved to be highly unstable and appeared to be lethal to bacterial cells. As an alternative, we engineered the integrative plasmid, pMH94, to express the BPs repressor and integration cassette from its native promote in place of the original L5 integration cassette. Our analysis suggested that expression of gp33 alone in *M. chelonae* (McProf) does not significantly change *whi*B7 expression (**Figure 3.4b**). Since gp33 is expressed as a leaderless transcript (Broussard et al., 2013), we wondered if gp5 expression was necessary to facilitate translation of gp33 by stabilizing the population of pre-formed 70S ribosomes. We co-expressed gp5 and gp33 in *M. chelonae* (McProf) but found that *whi*B7 expression was not altered under these conditions (**Figure 3.5b**). However, gp33 expression was nearly doubled in the co-expression strain relative to *M. chelonae* (BPs, McProf) (**Figure 3.5a**). This suggests that when expressed at a high level, gp5 may somehow enhance expression of gp33, potentially as a ribosome modulation factor that aids in stabilization of leaderless transcripts by recruiting 70S ribosomes to the 5’ end of transcripts to prevent degradation (Beck and Moll, 2018). This could explain

increased gp33 transcript detected in *M. chelonae* (McProf) cells carrying both pMHIR and pMOgp5.

While gp33 does not appear to impact *whi*B7 expression in *M. chelonae*, it is possible that it has an alternate role in regulating bacterial gene expression. Gp33 functions as a repressor by binding a 12-bp conserved palindromic sequence (5'- CGACATATGTCG - 3') upstream of lytic genes to block the binding of transcriptional machinery and prevent lytic gene expression during lysogenic infection (Villanueva et al., 2015). We identified eight related sequences within the regulatory region of the *M. chelonae* genome that could potentially serve as gp33 binding sites. Of interest are three binding sites located upstream of a *pad*R-like transcription factor, which is the second most downregulated gene in *M. chelonae* (BPs, McProf) (Cushman et al., 2021). The function of this transcription factor in *M. chelonae* is unknown, but *pad*R has been reported to regulate genes involved in stress responses, including those involved in antibiotic resistance, often by serving as a repressor in other bacterial species (Park et al., 2017; Vatlin et al., 2018). It is possible that gp33 inhibits *pad*R expression and subsequently results in de-repression of *pad*R-mediated genes in *M. chelonae* to alter antibiotic resistance. However, the relationship between gp33 and *pad*R in altering genotype and antibiotic resistance phenotype in *M. chelonae* would need to be investigated further.

BPs gp58 is moderately expressed and is encoded by mycobacteriophage mobile element 1 (MPME1) (Sampson et al., 2009). We generated two plasmid constructs to investigate the role of gp58 on *whi*B7: one overexpression vector and one vector carrying the native promoter for gp58. Additionally, we analyzed *whi*B7 expression in *M. chelonae* (CLED96, McProf). This essentially served as a gp58 deletion mutant since the genome of CLED96 is

nearly identical to BPs aside from a four-nucleotide difference and its lack of MPME1. Overexpression of gp58 did result in a statistically significant upregulation of *whi*B7 relative to the control strain at a 2-fold increase but was still nearly 40-fold lower than that observed in *M. chelonae* (BPs, McProf). Interestingly, the presence of the CLED96 prophage in *M. chelonae* (McProf) increased *whi*B7 expression by about 10-fold but was still significantly lower than the relative expression seen in *M. chelonae* (BPs, McProf) (**Figure 3.6b**). It is possible that background lytic infection in double lysogens, regardless of whether the second prophage is BPs or CLED96, could trigger an upregulation of *whi*B7 in the presence of McProf, but that another interaction is necessary to see the ~40-fold increase in *whi*B7 expression observed in *M. chelonae* (BPs, McProf). This suggests that while gp58 alone does not alter *whi*B7 expression, it may cooperatively interact with other factors to upregulate *whi*B7. This is evident by the 30-fold drop in *whi*B7 expression when MPME1 is absent, but the rest of the prophage remains intact, as seen in *M. chelonae* (CLED96, McProf) compared to the BPs double lysogen. We do not know the function of gp58, but it is possible that it possesses recombinase activity given that it is the only gene encoded on MPME1. If this is true, it is possible that gp58 has DNA binding potential and could interact with other BPs genes to alter bacterial gene expression. Given that *whi*B7 expression is known to fluctuate in a cell density-dependent manner, RNA isolations and qRT-PCR analysis should be repeated to confirm the impact of the CLED96 prophage on *whi*B7 expression in *M. chelonae* (McProf).

This work has allowed us to conclude that while both prophages, BPs and McProf, must be present to induce a drastic upregulation of *whi*B7, individual BPs genes do not interact with McProf to cause this effect. This implies that McProf may play a more important role in the

interaction between these two phages. Therefore, the impact of McProf viral gene products in the presence of BPs needs to be investigated to better understand *whi*B7 induction and increased antibiotic resistance in *M. chelonae* (BPs, McProf). In addition, the role of BPs lytic infection on *whi*B7 expression in *M. chelonae* (McProf) cells should be explored.

CHAPTER 4

DETERMINING THE ROLE OF THE MCPROF POLYMORPHIC TOXIN CASSETTE ON *WHI*B7 EXPRESSION AND ANTIBIOTIC RESISTANCE IN *MYCOBACTERIUM CHELONAE*

4.1 Chapter Summary

Mycobacterium abscessus is a nontuberculous pathogen associated with lung and disseminated infections. It is of growing concern due to its steady increase in incidence over the last decade (Griffith, 2019; Johansen et al., 2020) and the emergence of extensively drug resistant strains that have hindered effective treatment (Griffith, 2019). The majority of pathogenic mycobacteria carry integrated bacteriophage genomes (prophage) that are hypothesized to contribute to mycobacterial fitness and virulence (Fan et al., 2015). How prophage impact bacterial fitness, particularly when they don't encode an obvious virulence factor, is not understood.

M. chelonae is a member of the *M. abscessus*/*M. chelonae* complex which carries a naturally occurring prophage, McProf, that we hypothesize plays a role in mycobacterial fitness and antibiotic resistance of the host. *M. chelonae* carrying the prophage McProf were significantly more resistant to aminoglycosides relative to strains that lacked McProf (Cushman et al. 2021). Aminoglycoside resistance was further enhanced by the addition of a second prophage, BPs. RNAseq analysis of this strain, *M. chelonae* (BPs, McProf), showed drastic changes in bacterial gene expression relative to strains carrying only McProf, only BPs or no prophage. In the double lysogen strain (BPs, McProf) there was significant upregulation of *whi*B7, a conserved mycobacterial transcriptional activator that regulates genes associated with antibiotic resistance and stress adaptation (Morris et al., 2005; Burian et al., 2012; Cushman et

al., 2021). The role of BPs lysogenic gene products was evaluated and did not appear to alter *whi*B7 expression. There are numerous genes expressed from the McProf genome in the double lysogen but strong gene candidates for regulating bacterial genes involved in the stress response is a McProf-encoded polymorphic toxin system. To investigate the role of the polymorphic toxin system on *whi*B7 regulation and amikacin resistance, we constructed a strains of *M. chelonae* (ΔMcProf) that encodes three genes from the McProf putative Esx secreted polymorphic toxin (PT) system with and without the prophage BPs. qRT-PCR analysis demonstrated a 10-fold upregulation of *whi*B7 expression in the recombinant strain carrying BPs relative to control strains, indicating that the McProf PT cassette plays a role in *wh*iB7 expression levels when BPs is present. However, *whi*B7 expression levels were more than four times lower than that observed in the double lysogen (BPs, McProf). An increase in AMK resistance was not observed in recombinant strains. Taken together, these data suggest high *whi*B7 expression may require additional interactions between BPs and the naturally occurring prophage, McProf. Identifying prophage-encoded factors that contribute to drug resistance will be important in developing alternative treatment strategies for mycobacterial infections.

4.2 Introduction

Mycobacterial disease is the second leading cause of death by an infectious agent behind COVID-19 (WHO, 2020). Increasing prevalence of multi-drug resistant (MDR) strains has rendered previous treatment options ineffective**.** *M. abscessus* is a rapidly emerging nontuberculous pathogen that is primarily responsible for pulmonary infections but can also cause disseminated disease. It is a major contributor to mortality among cystic fibrosis patients and other immunocompromised individuals (Griffith, 2019). Currently, the only effective

treatment option consists of a combination therapy using amikacin and clarithromycin for as long as 2 years with harsh side effects (Hurst-Hess et al., 2017). Many strains have become extensively resistant, or resistant to all available drugs. In some cases, mutations in drug targets have been identified that cause this extensive resistance. However, the cause in many extensively resistant strains remains unknown, making treatment essentially impossible (Guo et al., 2020).

M. abscessus carries a broad range of antibiotic resistance genes that encode drug efflux pumps and proteins that modify either drug targets or the antibiotics themselves, resulting in inactivation (Johansen et al., 2020). Transcriptional activator, *whi*B7, regulates many of these genes associated with antibiotic resistance (Morris et al., 2005; Burian et al., 2012). Common among all extensively resistant clinical isolates of *M. abscessus* is increased expression of *whi*B7 compared to wild-type strains which may explain increased drug resistance (Burian et al., 2013; Hurst-Hess et al., 2017; Guo et al., 2020). *whi*B7 is known to be upregulated in the presence of environmental stressors, including the intracellular environment of a macrophage and subinhibitory drug exposure (Morris et al., 2005; Burian et al., 2012). Extensively resistant isolates exhibit this same upregulation without exposure to drug treatment or macrophage. What triggers this increased expression of *whi*B7 in the absence of cell stress is not understood

The majority of MDR strains identified to date also carry one or more integrated viral genomes, or prophage. Cells carrying prophage are called lysogens. Nearly all pathogens carry prophage that are known to contribute to fitness and virulence (Brussow et al., 2004; Wang et al., 2016). In some models, the role and mechanism of prophage impact is clear. This is the case with *E. coli* 0157:H7. This strain, responsible for enterohemorrhagic disease, is pathogenic due

to a toxin encoded by the Stx prophage (Kaper et al., 2004). In other models, the role is of prophage clear, but the mechanism is not understood. *E. coli* K12 carries 9 prophages. Research showed that as the number of prophages decreased through a series of curing experiments, so did resistance to antibiotics. The strain lacking all prophages was most susceptible to drugs (Wang et al., 2010). This work shows that there is a link between prophage and increased antibiotic resistance, however what this link is remains to be investigated. The majority of mycobacterial pathogens also carry prophage, and they are hypothesized to play a role in virulence yet remain largely uninvestigated (Fan et al., 2014; Fan et al., 2015; Bibb and Hatfull, 2002). Identifying the role of prophage in mediating intrinsic antibiotic resistance will provide insight for developing new and more effective therapies for mycobacterial disease.

M. chelonae is a very close relative of *M. abscessus*, sharing greater than 80% of protein-coding sequences. However, *M. chelonae* is a safer alternative to work with while still demonstrating characteristics of pathogenic mycobacteria (Morris et al., 2005; van Ingen et al., 2009; Jaen-Luchoro et al., 2016). This makes *M. chelonae* an effective model for studying the conserved mycobacterial WhiB7 regulon. We have shown that when *M. chelonae*, which carries a naturally occurring prophage, McProf, is infected with a second prophage, BPs, both *whi*B7 expression and antibiotic resistance is significantly increased (Cushman et al., 2021). We characterized the BPs and McProf prophages and investigated the role of BPs lysogenic gene products on *whi*B7 expression. We found that *whi*B7 expression was not significantly altered when individual BPs lysogenic genes were expressed in the presence of McProf, indicating that McProf must play a larger role in inducing this resistant phenotype.

The McProf prophage expresses 16 genes, of which the majority have no known function (Cushman et al., 2021). There is strong expression from a gene cassette located on the rightmost arm of the genome characterized as an ESX-secreted polymorphic toxin (PT) system that we predict is secreted by a mycobacterial type 7 secretion system (T7SS). Polymorphic toxin (PT) systems include a large multidomain PT protein with an N-terminal domain that allows export and/or delivery to other cells and a C-terminus toxin domain that targets cellular processes (DNAses, RNAses, NADases, etc) (Ruhe et al., 2020). Downstream of the PT gene is an immunity protein that neutralizes the toxin domain and prevents self-intoxication (Ruhe et al., 2020). Polymorphic toxins are secreted or delivered directly to adjacent cells, potentially providing a beneficial interaction in cells carrying the immunity protein such as sharing of nutrients and induction of cell signaling pathways (Wood et al., 2020; Garcia et al., 2016; Zhang et al., 2018). Alternatively, absence of an associated immunity protein results in cell death. The PT system of McProf is similar to PT systems described by Dedrick et al. (2021) in *M. abscessus* prophages and include a small ESAT6-like protein with a WXG-100 motif, a PT protein with a WXG-100 motif in the N-terminus followed by an immunity protein. The WXG-100 domains may allow formation of heterodimers between the ESAT6-like protein and the PT prior to export (Dedrick, 2021). McProf gp98 appears to encode the ESAT6-like protein which we are calling a WXG-100 family protein. Gp97 is a predicted Tde-like polymorphic toxin that was first characterized in *Agrobacterium tumefaciens* and likely exhibits DNase activity (Ma et al., 2018). Gp97 includes a WXG-100 motif, characteristic of T7SS substrates, and a potential T7SS secretion signal (YxxxD/E) in the N and C terminus respectively (Daleke et al., 2012). Gp96 encodes a predicted Tdi-like immunity protein that is typically paired with Tde polymorphic

toxins (Ma et al., 2014). RNAseq analysis showed that these genes were not differentially expressed in *M. chelonae* (BPs, McProf) relative to wildtype (McProf only) (Cushman et al., 2021).

Toxin systems are activated by danger signals such as phage infection and drug exposure, similar to *whi*B7, and may play a role in stress adaptation (Kumar et al., 2019; Morris et al., 2005; Burian et al., 2012; Cushman et al., 2021). It is therefore possible that an active McProf-encoded PT system could trigger a WhiB7 stress response. Other stress adaptation systems such as toxin/antitoxin (TA) systems encoded by prophage have been shown to increase resistance and persistence in the presence of antibiotics. In *E. coli,* prophage-encoded TA pair RalR/RalA increases resistance to broad-spectrum fosfomycin and the RelE toxin of prophage Qin leads to persistence in the presence of ciprofloxacin, ampicillin and tobramycin (Christensen et al., 2001; Guo et al., 2014; Neubauer et al., 2009). Additionally, prophage-encoded TA systems have been shown to mediate biofilm formation, stabilize mobile elements such as plasmids and prophages, and confer abortive infection (Wang et al., 2011; Yao et al., 2018; Fraikin et al., 2020; Wozniak et al., 2009; Dedrick et al., 2017). Toxin systems are abundant in pathogenic mycobacteria relative to nonpathogens and are highly expressed in especially virulent strains of *M. tuberculosis* (Kumar et al., 2019; Slayden et al., 2018). Further, diverse prophage-encoded PT systems have been identified in 25 *M. abscessus* prophages with close relation to McProf, as well as an additional 50 across 14 other Mab clusters, although their functions are largely unexplored (Molloy, Unpublished; Dedrick et al., 2021). The role of PT systems in mycobacterial drug resistance has not yet been described.

In this study we constructed recombinant strains of *M. chelonae* (ΔMcProf) with and without the prophage BPs to express the McProf PT cassette (gp96 – 98). We investigated the role of the PT cassette on BPs prophage stability and measured *whi*B7 expression and amikacin resistance in recombinant and control strains in the presence and absence of the BPs prophage.

4.3 Materials and Methods

4.3.1 Bacterial and viral strains

Mycobacterium chelonae (ATCC®35752, American Type Culture Collection, Manassas, VA) was grown in liquid Middlebrook 7H9 broth (BD, Sparks, MD) supplemented with 10% oleic acid, albumin, dextrose (OAD) and 0.05% Tween 80 at 30˚C with shaking at 230 RPM. The wildtype strain of *M. chelonae* carries a naturally occurring prophage, McProf, and will be referred to as *M. chelonae* (McProf). *M. smegmatis* MC^2155 (ATCC®700084, American Type Culture Collection) was cultivated in the same media in the absence of Tween 80 and grown at 37˚C with shaking. Kanamycin (KAN) was used as a selective measure for recombinant strains, at a concentration of 250 μg mL^{-1} in liquid and solid media. Competent *E. coli* DH5 cells were prepared by New England Biolabs, (Ipswich, MA) and grown in Luria broth base, Miller (BD) supplemented with 50 μg mL^{-1} of KAN at 37˚C with shaking at 230 RPM for propagation of plasmids. Bacterial strains used in this work are listed in **Table 4.1.** Plasmids used in this study are listed in **Table 4.2**.

Mycobacteriophage BPs was obtained from the Hatfull Laboratory (Sampson et al., 2009) and cultivated by plaque assay using *M. chelonae* (McProf) or *M. smegmatis* MC^2155. Serially diluted phage samples were incubated for 15 min at room temperature in 0.5-ml aliquots of late log phase bacteria. Aliquots were plated in 4.5 ml of 7H9 top agar (0.45% agar) onto 7H10

agar plates. High titer phage lysate stocks were generated by flooding bacterial lawns with nearly confluent lysis with phage buffer (10 mM Tris/HCl pH 7.5, 10 mM $MgSO_4$, 1 mM $CaCl_2$, 68.5 mM NaCl). Viral strains used in this study are listed in **Table 4.1**.

Table 4.1 Bacterial and viral strains used in this study.

Bacterial Strains	Strain Description	Source
Escherichia coli		
DH5α	Supercompetent cells	NEB
Mycobacterium chelonae		
Non-lysogen (ΔMcProf)	Mutant strain of *M. chelonae* ATCC 35752 lacking prophage McProf	Cushman et al., 2021
Single lysogen (BPs)	BPs lysogen of *M. chelonae* (ΔMcProf)	Cushman et al., 2021
Single lysogen (McProf)	*M. chelonae* ATCC 35752 with naturally-occurring prophage, McProf	ATCC
Double lysogen (BPs, McProf)	BPs lysogen of *M. chelonae* ATCC 35752	Cushman et al., 2021
Mycobacterium smegmatis		
MC^2155	*M. smegmatis* ATCC 700084	ATCC

Viral Strains	Virus Description	Source
BPs	Cluster G mycobacteriophage	Sampson et al., 2009

Table 4.2 Plasmids used in this study.

Plasmid Name	Vector	Phage Genes	Genome Coordinates	Description
pMHESX	pMH94	McProf gp96 – 98	63,600 – 68,223	Integration-dependent pMH94 subclone carrying the McProf ESX-like polymorphic toxin cassette with its native promoter.

4.3.2 RNA isolation

Total RNA was extracted from four replicates of 4-mL samples of *M. chelonae* strains at an OD_{600} of 1.0. Samples were harvested into 6-mL of RNAProtect Bacteria Reagent (Qiagen,

Germantown, MD) and centrifuged at 5,000 x *g* for 10 min. Cell pellets were resuspended in 100 μL of Tris-ethylenediaminetetraacetic acid (TE) with 20 mg mL^{-1} of lysozyme and incubated at room temperature for 40 min. Cells were treated with 700 μL of RLT buffer (Qiagen) and transferred to 2-mL Lysing Matrix B tubes (MP Biomedicals, Irvine, CA). Samples were homogenized for 8 min at 50 Hz in a TissueLyser LT (Qiagen). RNA was isolated from cell lysates using the RNeasy Mini Kit (Qiagen) according to the manufacturer's instructions. DNase (Qiagen) treatment was performed on the columns prior to elution in 50 μL of hot nuclease-free water. A second DNase treatment was performed using the Turbo DNA-Free Kit (Thermo Scientific, Waltham, MA) according to the manufacturer's recommendations. RNA concentrations were measured using a NanoDrop ND-1000 spectrophotometer (NanoDrop Technologies, Montchanin, DE). RNA quality was assessed through gel electrophoresis using the RNA FlashGel System (Lonza, Rockland, ME) according to the manufacturer's instructions.

4.3.3 Construction of recombinant strains

Bacterial expression vector, pMH94 (Lee et al., 1991) is integration-dependent and includes an L5 integration cassette and kanamycin resistance gene. The vector was linearized with *Eco*RI per the manufacturer's recommendations (NEB). The McProf polymorphic toxin cassette (gp96 – 98), including its native promoter (63,600 − 68,223 bp) was PCR amplified with primers that include 30-bp extensions that correspond to the ends of *Eco*RI-digested pMH94. The 3,628-bp insert was ligated into the vector using the Gibson Assembly Cloning Kit (NEB) and transformed into competent *E. coli* DH5α according to the manufacturer's instructions. Plasmid was propagated in *E. coli* and successful recombinant plasmid was confirmed by diagnostic PCR and sequencing (**Table 4.3**). The resulting plasmid is referred to as pMHESX (**Table 4.2**).

Recombinant plasmids were electroporated into competent *M. chelonae* (ΔMcProf) according to de Moura et al. (2014). Briefly, electrocompetent *M. chelonae* cells were prepared by washing with ice-cold 10% glycerol four times. Plasmid DNA in 500 ng quantities were electroporated with 100 µL of electrocompetent *M. chelonae* in 0.2-cm gap cuvettes. A sample of electrocompetent cells lacking plasmid DNA served as a negative control. Electroporation was carried out in a single pulse at 2.5 kV, 25 mF, 1,000 Ω. Cells were suspended in 900 µL of room-temperature 7H9-OAD and incubated at 30˚C with shaking for 4 h prior to plating on 7H10-OAD agar plates supplemented with 250 µg mL^{-1} of KAN. Transformants were PCR screened for the presence of the plasmid (**Table 4.3**). Because our work involved analysis of gene expression, specifically *whi*B7, plasmids were not maintained with antibiotic selection following generation of recombinant strains. pMH94 was maintained by integration into the L5 attachment site. Successful expression of target genes in recombinant strains was confirmed by qRT-PCR (**Figure 4.6**).

Table 4.3 Standard PCR primers used in this study.

Target	Primers	Sequence (5' to 3')
McProf attL	Mc_attL_F	CGTCACGTTGGGGACTATCT
	Mc_attL_R	TTGAGCTGCGGATAACCTCT
McProf attR	Mc_attR_F	CGCTTGTAATCGTCGTA
	McProphageRR	ATAACTTTCGGCGGTTCCTT
McProf attP	Mc_attR_F	CGCTTGTAATCGTCGTA
	Mc_attL_R	TTGAGCTGCGGATAACCTCT
McProf attB	Mc_attL_F	CGTCACGTTGGGGACTATCT
	McProphageRR	ATAACTTTCGGCGGTTCCTT
BPs attL	BPs_attB_F	GTCTCGTTACTGGCGAGCTT
	BPs_attP_R	CGGGTAGTAGGCAGATGAGC
BPs attR	BPs_attP_F	GCTTTATCCAGGGTTGACCA
	BPs_attB_R	CGGTAGTAGGCAGATGAGC
BPs attP	BPs_attP_F	GCTTTATCCAGGGTTGACCA
	BPs_attP_R	CGGGTAGTAGGCAGATGAGC
BPs attB	BPs_attB_F	GTCTCGTTACTGGCGAGCTT
	BPs_attB_R	CGGTAGTAGGCAGATGAGC
L5 attL	L5_attB_L	GGTGGAGGGAAGTTCAGGTC
	L5_attP_R	AGTCTTCAGCGATCCCCATC
L5 attR	L5_attP_L	GAATGCCCCTCGTCTGTTC
	L5_attB_R	ACCTGCGTCCATACTTCGTC
L5 attP	L5_attP_L	GAATGCCCCTCGTCTGTTC
	L5_attP_R	AGTCTTCAGCGATCCCCATC
L5 attB	L5_attB_L	GAATGCCCCTCGTCTGTTC
	L5_attB_R	ACCTGCGTCCATACTTCGTC
McProf ESX	pMH94_ESX_F	AGTCACGACGTTGTAAAACGACGGCCAGTG
		TGACTCTTAATCAGCGGGTCCGGGGTTCGA
	pMH94_ESX_R	GCATCACGCCATGTTCACCAAGATCGCGCT
		CGAGCTCGGTACCCGGGGATCCTCTAGAGT
pMHESX	pMH94_insert_seq_F	CTCTTCGCTATTACGCCAGC
	pMH94_insert_seq_R	GTTCGCCCTGTCGTTCAC

4.3.4 Isolation of lysogenic strains

To generate BPs lysogen strains, *M. chelonae* (ΔMcProf) recombinant strains were serially diluted and plated in 4.5 mL of 7H9 top agar onto 7H10-OAD agar plates. One set of plates was treated with 10^9 plaque forming units (PFUs) of BPs, while the second set was untreated. Plates were then incubated for 6 d at 30˚C. Resulting colonies were grown in 7H9 broth to test for phage particle release and superinfection immunity. Efficiency of lysogeny was

calculated by dividing the number of colonies on virus-treated plates by the number of colonies on non-treated plates and multiplying by 100 to yield a percentage. Primers were designed to PCR amplify BPs attachment sites, *att*L and *att*R, to confirm prophage integration for continued cultivation of lysogen strains (**Table 4.3**).

4.3.5 Phage particle release test

Cultures of recombinant *M. chelonae* (BPs) were grown to an optical density of 1.0. A 1-mL sample of each strain was harvested. Cells were pelleted by centrifuging at 16,000 x *g* for 1 min. Resulting supernatant was passed through a 2-μm filter (VWR International, Radnor, PA) to remove residual bacterial cells and serially diluted 10-fold. Lawns of *M. smegmatis* were created by mixing 0.5-mL of late log phase bacteria with 4.5 mL of 7H9 top agar and plating onto 7H10 solid agar. Supernatant dilutions were applied in 5-μL volumes onto bacterial lawns and incubated overnight at 37˚C.

4.3.6 cDNA synthesis and qRT-PCR

cDNA was synthesized in 20-μL reactions containing 500 ng of total RNA using the qScript cDNA Supermix (Quantabio, Beverly, MA) according to the manufacturer's recommendations. Reactions were run under the following thermal cycle: 5 min at 25˚C, 20 min at 42˚C, and 5 min at 85˚C for inactivation. Working stocks of cDNA were prepared by diluting samples 1:6 in 10 mM Tris.

Primers for quantitative real-time PCR (qRT-PCR) assays were designed to amplify a 100-bp region with the gene of interest using Primer3 (**Table 4.4**). qRT-PCR assays were carried out in triplicate reactions in 25-μL volumes containing 200 nM of each primer, 1 μL of cDNA (diluted 1:6), and PerfeCTa SYBR Green Supermix (Quantabio) according to the manufacturer's

instructions. Positive and no-template controls were included in each assay. Reactions were run using the Bio-Rad CFX96 Real-Time system (Bio-Rad Laboratories, Hercules, CA). Reactions were initially incubated for 3 min at 95˚C, followed by 40 cycles of 10 s at 95˚C and 30 s at 60˚C, and lastly a melt curve to confirm a single amplicon per target gene. Change in RNA abundance was normalized to *M. chelonae* 16S rRNA, and relative expression determined using the $2^{-\Delta\Delta CT}$ method (Livak et al., 2001).

Table 4.4 qRT-PCR primers used in this study.

Target	Primers	Sequence (5' to 3')
16S	16S_qPCR_F1	CCGGATAGGACCACACACTT
	16S_qPCR_R1	ATTACCCCACCAACAAGCTG
whi B7	whiB7_qPCR_F4	ACTTTCCGCGAACCACAG
	whiB7_qPCR_R1a	ATGATGACCGTCGAAGTGG
MP Tdi	MP96_qPCR_F2	ACTCGATCGGATCAACAAGC
	MP96_qPCR_R2	CGAGAGTTTGGCTTCTCAGG
MP Tde	MP97_qPCR_F2	CTGAGAGCGTCCTTTTCCTG
	MP97_qPCR_R2	TAGGGAACCAGGGCTTATCC
MP EsxA	MP98_qPCR_F1	GTTGGTATCCGGTGTTGAGC
	MP98_qPCR_R1	CGATCAGCGACATCTACGAC

4.3.7 Minimum inhibitory concentration assays

Minimum inhibitory concentration (MIC) assays were performed according to Burian and coworkers (Burian et al., 2012) and Ramon-Garcia and coworkers (Ramon-Garcia et al., 2013). Cultures were grown in 7H9-OAD supplemented with 0.05% Tween80 at 30˚C with shaking and sub-cultured such that overnight incubation resulted in an OD_{600} of 0.1 - 0.3. Cultures were diluted to an OD of 0.005 without Tween and incubated for a 1 h and applied in 50-μL volumes to wells of a 96-well plate containing 50-μL 7H9 media with amikacin (AMK) concentrations that

varied by 2-fold dilutions (528 – 4 μg mL^{-1}). Each strain was applied in replicates of six at each drug concentration and no-antibiotic controls were performed in replicates of 16. Additionally, no-bacteria controls were included to serve as an absorbance blank. Inoculated plates were sealed with porous adhesive culture plate films (VWR International), wrapped with parafilm and incubated at 30°C for 2 d. A 5% solution of Tween80 and AlamarBlue (Bio-Rad) was added to each well in 25- and 2-μL volumes respectively, incubated at 30˚C for 1 d, and OD measured at 570- and 600 nm. Percent viability of cells was calculated as the percent difference in reduction between antibiotic-treated cells and untreated cells according to the manufacturer's instructions. Each assay was replicated in three independent experiments.

4.4 Results

4.4.1 Generation of recombinant *M. chelonae* strains

Bacterial expression vector, pMH94, is integration-dependent and includes an L5 integration cassette and kanamycin resistance gene for plasmid maintenance (Lee et al., 1991). Because our work involved analysis of gene expression and antibiotic resistance, it was important to utilize a vector that would not require antibiotic selection. The region of the McProf genome (coordinates 63,600 − 68,223 bp) that includes the polymorphic toxin cassette (gp96 − 98) and its native promoter was PCR amplified and inserted into linearized pMH94 to create pMHESX (**Table 4.2**). pMHESX and control vector, pMH94, were electroporated into *M. chelonae* (ΔMcProf). BPs lysogens were created from strains *M. chelonae* (pMHESX) and *M. chelonae* (pMH94) in order to determine if the McProf PT system stabilizes the BPs prophage and how the PT cassette interacts with BPs to alter *whi*B7 expression and amikacin resistance.

4.4.2 Expression of the McProf polymorphic toxin cassette stabilizes BPs single lysogens of *M. chelonae*

Phage-encoded toxin systems are reported to aid in stabilization of replicative elements, including plasmids and prophages (Yao et al., 2018). We wondered if the McProf PT cassette stabilizes the BPs prophage given the increased efficiency of lysogeny and reduced particle release observed in *M. chelonae* (BPs, McProf) relative to the BPs single lysogen (Cushman et al., 2021). BPs lysogens of *M. chelonae* (pMHESX) and the control strain, *M. chelonae* (pMH94), were grown to an optical density of 1.0 and phage particle release was measured in culture supernatant (**Figure 4.1**). There was a difference of two orders of magnitude between the two strains, with phage particles detected at concentrations of 2×10^7 PFU mL^{-1} and 2×10^5 for *M. chelonae* (BPs) (pMH94) and *M. chelonae* (BPs) (pMHESX) respectively. Although we did not determine if McProf PT system proteins are produced from the pMHESX plasmid, the stabilization of the BPs prophage in the presence of pMHESX suggests that McProf PT system gene products are being made in the recombinant strains.

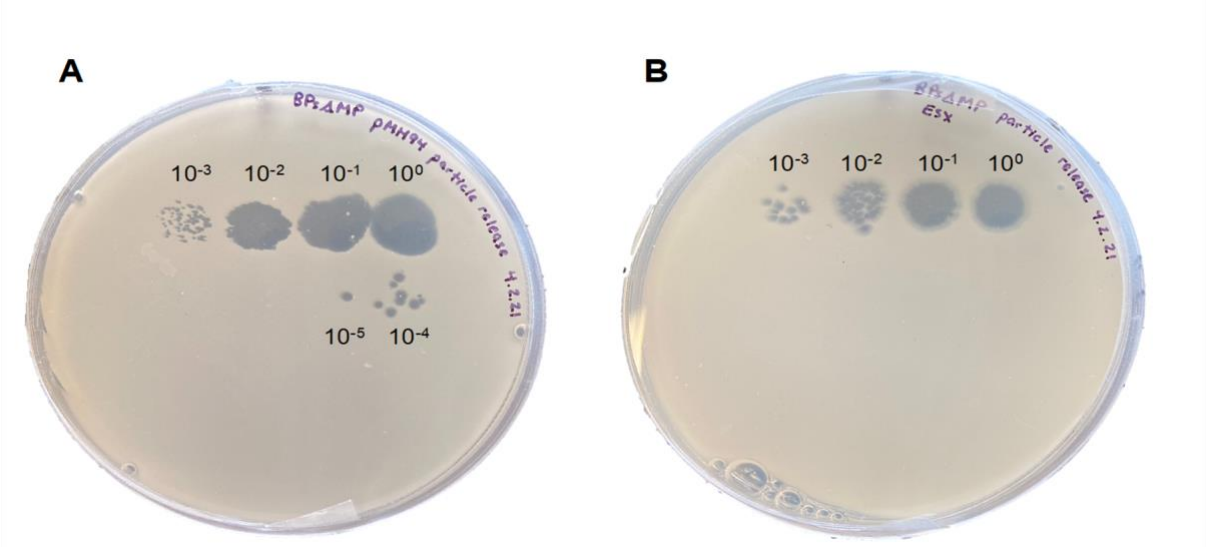

Figure 4.1 Phage particle release in recombinant *M. chelonae* (BPs). Supernatant of recombinant *M. chelonae* (BPs) (pMH94) (**A**) and *M. chelonae* (BPs) (pMHESX) (**B**) were serially diluted and applied to lawns of *M. smegmatis*.

4.4.3 The McProf polymorphic toxin cassette triggers upregulation of *whi*B7 in the presence of phage BPs

To determine whether expression of the McProf-encoded PT cassette alters *whi*B7 expression in the presence of BPs, we measured relative *whi*B7 expression in recombinant strains, and in *M. chelonae* (McProf) and *M. chelonae* (BPs, McProf) by qRT-PCR (**Figure 4.2**). Expression of *whi*B7 was significantly elevated (approximately 10-fold) in *M. chelonae* (BPs) (pMHESX) relative to *M. chelonae* (ΔMcProf) (pMH94). However, expression of *whi*B7 in *M. chelonae* (BPs) (pMHESX) was not as high as *whi*B7 expression levels in the double lysogen strain, which demonstrated a 45-fold increase relative to *M. chelonae* (ΔMcProf) (pMH94). As expected, expression of the PT cassette in the absence of BPs (*M. chelonae* (ΔMcProf) (pMHESX)) did not alter *whi*B7 expression. This suggests that while the McProf PT cassette

elevates *whi*B7 expression in the presence of BPs, it is not the only factor causing the drastic increase in *whi*B7 expression observed in *M. chelonae* (BPs, McProf).

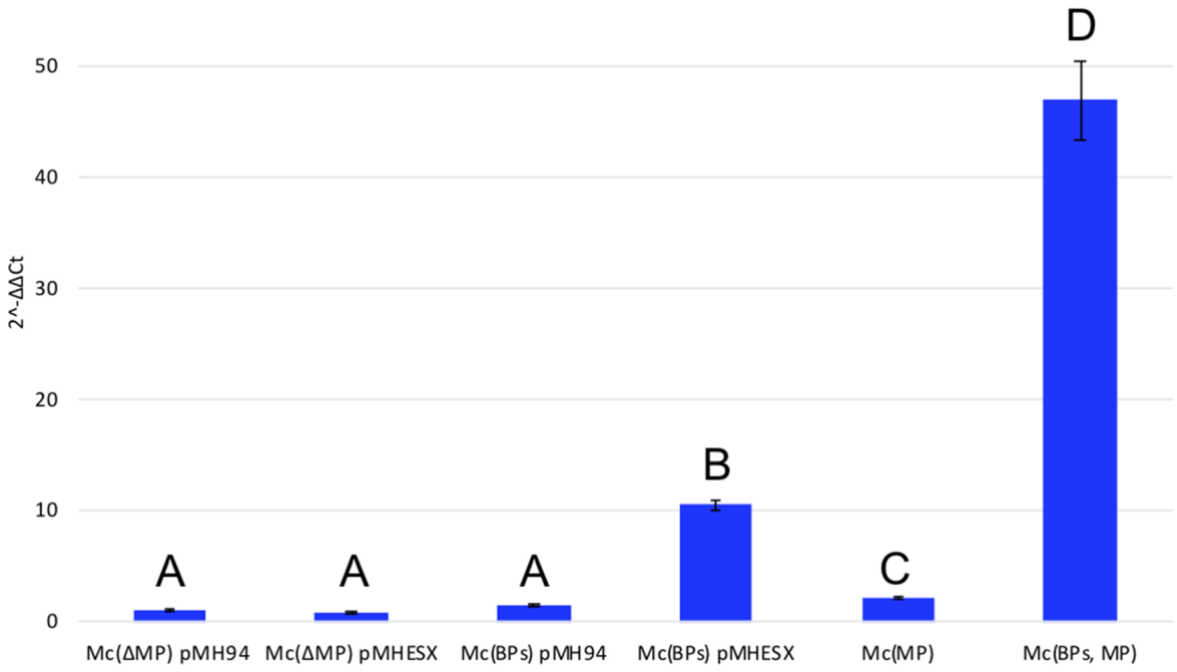

Figure 4.2 qRT-PCR analysis of *whi*B7 in recombinant strains of *M. chelonae* expressing the McProf polymorphic toxin cassette. The average relative expression levels of *whi*B7 was measured in recombinant strains of *M. chelonae* (ΔMcProf) and *M. chelonae* (BPs) carrying pMHESX or empty vector (pMH94) and compared to *whi*B7 expression in *M. chelonae* (McProf) and *M. chelonae* (BPs, McProf) by SYBR Green by qRT-PCR. Cultures were grown to an OD_{600} of 1.0 before harvesting RNA in triplicate. Graphs represent average values ± standard error of the mean with n=3 and are representative of two independent trials. Means with different letters are significantly different (Tukey's HSD, α=0.05).

4.4.4 The McProf polymorphic toxin cassette is downregulated in *M. chelonae* (BPs, McProf)

We confirmed that each of the PT cassette genes were expressed from pMHESX recombinant *M. chelonae* strains by qRT-PCR and compared expression to that observed in *M. chelonae* (McProf) and *M. chelonae* (BPs, McProf) (**Figure 4.3**). The expression profile of the recombinant strains differed from that of the double lysogen (BPs, McProf). The WXG-100

family protein and Tdi-like immunity protein were expressed at similar levels in both *M. chelonae* (ΔMcProf) (pMHESX) and *M. chelonae* (ΔMcProf) (BPs) (pMHESX) relative to *M. chelonae* (McProf) (**Figure 4.3a** and **Figure 4.3c**). However, expression of these genes in the double lysogen was significantly lower. The expression levels of gp97, the Tde-like PT, was higher in both recombinant strains, *M. chelonae* (ΔMcProf) (pMHESX) and *M. chelonae* (BPs) (pMHESX) by approximately 6.5-fold and 5-fold relative to *M. chelonae* (McProf) whereas expression levels in the double lysogen were the lowest (**Figure 4.3b**). This suggests that the presence of an intact McProf prophage affects expression of gp97. Interestingly, all three genes in the PT cassette were downregulated in *M. chelonae* (BPs, McProf). The presence of the BPs prophage also appears to affect expression of genes in the PT system. The different expression profiles between the single McProf and double lysogen (BPs, McProf) strains is in contrast from the RNAseq data which did not detect significant differential expression of these genes.

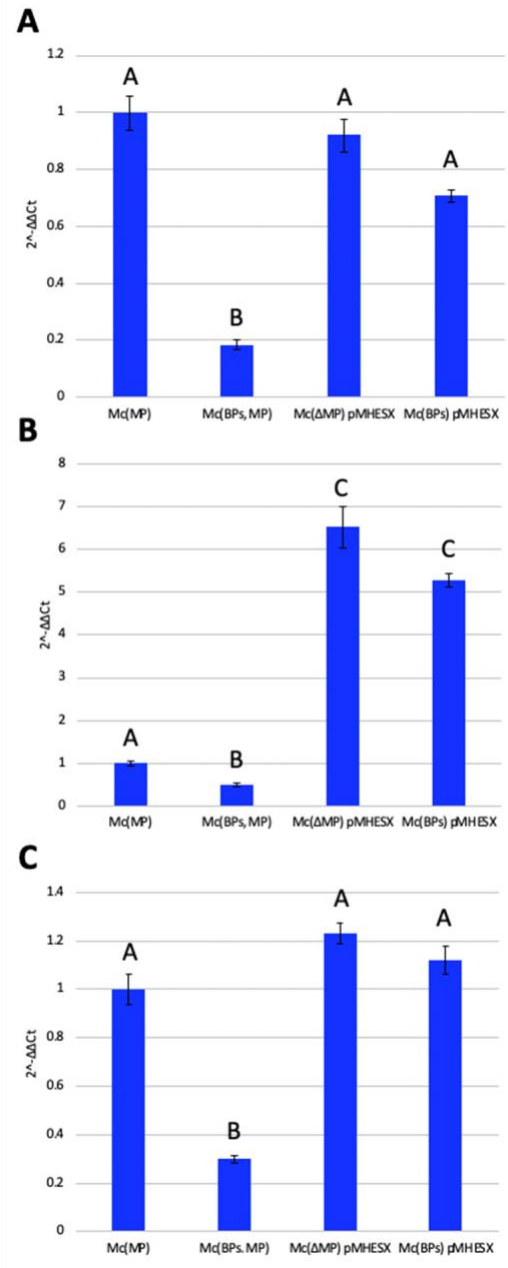

Figure 4.3 $2^{-\Delta\Delta Ct}$ qRT-PCR analysis of polymorphic toxin cassette genes in *recombinant M. chelonae* strains. The average expression of the WXG-100-like protein (**A**), the Tde-like polymorphic toxin (**B**), and the Tdi-like immunity protein (**C**) was measured in recombinant strains of *M. chelonae* (ΔMcProf) and *M. chelonae* (BPs) carrying pMHESX, as well as in *M. chelonae* (McProf) and *M. chelonae* (BPs, McProf), by SYBR Green qRT-PCR. Cultures were grown to an OD_{600} of 1.0 before harvesting RNA in triplicate. Graphs represent average values ± standard error of the mean with n=3 and are representative of two independent trials. Means with different letters are significantly different (Tukey's HSD, α=0.05).

To compare the ratio of PT to immunity protein, we plotted the average ΔCt for each gene by strain (**Figure 4.5**). The Tdi-like immunity protein is the most highly expressed gene in the PT cassette in McProf-carrying strains, and PT expression is lower in McProf-carrying strains compared to recombinant strains. In contrast, PT expression is higher in the recombinant strains and immunity protein expression in nearly equivalent to that of the toxin, indicating that the ratio of immunity protein to PT transcripts differ in the absence of an intact McProf prophage (**Figures 4.4** and **4.5**). *M. chelonae* (BPs, McProf) has lower expression across the entire cassette compared to other strains and the WXG-100 protein has the lowest expression of the three PT cassette genes across all strains, as indicated by elevated ΔCt values.

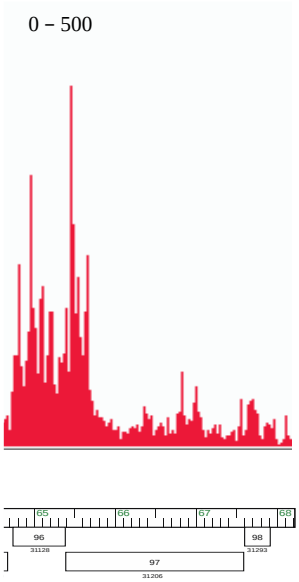

Figure 4.4 McProf polymorphic toxin cassette gene expression profile. The coordinates of the McProf genome are represented by the ruler. Genes are shown as boxes above (transcribed rightwards) or below (transcribed leftward) the ruler. RNAseq profiles are shown reverse (red) DNA strands. The number of reads mapped are shown on the y-axis. The map was generated using Phamerator (Cresawn et al., 2011).

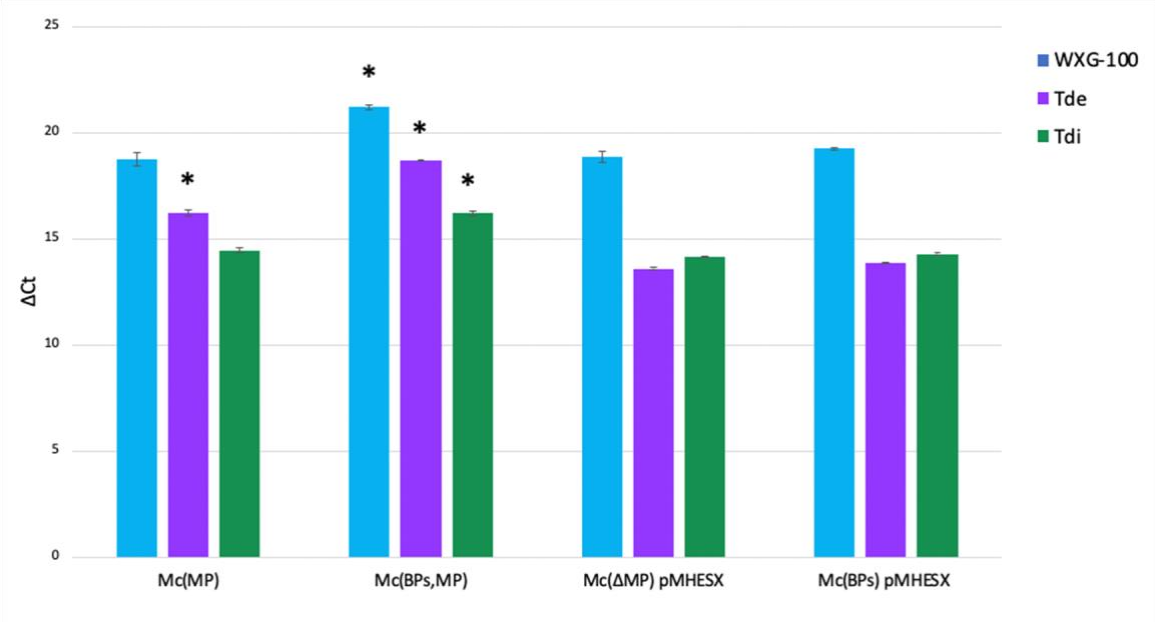

Figure 4.5 ΔCt qRT-PCR analysis of McProf polymorphic toxin cassette genes in *recombinant M. chelonae* strains. The average expression of the WXG-100-like protein (blue), the Tde-like polymorphic toxin (purple), and the Tdi-like immunity protein (green) was measured in recombinant strains of *M. chelonae* (ΔMcProf) and *M. chelonae* (BPs) carrying pMHESX, as well as in *M. chelonae* (McProf) and *M. chelonae* (BPs, McProf), by SYBR Green qRT-PCR. Cultures were grown to an OD_{600} of 1.0 before harvesting RNA in triplicate. Graphs represent average values ± standard error of the mean with n=3 and are representative of two independent trials. Significantly different means by gene across all strains are represented by asterix (Tukey's HSD, α=0.05).

4.4.5 Expression of the McProf polymorphic toxin cassette does not alter amikacin resistance

Previous work demonstrated that the presence of both BPs and McProf prophages significantly increased the resistance of *M. chelonae* to aminoglycoside, amikacin, relative to strains carrying one or no prophage (Cushman et al., 2021). We investigated whether expression of the McProf PT genes in the recombinant strains in the presence and absence of BPs increased AMK resistance through MIC assays (**Figure 4.6**). The AMK MIC was measured in recombinant *M. chelonae* (ΔMcProf) and *M. chelonae* (BPs) expressing the PT cassette (pMHESX) compared to respective strains carrying empty vector (pMH94). There was no

significant difference in AMK resistance between the PT recombinant strains relative to control strains carrying empty vector. The presence of the BPs prophage also did not affect AMK resistance. The MIC for all four recombinant strains with and without the BPs prophage was 16 μg mL^{-1}. All strains showed enhanced resistance upon ACI treatment at an MIC of 32 μg mL^{-1}. However, ACI treatment did not have a greater effect on *M. chelonae* (BPs) (pMHESX) compared to *M. chelonae* (ΔMcProf) (pMHESX), nor did strains carrying the control vector demonstrate lower resistance upon ACI treatment relative to pMHESX-carrying strains.

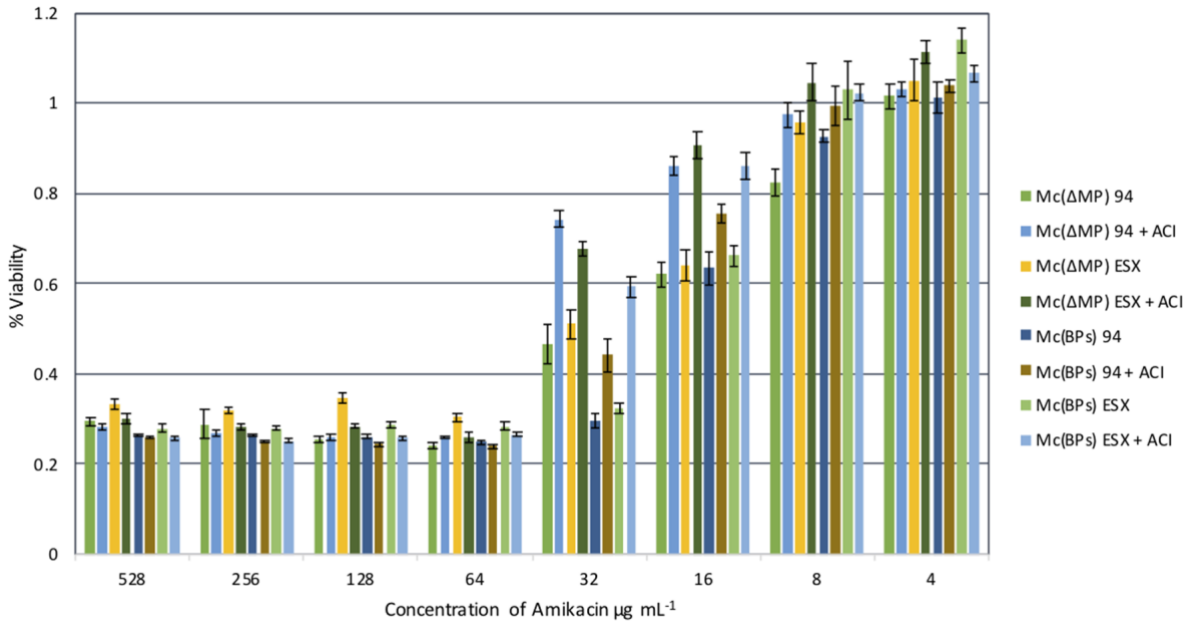

Figure 4.6 Percent viability of recombinant *M. chelonae* strains upon AMK treatment in the presence and absence of ACI. Percent viability of *M. chelonae* (ΔMcProf) (McΔMP), and *M. chelonae* (BPs) (Mc (BPs) carrying pMHESX (ESX) or empty vector (94)) in the presence of varying concentrations of amikacin. To determine if the presence of the McProf PT cassette interacts with sub-inhibitory concentrations of antibiotics, each strain was treated or not treated with 75 µM acivicin (ACI). Graphs represent average values ± SE of the mean with n=3. The optical density of was measured at 570- and 600 nm after the addition of 2 µL of AlamarBlue and the percent difference in reduction between antibiotic-treated cells and untreated cells was calculated. Data is representative of two independent experiments.

4.4 Discussion

The incidence of non-tuberculous mycobacterial disease has been on the rise and poses a major public health threat. Effective treatment of these diseases, especially *M. abscessus* infections, has proven to be difficult as a result of high levels of intrinsic drug resistance (Johansen et al., 2020). Further, emergence of extensively antibiotic resistant isolates of *M. abscessus* has rendered successful clearance of infections nearly impossible (Johansen et al., 2020). Extensive resistance in some *M. abscessus* strains can be attributed to mutations in 16S or 23S rRNA, the targets for aminoglycosides and macrolides respectively. However, mutations

do not account for extensive resistance observed in all clinical isolates (Guo et al., 2020). Common among extensively resistant *M. abscessus* strains is upregulation of transcriptional activator, *whi*B7, which positively regulates many genes associated with antibiotic resistance and stress adaptation (Guo et al., 2020). While *whi*B7 expression is known to be induced by stress conditions such as sub-lethal drug exposure, phage infection, and the intracellular environment of macrophages, the cause of upregulation in extensively resistant *M. abscessus* is not completely understood (Cushman et al., 2021 and Burian et al., 2012). Better understanding mechanisms of intrinsic drug resistance in pathogenic mycobacteria is essential for developing more effective treatments.

We recently demonstrated for the first time that phage infection impacts *whi*B7 expression in mycobacteria. The presence of prophage BPs increases expression of *whi*B7 in *M. chelonae*, but only in strains carrying the naturally occurring prophage, McProf. This suggests that an interaction between BPs and McProf triggers an upregulation of *whi*B7 (Cushman et al., 2021). Expression of individual BPs lysogenic gene products did not significantly alter *whi*B7 expression, suggesting that lytic infection by BPs and/or McProf gene products play a more important role in altering *whi*B7 expression and antibiotic resistance (Molloy, Unpublished). Here we explore the role of the McProf-encoded polymorphic toxin (PT) cassette on prophage stability, *whi*B7 expression and amikacin resistance. We show that expression of the PT cassette alone in the presence of the BPs prophage does significantly increase *whi*B7 expression but not to the same degree of high expression levels observed in *M. chelonae* (BPs, McProf).

The genes in the McProf PT system play a role in stabilizing the BPs prophage in mycobacteria. BPs forms comparatively unstable lysogens in mycobacterial strains that lack the

McProf prophage with culture supernatant titers approaching 10^{10} PFU mL^{-1}. In contrast, culture supernatant titers of BPs lysogens of *M. chelonae* (McProf) or the PT recombinant strain are 2 – 4 orders of magnitude lower (**Figure 4.1**) (Cushman et al., 2021). Active polymorphic toxin systems are known to aid in the stabilization of replication elements, including prophage and plasmids (Yao et al., 2018; Fraikin et al., 2020; Wozniak et al., 2009). We did not measure protein production from gp96 – 98 in the recombinant strains. However, the drastic difference in BPs titer in culture supernatants in the recombinant strains relative to controls suggests that active gene products are likely being made at a high enough level to stabilize the BPs prophage, possibly by killing cells in which BPs induction occurs.

The McProf PT system contributes to the *whi*B7 response, but not to the same degree as strains carrying an intact McProf prophage. Toxin/antitoxin and polymorphic toxin systems are activated by stressors such as phage infection and antibiotic exposure, and are abundant in pathogenic mycobacteria (Kumar et al., 2019; Slayden et al., 2018; Wang et al., 2011). These systems may also contribute to stress adaptation responses (Slayden et al., 2018). Our analysis suggested that while expression of the PT cassette in *M. chelonae* (BPs) (pMHESX) does increase *whi*B7 expression by approximately 10-fold, this system alone does not explain the >40-fold increase observed in the double lysogen (BPs, McProf) (**Figure 4.2**). This likely explains why there is not a difference in AMK resistance observed in pMHESX strains (**Figure 4.5**), although MIC data is preliminary and should be repeated. It is possible that an additional McProf-encoded factor(s), independently or through interactions with the PT cassette, are necessary for high *whi*B7 expression in the presence of BPs. Therefore, the role of the other 13 genes expressed from the McProf prophage should be investigated.

The PT cassette was actively expressed in recombinant strains; however, the expression profiles contrasted those observed from RNAseq. While it remains true that the immunity protein is the most highly expressed gene in the cassette, we found that expression of all three PT cassette genes is significantly lower in *M. chelonae* (BPs, McProf) compared to both wildtype *M. chelonae* and the recombinant strains (**Figure 4.3**). It is possible that differential expression was not detected in RNAseq analysis as a result of low read coverage. While the McProf PT cassette appears to be transcribed on the same operon, the stark difference in reads mapped to the WXG-100 protein and the N-terminus of the toxin compared to the immunity proteins suggests that there may be a hidden promoter within the C-terminus of the PT ORF that would explain the heightened expression of the immunity protein in McProf-carrying strains (**Figure 4.4**). Together, this suggests that the McProf PT cassette is downregulated in the double lysogen (BPs, McProf) but not when BPs alone is present, indicating that another McProf-encoded component plays a role in regulating the polymorphic toxin system.

The difference in *whi*B7 expression between the recombinant BPs lysogen and the double lysogen may be due to differences in the gene expression profile of the PT cassette between strains. The Tdi-like immunity protein (McProf gp96) is more highly expressed than its associated Tde-like toxin (McProf gp97) in McProf-carrying strains, whereas in the recombinant strains, expression of the immunity protein and PT were nearly equal (**Figure 4.5**). It makes sense for the ratio of immunity protein to toxin to be high in order to protect cells from PT activity and similar expression profiles have been observed in prophage-encoded PT systems identified in clinical *M. abscessus* strains (Dedrick et al., 2021; Harms et al., 2018). If PT enzymatic activity is important for *whi*B7 expression, then a lower ratio of immunity protein to

PT would likely affect residual toxin activity and potentially *whi*B7 expression. However, though the PT cassette expression profiles between the recombinant strains are highly similar, this would not explain the 10-fold difference in *whi*B7 expression in the presence and absence of BPs. This suggests that the presence of the BPs phage likely affects regulation of the toxin system at the post-transcriptional level. Because an intact McProf prophage is also important for high *whi*B7 expression, it too may be important to PT protein activity and potentially results in increased *whi*B7 expression. In *Enterococcus*, T7SS PT systems are known to be upregulated by phage infection (Chaterjee et al., 2021). The presence of an intact McProf genome may result in phage gene expression that activates the PT system in a way that affects *whi*B7 expression which cannot be observed in our recombinant strains.

We have shown that the McProf PT system does contribute to the *whi*B7 response in the presence of the BPs prophage; however, the PT cassette alone does not explain the 45-fold increase in *whi*B7 expression observed in *M. chelonae* (BPs, McProf). The impact of the other genes expressed from the McProf prophage should be investigated in the presence of both the PT cassette and BPs to explore whether a combination of McProf-encoded gene products is responsible for inducing *whi*B7 expression upon infection by BPs.

CHAPTER 5

CONCLUDING REMARKS AND FUTURE DIRECTIONS

Pathogenic mycobacteria pose a major public health threat and are the second leading cause of death by an infectious agent behind COVID-19 (WHO, 2020). Nontuberculous mycobacterial pathogens are gaining prevalence, surpassing the incidence of tuberculosis in most developed countries (Johansen et al., 2020). *Mycobacterium abscessus* is the most intrinsically antibiotic-resistant species known. It is the causative agent of lung infections that disproportionately affect immunocompromised individuals, such as cystic fibrosis patients. These characteristics make *M. abscessus* infections difficult to treat, with a success rate of only 45% (Griffith, 2019; Johansen et al., 2020). Further, emergence of extensively antibiotic resistant isolates of *M. abscessus* has rendered successful clearance of disease nearly impossible (Johansen et al., 2020). While some extensively resistant isolates are caused by mutations in drug targets, others appear to be a result of increased intrinsic drug resistance with no known cause (Guo et al., 2020). Common among extensively resistant *M. abscessus* strains is upregulation of conserved mycobacterial transcriptional activator, *whi*B7, which regulates many genes associated with antibiotic resistance and stress adaptation (Guo et al., 2020; Morris et al., 2005; Burian et al., 2012). The majority of extensively resistant clinical *M. abscessus* strains identified thus far carry one or more prophage (Dedrick et al., 2021; Molloy, Unpublished). Prophage are known to contribute to fitness and virulence in many pathogens, but their role in mycobacteria has not been established (Fan et al., 2014). Characterizing the pathways that lead to increased *whi*B7 expression and intrinsic drug resistance in pathogenic

mycobacteria will be important for identifying new targets for novel drug development (Nessar et al., 2012; Dheda et al., 2018).

This thesis has contributed to understanding the role of prophage on *whi*B7 expression and intrinsic drug resistance in pathogenic mycobacteria. The McProf prophage is found naturally in the pathogen *M. chelonae* where it plays a major role in regulating intrinsic drug resistance via upregulating *whi*B7. My work suggests it does through the polymorphic toxin system encoded within McProf. McProf belongs to a novel cluster, MabR (Molloy, Unpublished). At least 25 clinical isolates of *M. abscessus* have been identified carrying McProf-like or MabR prophage sequences (Molloy, Unpublished). Therefore, this work is significant to the study of drug resistance in *M. abscessus* because the polymorphic toxin system encoded by McProf is also common in strains of *M. abscessus whi*B7 pathway that is conserved in all mycobacteria.

We expanded our understanding of this regulatory system by showing that the addition of a second prophage, BPs, to *M. chelonae* (McProf) triggers a >40-fold increase in *whi*B7 expression and results in enhanced aminoglycoside resistance. In fact, whole genome RNAseq analysis showed differential expression of 8.5% of *M. chelonae* genes in the presence of BPs. We developed a four-strain model including single, double, and non-lysogens of *M. chelonae* and found that both prophages must be present to observe a drastic increase in *whi*B7 expression and antibiotic resistance. Sub-lethal levels of Acivicin (ACI), are known to induce increased expression of *whi*B7. We showed that it not only significantly increased amikacin (AMK) resistance in all four strains but had the most pronounced effect on strains carrying McProf. Not surprisingly, ACI treatment also significantly increased *whi*B7 expression in each

strain. This allowed us to conclude that an interaction between McProf and BPs induces *whi*B7 expression and that exposure to sub-lethal drugs further enhances this effect. Notably, this is the first report of phage infection serving as a trigger for the WhiB7 response. However, we saw that when exposed to sub-lethal AMK, *whi*B7 expression was only substantially increased in *M. chelonae* strains lacking McProf. We noted that ACI is a smaller molecule compared to AMK and wondered if McProf somehow alters cell wall permeability. This could explain increased AMK resistance in McProf-carrying strains, and why sub-lethal AMK doesn't appear to significantly impact *whi*B7 expression in *M. chelonae* (McProf) and *M. chelonae* (BPs, McProf). It would be interesting to assess differences in cell wall permeability between all four *M. chelonae* strains by measuring dye uptake using fluorescent microscopy. Ethidium bromide has been successfully used to measure rate of uptake and efflux in mycobacteria, as it strongly fluoresces when concentrated in the cytoplasm of Gram-positive bacteria (Rodrigues et al., 2011). Therefore, these methods could be optimized to measure ethidium bromide uptake in *M. chelonae*, and potentially uncover another layer of intrinsic resistance in mycobacterial pathogens.

Given the dramatic increase in *whi*B7 expression and aminoglycoside resistance observed in *M. chelonae* (BPs, McProf), but not in single or non-lysogens of *M. chelonae*, we investigated the impact of BPs lysogenic gene products on *whi*B7 expression in the presence of McProf. We identified three genes expressed by the BPs prophage and generated recombinant strains of *M. chelonae* (McProf) to individually express these genes. qRT-PCR analysis demonstrated that BPs lysogenic gene products do not significantly alter *whi*B7 expression. In a population of lysogens, a random subset of cells spontaneously goes through induction, or a

switch from lysogenic to lytic replication (Casjens, 2003). Therefore, the impact of BPs lytic infection on *whi*B7 expression also needs to be investigated. This can be achieved by infecting *M. chelonae* (McProf) with a BPs mutant that lacks the immunity repressor so that it is only capable of lytic growth. We have generated such a strain using BRED technology (Marinelli et al., 2008). RNA can be harvested throughout the infection cycle and temporal *whi*B7 expression measured by qRT-PCR. Because the presence of McProf is necessary for *whi*B7 induction upon BPs infection, as seen in *M. chelonae* (BPs, McProf), it is likely that BPs infection does not directly alter *whi*B7 expression, but rather activates McProf gene products that results in stress signaling that triggers a WhiB7 response. Therefore, the relative expression of McProf genes should be monitored during lytic infection as well. Alternately, generation of a "super" double lysogen by overexpressing the BPs immunity repressor in *M. chelonae* (BPs, McProf) would serve two purposes. First, it could confirm that BPs lysogenic gene products truly do not influence *whi*B7 expression. Second, overexpression of the immunity repressor would greatly minimize or entirely prevent induction events. Overexpression of the BPs immunity repressor was previously attempted using a constitutive Hsp60 promoter and appeared to be lethal to the cell. To circumvent this, an inducible promoter could be used to control repressor expression levels. If *whi*B7 expression is not upregulated in a super double lysogen, then it would be plausible to further investigate BPs induction events as a contributor to *whi*B7 induction in the presence of McProf.

Since BPs lysogenic gene products did not contribute to *whi*B7 upregulation, we looked into the role of McProf gene products, specifically the polymorphic toxin (PT) cassette. While expression of the McProf PT cassette did result in a 10-fold increase in *whi*B7 expression in *M.*

chelonae (BPs), it did not fully account for the 45-fold increase observed in *M. chelonae* (BPs, McProf). This suggests that other McProf-encoded factors may contribute to the induction of *whi*B7 or affect the expression and/or activation of the McProf PT system such that higher whib7 expression occurs and therefore should be investigated. McProf expresses 13 genes in addition to the PT cassette. Each of these genes should be cloned into *M. chelonae* (BPs) and the impact on *whi*B7 expression and aminoglycoside resistance evaluated. Of specific interest is gp84. It does not have a predicted function; however, it is the most highly expressed McProf gene. It is therefore possible that this gene product is somehow beneficial to McProf and/or its bacterial host.

Another aspect to consider is a potential interaction between the McProf PT system and an *M. chelonae*-encoded flotillin protein. The most highly upregulated gene in *M. chelonae* (BPs, McProf) relative to the wildtype strain encodes a predicted flotillin protein with a 99-fold increase in expression (Cushman et al., 2021). As it is not a member of the WhiB7 regulon, it was not previously investigated, but orthologs have been identified in *M. tuberculosis* and *M. abscessus*. The function of this gene in *M. chelonae* in unknown; however, in multidrug resistant *Staphylococcus aureus*, it serves as a chaperone and contributes to virulence by interacting with functional membrane microdomains and type 7 secretion system (T7SS) components (Mielich-Suss et al., 2017). Further, phage infection in *Enterococcus faecalis* results in increased expression of T7SS components and its substrates (Chaterjee et al., 2021). Taken together, it is possible that the *M. chelonae* flotillin protein could be facilitating interactions between T7SS substrates, such as the McProf-encoded polymorphic toxin, and the bacterial membrane upon activation by BPs infection, potentially triggering a population-based WhiB7

response. The impact of the McProf PT cassette on flotillin expression should be measured by qRT-PCR to determine whether there is a link between the two systems. Additionally, a flotillin knockout strain should be created from *M. chelonae* (BPs, McProf) to assess whether the flotillin protein is involved in triggering an upregulation of *whiB*7.

In summary, this work has identified phage infection as a novel trigger of the WhiB7 stress response and increased drug resistance and has begun to uncover potential mechanisms responsible for this response. Continuing to characterize these phage-host interactions is important to better understanding the virulence of mycobacterial pathogens. Elucidating the mechanisms of *whi*B7 upregulation and increased antibiotic resistance in pathogenic mycobacteria will be essential to developing new therapeutic targets for multidrug resistant infections.

LITERATURE CITED

Afgan, E., Baker, D., Batut, B., van den Beek, M., Bouvier, D., Cech, M., Chilton, J., Clements, D., Coraor, N., Grüning, B. A., Guerler, A., Hillman-Jackson, J., Hiltemann, S., Jalili, V., Rasche, H., Soranzo, N., Goecks, J., Taylor, J., Nekrutenko, A., & Blankenberg, D. (2018). The Galaxy platform for accessible, reproducible and collaborative biomedical analyses: 2018 update. *Nucleic acids research*, *46*(W1), W537–W544. https://doi.org/10.1093/nar/gky379

Aínsa, J. A., Blokpoel, M. C., Otal, I., Young, D. B., De Smet, K. A., & Martín, C. (1998). Molecular cloning and characterization of Tap, a putative multidrug efflux pump present in *Mycobacterium fortuitum* and *Mycobacterium tuberculosis*. *Journal of bacteriology*, *180*(22), 5836–5843. https://doi.org/10.1128/JB.180.22.5836-5843.1998

Alderwick, L. J., Harrison, J., Lloyd, G. S., & Birch, H. L. (2015). The Mycobacterial Cell Wall--Peptidoglycan and Arabinogalactan. *Cold Spring Harbor perspectives in medicine*, *5*(8), a021113. https://doi.org/10.1101/cshperspect.a021113

Altschul, S. F., Gish, W., Miller, W., Myers, E. W., & Lipman, D. J. (1990). Basic local alignment search tool. *Journal of molecular biology*, *215*(3), 403–410. https://doi.org/10.1016/S0022-2836(05)80360-2

Andrews, S. (2017). FastQC: a quality control tool for high throughput sequence data. 2010.

Arndt, D., Grant, J. R., Marcu, A., Sajed, T., Pon, A., Liang, Y., & Wishart, D. S. (2016). PHASTER: a better, faster version of the PHAST phage search tool. *Nucleic acids research*, *44*(W1), W16–W21. https://doi.org/10.1093/nar/gkw387

Bachmann, N. L., Salamzade, R., Manson, A. L., Whittington, R., Sintchenko, V., Earl, A. M., & Marais, B. J. (2020). Key Transitions in the Evolution of Rapid and Slow Growing *Mycobacteria* Identified by Comparative Genomics. *Frontiers in microbiology*, *10*, 3019. https://doi.org/10.3389/fmicb.2019.03019

Barka, E. A., Vatsa, P., Sanchez, L., Gaveau-Vaillant, N., Jacquard, C., Meier-Kolthoff, J. P., Klenk, H. P., Clément, C., Ouhdouch, Y., & van Wezel, G. P. (2015). Taxonomy, Physiology, and Natural Products of Actinobacteria. *Microbiology and molecular biology reviews : MMBR*, *80*(1), 1–43. https://doi.org/10.1128/MMBR.00019-15

Beck, H. J., & Moll, I. (2018). Leaderless mRNAs in the Spotlight: Ancient but Not Outdated!. *Microbiology spectrum*, *6*(4), 10.1128/microbiolspec.RWR-0016-2017. https://doi.org/10.1128/microbiolspec.RWR-0016-2017

Bibb, L. A., & Hatfull, G. F. (2002). Integration and excision of the *Mycobacterium tuberculosis* prophage-like element, phiRv1. *Molecular microbiology*, *45*(6), 1515–1526. https://doi.org/10.1046/j.1365-2958.2002.03130.x

Borodovsky, M., & Lomsadze, A. (2011). Eukaryotic gene prediction using GeneMark.hmm-E and GeneMark-ES. *Current protocols in bioinformatics*, *Chapter 4*, Unit–4.6.10. https://doi.org/10.1002/0471250953.bi0406s35

Broussard, G. W., Oldfield, L. M., Villanueva, V. M., Lunt, B. L., Shine, E. E., & Hatfull, G. F. (2013). Integration-dependent bacteriophage immunity provides insights into the evolution of genetic switches. *Molecular cell*, *49*(2), 237–248. https://doi.org/10.1016/j.molcel.2012.11.012

Brüssow, H., Canchaya, C., & Hardt, W. D. (2004). Phages and the evolution of bacterial pathogens: from genomic rearrangements to lysogenic conversion. *Microbiology and molecular biology reviews : MMBR*, *68*(3), 560–602. https://doi.org/10.1128/MMBR.68.3.560-602.2004

Burian, J., Ramón-García, S., Sweet, G., Gómez-Velasco, A., Av-Gay, Y., & Thompson, C. J. (2012). The mycobacterial transcriptional regulator *whi*B7 gene links redox homeostasis and intrinsic antibiotic resistance. *The Journal of biological chemistry*, *287*(1), 299–310. https://doi.org/10.1074/jbc.M111.302588

Burian, J., Ramón-García, S., Howes, C. G., & Thompson, C. J. (2012). WhiB7, a transcriptional activator that coordinates physiology with intrinsic drug resistance in *Mycobacterium tuberculosis*. *Expert review of anti-infective therapy*, *10*(9), 1037–1047. https://doi.org/10.1586/eri.12.90

Burian, J., Yim, G., Hsing, M., Axerio-Cilies, P., Cherkasov, A., Spiegelman, G. B., & Thompson, C. J. (2013). The mycobacterial antibiotic resistance determinant WhiB7 acts as a transcriptional activator by binding the primary sigma factor SigA (RpoV). *Nucleic acids research*, *41*(22), 10062–10076. https://doi.org/10.1093/nar/gkt751

Burian, J., & Thompson, C. J. (2018). Regulatory genes coordinating antibiotic-induced changes in promoter activity and early transcriptional termination of the mycobacterial intrinsic resistance gene *whi*B7. *Molecular microbiology*, *107*(3), 402–415. https://doi.org/10.1111/mmi.13890

Bush M. J. (2018). The actinobacterial WhiB-like (Wbl) family of transcription factors. *Molecular microbiology*, *110*(5), 663–676. https://doi.org/10.1111/mmi.14117

Canestrari, J. G., Lasek-Nesselquist, E., Upadhyay, A., Rofaeil, M., Champion, M. M., Wade, J. T., Derbyshire, K. M., & Gray, T. A. (2020). Polycysteine-encoding leaderless short ORFs function as cysteine-responsive attenuators of operonic gene expression in mycobacteria. *Molecular microbiology*, *114*(1), 93–108. https://doi.org/10.1111/mmi.14498

Carrigy, N. B., Larsen, S. E., Reese, V., Pecor, T., Harrison, M., Kuehl, P. J., Hatfull, G. F., Sauvageau, D., Baldwin, S. L., Finlay, W. H., Coler, R. N., & Vehring, R. (2019). Prophylaxis of *Mycobacterium tuberculosis* H37Rv Infection in a Preclinical Mouse Model via Inhalation of Nebulized Bacteriophage D29. *Antimicrobial agents and chemotherapy*, *63*(12), e00871-19. Advance online publication. https://doi.org/10.1128/AAC.00871-19

Casjens S. (2003). Prophages and bacterial genomics: what have we learned so far?. *Molecular microbiology*, *49*(2), 277–300. https://doi.org/10.1046/j.1365-2958.2003.03580.x

Chatterjee, A., Willett, J., Dunny, G. M., & Duerkop, B. A. (2021). Phage infection and sub-lethal antibiotic exposure mediate *Enterococcus faecalis* type VII secretion system dependent inhibition of bystander bacteria. *PLoS genetics*, *17*(1), e1009204. https://doi.org/10.1371/journal.pgen.1009204

Chen, W., Green, K. D., Tsodikov, O. V., & Garneau-Tsodikova, S. (2012). Aminoglycoside multiacetylating activity of the enhanced intracellular survival protein from *Mycobacterium smegmatis* and its inhibition. *Biochemistry*, *51*(24), 4959–4967. https://doi.org/10.1021/bi3004473

Christensen, S. K., Mikkelsen, M., Pedersen, K., & Gerdes, K. (2001). RelE, a global inhibitor of translation, is activated during nutritional stress. *Proceedings of the National Academy of Sciences of the United States of America*, *98*(25), 14328–14333. https://doi.org/10.1073/pnas.251327898

Coray, D. S., Wheeler, N. E., Heinemann, J. A., & Gardner, P. P. (2017). Why so narrow: Distribution of anti-sense regulated, type I toxin-antitoxin systems compared with type II and type III systems. *RNA biology*, *14*(3), 275–280. https://doi.org/10.1080/15476286.2016.1272747

Cresawn, S. G., Bogel, M., Day, N., Jacobs-Sera, D., Hendrix, R. W., & Hatfull, G. F. (2011). Phamerator: a bioinformatic tool for comparative bacteriophage genomics. *BMC bioinformatics*, *12*, 395. https://doi.org/10.1186/1471-2105-12-395

Cushman, J., Freeman, E., McCallister, S., Schumann, A., Hutchison, K. W., & Molloy, S. D. (2021). Increased *whi*B7 expression and antibiotic resistance in *Mycobacterium chelonae* carrying two prophages. *BMC microbiology*, *21*(1), 176. https://doi.org/10.1186/s12866-021-02224-z

Daleke, M. H., Ummels, R., Bawono, P., Heringa, J., Vandenbroucke-Grauls, C. M., Luirink, J., & Bitter, W. (2012). General secretion signal for the mycobacterial type VII secretion pathway. *Proceedings of the National Academy of Sciences of the United States of America*, *109*(28), 11342–11347. https://doi.org/10.1073/pnas.1119453109

Dar, D., Shamir, M., Mellin, J. R., Koutero, M., Stern-Ginossar, N., Cossart, P., & Sorek, R. (2016). Term-seq reveals abundant ribo-regulation of antibiotics resistance in bacteria. *Science (New York, N.Y.)*, *352*(6282), aad9822. https://doi.org/10.1126/science.aad9822

Dedrick, R. M., Marinelli, L. J., Newton, G. L., Pogliano, K., Pogliano, J., & Hatfull, G. F. (2013). Functional requirements for bacteriophage growth: gene essentiality and expression in mycobacteriophage Giles. *Molecular microbiology*, *88*(3), 577–589. https://doi.org/10.1111/mmi.12210

Dedrick, R. M., Mavrich, T. N., Ng, W. L., Cervantes Reyes, J. C., Olm, M. R., Rush, R. E., Jacobs-Sera, D., Russell, D. A., & Hatfull, G. F. (2016). Function, expression, specificity, diversity and incompatibility of actinobacteriophage parABS systems. *Molecular microbiology*, *101*(4), 625–644. https://doi.org/10.1111/mmi.13414

Dedrick, R. M., Jacobs-Sera, D., Bustamante, C. A., Garlena, R. A., Mavrich, T. N., Pope, W. H., Reyes, J. C., Russell, D. A., Adair, T., Alvey, R., Bonilla, J. A., Bricker, J. S., Brown, B. R., Byrnes, D., Cresawn, S. G., Davis, W. B., Dickson, L. A., Edgington, N. P., Findley, A. M., Golebiewska, U., … Hatfull, G. F. (2017). Prophage-mediated defence against viral attack and viral counter-defence. *Nature microbiology*, *2*, 16251. https://doi.org/10.1038/nmicrobiol.2016.251

Dedrick, R. M., Guerrero-Bustamante, C. A., Garlena, R. A., Russell, D. A., Ford, K., Harris, K., Gilmour, K. C., Soothill, J., Jacobs-Sera, D., Schooley, R. T., Hatfull, G. F., & Spencer, H. (2019). Engineered bacteriophages for treatment of a patient with a disseminated drug-resistant *Mycobacterium abscessus*. *Nature medicine*, *25*(5), 730–733. https://doi.org/10.1038/s41591-019-0437-z

Dedrick, R. M., Aull, H. G., Jacobs-Sera, D., Garlena, R. A., Russell, D. A., Smith, B. E., Mahalingam, V., Abad, L., Gauthier, C. H., & Hatfull, G. F. (2021). The Prophage and Plasmid Mobilome as a Likely Driver of *Mycobacterium abscessus* Diversity. *mBio*, *12*(2), e03441-20. https://doi.org/10.1128/mBio.03441-20

Delcher, A. L., Harmon, D., Kasif, S., White, O., & Salzberg, S. L. (1999). Improved microbial gene identification with GLIMMER. *Nucleic acids research*, *27*(23), 4636–4641. https://doi.org/10.1093/nar/27.23.4636

De Rossi, E., Blokpoel, M. C., Cantoni, R., Branzoni, M., Riccardi, G., Young, D. B., De Smet, K. A., & Ciferri, O. (1998). Molecular cloning and functional analysis of a novel tetracycline resistance determinant, *tet*(V), from *Mycobacterium smegmatis*. *Antimicrobial agents and chemotherapy*, *42*(8), 1931–1937. https://doi.org/10.1128/AAC.42.8.1931

De Rossi, E., Arrigo, P., Bellinzoni, M., Silva, P. A., Martín, C., Aínsa, J. A., Guglierame, P., & Riccardi, G. (2002). The multidrug transporters belonging to major facilitator superfamily in *Mycobacterium tuberculosis*. *Molecular medicine (Cambridge, Mass.)*, *8*(11), 714–724. https://doi.org/10.1007/BF03402035

Dheda, K., Lenders, L., Magombedze, G., Srivastava, S., Raj, P., Arning, E., Ashcraft, P., Bottiglieri, T., Wainwright, H., Pennel, T., Linegar, A., Moodley, L., Pooran, A., Pasipanodya, J. G., Sirgel, F. A., van Helden, P. D., Wakeland, E., Warren, R. M., & Gumbo, T. (2018). Drug-Penetration Gradients Associated with Acquired Drug Resistance in Patients with Tuberculosis. *American journal of respiratory and critical care medicine*, *198*(9), 1208–1219. https://doi.org/10.1164/rccm.201711-2333OC

Ehrt, S., Guo, X. V., Hickey, C. M., Ryou, M., Monteleone, M., Riley, L. W., & Schnappinger, D. (2005). Controlling gene expression in mycobacteria with anhydrotetracycline and Tet repressor. *Nucleic acids research*, *33*(2), e21. https://doi.org/10.1093/nar/gni013

Fan, X., Xie, L., Li, W., & Xie, J. (2014). Prophage-like elements present in Mycobacterium genomes. *BMC genomics*, *15*(1), 243. https://doi.org/10.1186/1471-2164-15-243

Fan, X., Abd Alla, A. A., & Xie, J. (2016). Distribution and function of prophage phiRv1 and phiRv2 among *Mycobacterium tuberculosis* complex. *Journal of biomolecular structure & dynamics*, *34*(2), 233–238. https://doi.org/10.1080/07391102.2015.1022602

Fedrizzi, T., Meehan, C. J., Grottola, A., Giacobazzi, E., Fregni Serpini, G., Tagliazucchi, S., Fabio, A., Bettua, C., Bertorelli, R., De Sanctis, V., Rumpianesi, F., Pecorari, M., Jousson, O., Tortoli, E., & Segata, N. (2017). Genomic characterization of Nontuberculous Mycobacteria. *Scientific reports*, *7*, 45258. https://doi.org/10.1038/srep45258

Fineran, P. C., Blower, T. R., Foulds, I. J., Humphreys, D. P., Lilley, K. S., & Salmond, G. P. (2009). The phage abortive infection system, ToxIN, functions as a protein-RNA toxin-antitoxin pair. *Proceedings of the National Academy of Sciences of the United States of America*, *106*(3), 894–899. https://doi.org/10.1073/pnas.0808832106

Fraikin, N., Goormaghtigh, F., & Van Melderen, L. (2020). Type II Toxin-Antitoxin Systems: Evolution and Revolutions. *Journal of bacteriology*, *202*(7), e00763-19. https://doi.org/10.1128/JB.00763-19

Gao, N., Shearwin, K., Mack, J., Finzi, L., & Dunlap, D. (2013). Purification of bacteriophage lambda repressor. *Protein expression and purification*, *91*(1), 30–36. https://doi.org/10.1016/j.pep.2013.06.013

Garcia, E. C., Perault, A. I., Marlatt, S. A., & Cotter, P. A. (2016). Interbacterial signaling via Burkholderia contact-dependent growth inhibition system proteins. *Proceedings of the National Academy of Sciences of the United States of America*, *113*(29), 8296–8301. https://doi.org/10.1073/pnas.1606323113

Glickman, C., Kammlade, S. M., Hasan, N. A., Epperson, L. E., Davidson, R. M., & Strong, M. (2020). Characterization of integrated prophages within diverse species of clinical nontuberculous mycobacteria. *Virology journal*, *17*(1), 124. https://doi.org/10.1186/s12985-020-01394-y

Gordillo Altamirano, F. L., & Barr, J. J. (2019). Phage Therapy in the Postantibiotic Era. *Clinical microbiology reviews*, *32*(2), e00066-18. https://doi.org/10.1128/CMR.00066-18
Guerrero-Bustamante, C. A., Dedrick, R. M., Garlena, R. A., Russell, D. A., & Hatfull, G. F. (2021). Toward a Phage Cocktail for Tuberculosis: Susceptibility and Tuberculocidal Action of Mycobacteriophages against Diverse *Mycobacterium tuberculosis* Strains. *mBio*, *12*(3), e00973-21. https://doi.org/10.1128/mBio.00973-21

Guo, Y., Quiroga, C., Chen, Q., McAnulty, M. J., Benedik, M. J., Wood, T. K., & Wang, X. (2014). RalR (a DNase) and RalA (a small RNA) form a type I toxin-antitoxin system in *Escherichia coli*. *Nucleic acids research*, *42*(10), 6448–6462. https://doi.org/10.1093/nar/gku279

Guo, Q., Chen, J., Zhang, S., Zou, Y., Zhang, Y., Huang, D., Zhang, Z., Li, B., & Chu, H. (2020). Efflux Pumps Contribute to Intrinsic Clarithromycin Resistance in Clinical, *Mycobacterium abscessus* Isolates. *Infection and drug resistance*, *13*, 447–454. https://doi.org/10.2147/IDR.S239850

Haq, I. U., Chaudhry, W. N., Akhtar, M. N., Andleeb, S., & Qadri, I. (2012). Bacteriophages and their implications on future biotechnology: a review. *Virology journal*, *9*, 9. https://doi.org/10.1186/1743-422X-9-9

Harms, A., Fino, C., Sørensen, M. A., Semsey, S., & Gerdes, K. (2017). Prophages and Growth Dynamics Confound Experimental Results with Antibiotic-Tolerant Persister Cells. *mBio*, *8*(6), e01964-17. https://doi.org/10.1128/mBio.01964-17

Harms, A., Brodersen, D. E., Mitarai, N., & Gerdes, K. (2018). Toxins, Targets, and Triggers: An Overview of Toxin-Antitoxin Biology. *Molecular cell*, *70*(5), 768–784. https://doi.org/10.1016/j.molcel.2018.01.003

Hatfull, G. F., & Hendrix, R. W. (2011). Bacteriophages and their genomes. *Current opinion in virology*, *1*(4), 298–303. https://doi.org/10.1016/j.coviro.2011.06.009

Hatfull G. F. (2014). Mycobacteriophages: windows into tuberculosis. *PLoS pathogens*, *10*(3), e1003953. https://doi.org/10.1371/journal.ppat.1003953

Hurst-Hess, K., Rudra, P., & Ghosh, P. (2017). *Mycobacterium abscessus* WhiB7 Regulates a Species-Specific Repertoire of Genes To Confer Extreme Antibiotic Resistance. *Antimicrobial agents and chemotherapy*, *61*(11), e01347-17. https://doi.org/10.1128/AAC.01347-17

Hyder, S. L., & Streitfeld, M. M. (1978). Transfer of erythromycin resistance from clinically isolated lysogenic strains of *Streptococcus pyogenes via* their endogenous phage. *The Journal of infectious diseases*, *138*(3), 281–286. https://doi.org/10.1093/infdis/138.3.281

van Ingen, J., Boeree, M. J., van Soolingen, D., & Mouton, J. W. (2012). Resistance mechanisms and drug susceptibility testing of nontuberculous mycobacteria. *Drug resistance updates : reviews and commentaries in antimicrobial and anticancer chemotherapy*, *15*(3), 149–161. https://doi.org/10.1016/j.drup.2012.04.001

Jacobs, J. M., Stine, C. B., Baya, A. M., & Kent, M. L. (2009). A review of mycobacteriosis in marine fish. *Journal of fish diseases*, *32*(2), 119–130. https://doi.org/10.1111/j.1365-2761.2008.01016.x

Jaén-Luchoro, D., Salvà-Serra, F., Aliaga-Lozano, F., Seguí, C., Busquets, A., Ramírez, A., Ruíz, M., Gomila, M., Lalucat, J., & Bennasar-Figueras, A. (2016). Complete Genome Sequence of *Mycobacterium chelonae* Type Strain CCUG 47445, a Rapidly Growing Species of Nontuberculous Mycobacteria. *Genome announcements*, *4*(3), e00550-16. https://doi.org/10.1128/genomeA.00550-16

Johansen, M. D., Herrmann, J. L., & Kremer, L. (2020). Non-tuberculous mycobacteria and the rise of *Mycobacterium abscessus*. *Nature reviews. Microbiology*, *18*(7), 392–407. https://doi.org/10.1038/s41579-020-0331-1

Jault, P., Leclerc, T., Jennes, S., Pirnay, J. P., Que, Y. A., Resch, G., Rousseau, A. F., Ravat, F., Carsin, H., Le Floch, R., Schaal, J. V., Soler, C., Fevre, C., Arnaud, I., Bretaudeau, L., & Gabard, J. (2019). Efficacy and tolerability of a cocktail of bacteriophages to treat burn wounds infected by *Pseudomonas aeruginosa* (PhagoBurn): a randomised, controlled, double-blind phase 1/2 trial. *The Lancet. Infectious diseases*, *19*(1), 35–45. https://doi.org/10.1016/S1473-3099(18)30482-1

Kaper, J. B., Nataro, J. P., & Mobley, H. L. (2004). Pathogenic *Escherichia coli*. *Nature reviews. Microbiology*, *2*(2), 123–140. https://doi.org/10.1038/nrmicro818

Kapopoulou, A., Lew, J. M., & Cole, S. T. (2011). The MycoBrowser portal: a comprehensive and manually annotated resource for mycobacterial genomes. *Tuberculosis (Edinburgh, Scotland)*, *91*(1), 8–13. https://doi.org/10.1016/j.tube.2010.09.006

van Kessel, J. C., & Hatfull, G. F. (2007). Recombineering in *Mycobacterium tuberculosis*. *Nature methods*, *4*(2), 147–152. https://doi.org/10.1038/nmeth996

Knezevic, P., Adriaenssens, E. M., & Ictv Report Consortium (2021). ICTV Virus Taxonomy Profile: *Inoviridae*. *The Journal of general virology*, *102*(7), 10.1099/jgv.0.001614. https://doi.org/10.1099/jgv.0.001614

Kreuger F. (2019) Trim Galore! v0.6.3
http://www.bioinformatics.babraham.ac.uk/projects/trim_galore/

Kumar, A., Alam, A., Bharadwaj, P., Tapadar, S., Rani, M., & Hasnain, S. E. (2019). Toxin-antitoxin (TA) systems in stress survival and pathogenesis. In *Mycobacterium tuberculosis: molecular infection biology, pathogenesis, diagnostics and new interventions* (pp. 257-274). Springer, Singapore.

Larsson, C., Luna, B., Ammerman, N. C., Maiga, M., Agarwal, N., & Bishai, W. R. (2012). Gene expression of *Mycobacterium tuberculosis* putative transcription factors *whi*B1-7 in redox environments. *PloS one*, *7*(7), e37516. https://doi.org/10.1371/journal.pone.0037516

LeRoux, M., Kirkpatrick, R. L., Montauti, E. I., Tran, B. Q., Peterson, S. B., Harding, B. N., Whitney, J. C., Russell, A. B., Traxler, B., Goo, Y. A., Goodlett, D. R., Wiggins, P. A., & Mougous, J. D. (2015). Kin cell lysis is a danger signal that activates antibacterial pathways of *Pseudomonas aeruginosa*. *eLife*, *4*, e05701. https://doi.org/10.7554/eLife.05701

Leplae, R., Geeraerts, D., Hallez, R., Guglielmini, J., Drèze, P., & Van Melderen, L. (2011). Diversity of bacterial type II toxin-antitoxin systems: a comprehensive search and functional analysis of novel families. *Nucleic acids research*, *39*(13), 5513–5525. https://doi.org/10.1093/nar/gkr131

Livak, K. J., & Schmittgen, T. D. (2001). Analysis of relative gene expression data using real-time quantitative PCR and the 2(-Delta Delta C(T)) Method. *Methods (San Diego, Calif.)*, *25*(4), 402–408. https://doi.org/10.1006/meth.2001.1262

Langmead, B., & Salzberg, S. L. (2012). Fast gapped-read alignment with Bowtie 2. *Nature methods*, *9*(4), 357–359. https://doi.org/10.1038/nmeth.1923

Love, M. I., Huber, W., & Anders, S. (2014). Moderated estimation of fold change and dispersion for RNA-seq data with DESeq2. *Genome biology*, *15*(12), 550. https://doi.org/10.1186/s13059-014-0550-8

Luthra, S., Rominski, A., & Sander, P. (2018). The Role of Antibiotic-Target-Modifying and Antibiotic-Modifying Enzymes in *Mycobacterium abscessus* Drug Resistance. *Frontiers in microbiology*, *9*, 2179. https://doi.org/10.3389/fmicb.2018.02179

Ma, L. S., Hachani, A., Lin, J. S., Filloux, A., & Lai, E. M. (2014). *Agrobacterium tumefaciens* deploys a superfamily of type VI secretion DNase effectors as weapons for interbacterial competition in planta. *Cell host & microbe*, *16*(1), 94–104. https://doi.org/10.1016/j.chom.2014.06.002

Marinelli, L. J., Piuri, M., Swigonová, Z., Balachandran, A., Oldfield, L. M., van Kessel, J. C., & Hatfull, G. F. (2008). BRED: a simple and powerful tool for constructing mutant and recombinant bacteriophage genomes. *PloS one*, *3*(12), e3957. https://doi.org/10.1371/journal.pone.0003957

Mielich-Süss, B., Wagner, R. M., Mietrach, N., Hertlein, T., Marincola, G., Ohlsen, K., Geibel, S., & Lopez, D. (2017). Flotillin scaffold activity contributes to type VII secretion system assembly in *Staphylococcus aureus*. *PLoS pathogens*, *13*(11), e1006728. https://doi.org/10.1371/journal.ppat.1006728

Morris, R. P., Nguyen, L., Gatfield, J., Visconti, K., Nguyen, K., Schnappinger, D., Ehrt, S., Liu, Y., Heifets, L., Pieters, J., Schoolnik, G., & Thompson, C. J. (2005). Ancestral antibiotic resistance in *Mycobacterium tuberculosis*. *Proceedings of the National Academy of Sciences of the United States of America*, *102*(34), 12200–12205. https://doi.org/10.1073/pnas.0505446102

de Moura, V., Gibbs, S., & Jackson, M. (2014). Gene replacement in *Mycobacterium chelonae*: application to the construction of porin knock-out mutants. *PloS one*, *9*(4), e94951. https://doi.org/10.1371/journal.pone.0094951

Muniesa, M., Colomer-Lluch, M., & Jofre, J. (2013). Potential impact of environmental bacteriophages in spreading antibiotic resistance genes. *Future microbiology*, *8*(6), 739–751. https://doi.org/10.2217/fmb.13.32

Nasiri, M. J., Haeili, M., Ghazi, M., Goudarzi, H., Pormohammad, A., Imani Fooladi, A. A., & Feizabadi, M. M. (2017). New Insights in to the Intrinsic and Acquired Drug Resistance Mechanisms in Mycobacteria. *Frontiers in microbiology*, *8*, 681. https://doi.org/10.3389/fmicb.2017.00681

Nash, K. A., Brown-Elliott, B. A., & Wallace, R. J., Jr (2009). A novel gene, *erm*(41), confers inducible macrolide resistance to clinical isolates of *Mycobacterium abscessus* but is absent from *Mycobacterium chelonae*. *Antimicrobial agents and chemotherapy*, *53*(4), 1367–1376. https://doi.org/10.1128/AAC.01275-08

Nessar, R., Cambau, E., Reyrat, J. M., Murray, A., & Gicquel, B. (2012). *Mycobacterium abscessus*: a new antibiotic nightmare. *The Journal of antimicrobial chemotherapy*, *67*(4), 810–818. https://doi.org/10.1093/jac/dkr578

Neubauer, C., Gao, Y. G., Andersen, K. R., Dunham, C. M., Kelley, A. C., Hentschel, J., Gerdes, K., Ramakrishnan, V., & Brodersen, D. E. (2009). The structural basis for mRNA recognition and cleavage by the ribosome-dependent endonuclease RelE. *Cell*, *139*(6), 1084–1095. https://doi.org/10.1016/j.cell.2009.11.015

Pai, M., Behr, M. A., Dowdy, D., Dheda, K., Divangahi, M., Boehme, C. C., Ginsberg, A., Swaminathan, S., Spigelman, M., Getahun, H., Menzies, D., & Raviglione, M. (2016). Tuberculosis. *Nature reviews. Disease primers*, *2*, 16076. https://doi.org/10.1038/nrdp.2016.76

Pallen M. J. (2002). The ESAT-6/WXG100 superfamily -- and a new Gram-positive secretion system?. *Trends in microbiology*, *10*(5), 209–212. https://doi.org/10.1016/s0966-842x(02)02345-4

Parikh, A., Kumar, D., Chawla, Y., Kurthkoti, K., Khan, S., Varshney, U., & Nandicoori, V. K. (2013). Development of a new generation of vectors for gene expression, gene replacement, and protein-protein interaction studies in mycobacteria. *Applied and environmental microbiology*, *79*(5), 1718–1729. https://doi.org/10.1128/AEM.03695-12

Park, S. C., Kwak, Y. M., Song, W. S., Hong, M., & Yoon, S. I. (2017). Structural basis of effector and operator recognition by the phenolic acid-responsive transcriptional regulator PadR. *Nucleic acids research*, *45*(22), 13080–13093. https://doi.org/10.1093/nar/gkx1055

Patro, R., Duggal, G., Love, M. I., Irizarry, R. A., & Kingsford, C. (2017). Salmon provides fast and bias-aware quantification of transcript expression. *Nature methods*, *14*(4), 417–419. https://doi.org/10.1038/nmeth.4197

Percival, S., & Williams, D. 2014. Microbiology of Waterborne Diseases (Second Edition). *Mycobacterium*. 177-207. https://doi.org/10.1016/B978-0-12-415846-7.00009-3.

Petrova, Z. O., Broussard, G. W., & Hatfull, G. F. (2015). Mycobacteriophage-repressor-mediated immunity as a selectable genetic marker: Adephagia and BPs repressor selection. *Microbiology (Reading, England)*, *161*(8), 1539–1551. https://doi.org/10.1099/mic.0.000120

Pope, W. H., Mavrich, T. N., Garlena, R. A., Guerrero-Bustamante, C. A., Jacobs-Sera, D., Montgomery, M. T., Russell, D. A., Warner, M. H., Science Education Alliance-Phage Hunters Advancing Genomics and Evolutionary Science (SEA-PHAGES), & Hatfull, G. F. (2017). Bacteriophages of *Gordonia* spp. Display a Spectrum of Diversity and Genetic Relationships. *mBio*, *8*(4), e01069-17. https://doi.org/10.1128/mBio.01069-17

Prasanna, A. N., & Mehra, S. (2013). Comparative phylogenomics of pathogenic and non-pathogenic mycobacterium. *PloS one*, *8*(8), e71248. https://doi.org/10.1371/journal.pone.0071248

Pryjma, M., Burian, J., Kuchinski, K., & Thompson, C. J. (2017). Antagonism between Front-Line Antibiotics Clarithromycin and Amikacin in the Treatment of *Mycobacterium abscessus* Infections Is Mediated by the *whiB7* Gene. *Antimicrobial agents and chemotherapy*, *61*(11), e01353-17. https://doi.org/10.1128/AAC.01353-17

Rabinovich, L., Sigal, N., Borovok, I., Nir-Paz, R., & Herskovits, A. A. (2012). Prophage excision activates Listeria competence genes that promote phagosomal escape and virulence. *Cell*, *150*(4), 792–802. https://doi.org/10.1016/j.cell.2012.06.036

Ramón-García, S., Mick, V., Dainese, E., Martín, C., Thompson, C. J., De Rossi, E., Manganelli, R., & Aínsa, J. A. (2012). Functional and genetic characterization of the *tap* efflux pump in *Mycobacterium bovis* BCG. *Antimicrobial agents and chemotherapy*, *56*(4), 2074–2083. https://doi.org/10.1128/AAC.05946-11

Ramón-García, S., Ng, C., Jensen, P. R., Dosanjh, M., Burian, J., Morris, R. P., Folcher, M., Eltis, L. D., Grzesiek, S., Nguyen, L., & Thompson, C. J. (2013). WhiB7, an Fe-S-dependent transcription factor that activates species-specific repertoires of drug resistance determinants in actinobacteria. *The Journal of biological chemistry*, *288*(48), 34514–34528. https://doi.org/10.1074/jbc.M113.516385

Rice, S. A., Tan, C. H., Mikkelsen, P. J., Kung, V., Woo, J., Tay, M., Hauser, A., McDougald, D., Webb, J. S., & Kjelleberg, S. (2009). The biofilm life cycle and virulence of *Pseudomonas aeruginosa* are dependent on a filamentous prophage. *The ISME journal*, *3*(3), 271–282. https://doi.org/10.1038/ismej.2008.109

Rodrigues, L., Ramos, J., Couto, I., Amaral, L., & Viveiros, M. (2011). Ethidium bromide transport across *Mycobacterium smegmatis* cell-wall: correlation with antibiotic resistance. *BMC microbiology*, *11*, 35. https://doi.org/10.1186/1471-2180-11-35

Rominski, A., Roditscheff, A., Selchow, P., Böttger, E. C., & Sander, P. (2017). Intrinsic rifamycin resistance of *Mycobacterium abscessus* is mediated by ADP-ribosyltransferase MAB_0591. *The Journal of antimicrobial chemotherapy*, *72*(2), 376–384. https://doi.org/10.1093/jac/dkw466

Rudra, P., Hurst-Hess, K. R., Cotten, K. L., Partida-Miranda, A., & Ghosh, P. (2020). Mycobacterial HflX is a ribosome splitting factor that mediates antibiotic resistance. *Proceedings of the National Academy of Sciences of the United States of America*, *117*(1), 629–634. https://doi.org/10.1073/pnas.1906748117

Ruhe, Z. C., Low, D. A., & Hayes, C. S. (2020). Polymorphic Toxins and Their Immunity Proteins: Diversity, Evolution, and Mechanisms of Delivery. *Annual review of microbiology*, *74*, 497–520. https://doi.org/10.1146/annurev-micro-020518-115638

Russell, D. A., & Hatfull, G. F. (2017). PhagesDB: the actinobacteriophage database. *Bioinformatics (Oxford, England)*, *33*(5), 784–786. https://doi.org/10.1093/bioinformatics/btw711

Sampson, T., Broussard, G. W., Marinelli, L. J., Jacobs-Sera, D., Ray, M., Ko, C. C., Russell, D., Hendrix, R. W., & Hatfull, G. F. (2009). Mycobacteriophages BPs, Angel and Halo: comparative genomics reveals a novel class of ultra-small mobile genetic elements. *Microbiology (Reading, England)*, *155*(Pt 9), 2962–2977. https://doi.org/10.1099/mic.0.030486-0

Sawyer, E. B., Grabowska, A. D., & Cortes, T. (2018). Translational regulation in mycobacteria and its implications for pathogenicity. *Nucleic acids research*, *46*(14), 6950–6961. https://doi.org/10.1093/nar/gky574

Shur, K. V., Maslov, D. A., Mikheecheva, N. E., Akimova, N. I., Bekker, O. B., & Danilenko, V. N. (2017). The intrinsic antibiotic resistance to β-lactams, macrolides, and fluoroquinolones of mycobacteria is mediated by the *whi*B7 and *tap* genes. *Russian Journal of Genetics*, *53*(9), 1006-1015. https://doi.org/10.1134/S1022795417080087

Slayden, R. A., Dawson, C. C., & Cummings, J. E. (2018). Toxin-antitoxin systems and regulatory mechanisms in *Mycobacterium tuberculosis. Pathogens and disease*, *76*(4), 10.1093/femspd/fty039. https://doi.org/10.1093/femspd/fty039

Söding, J., Biegert, A., & Lupas, A. N. (2005). The HHpred interactive server for protein homology detection and structure prediction. *Nucleic acids research*, *33*(Web Server issue), W244–W248. https://doi.org/10.1093/nar/gki408

Stone, E., Campbell, K., Grant, I., & McAuliffe, O. (2019). Understanding and Exploiting Phage-Host Interactions. *Viruses*, *11*(6), 567. https://doi.org/10.3390/v11060567

Suttle C. A. (2016). Environmental microbiology: Viral diversity on the global stage. *Nature microbiology*, *1*(11), 16205. https://doi.org/10.1038/nmicrobiol.2016.205

Vatlin, A. A., Bekker, O. B., Lysenkova, L. N., Shchekotikhin, A. E., & Danilenko, V. N. (2018). A functional study of the global transcriptional regulator PadR from a strain *Streptomyces fradiae*-nitR+bld, resistant to nitrone-oligomycin. *Journal of basic microbiology*, *58*(9), 739–746. https://doi.org/10.1002/jobm.201800095

Villanueva, V. M., Oldfield, L. M., & Hatfull, G. F. (2015). An Unusual Phage Repressor Encoded by Mycobacteriophage BPs. *PloS one*, *10*(9), e0137187. https://doi.org/10.1371/journal.pone.0137187

Wang, X., Kim, Y., Ma, Q., Hong, S. H., Pokusaeva, K., Sturino, J. M., & Wood, T. K. (2010). Cryptic prophages help bacteria cope with adverse environments. *Nature communications*, *1*, 147. https://doi.org/10.1038/ncomms1146

Wang, X., & Wood, T. K. (2011). Toxin-antitoxin systems influence biofilm and persister cell formation and the general stress response. *Applied and environmental microbiology*, *77*(16), 5577–5583. https://doi.org/10.1128/AEM.05068-11

Wang, X., Kim, Y., Hong, S. H., Ma, Q., Brown, B. L., Pu, M., Tarone, A. M., Benedik, M. J., Peti, W., Page, R., & Wood, T. K. (2011). Antitoxin MqsA helps mediate the bacterial general stress response. *Nature chemical biology*, *7*(6), 359–366. https://doi.org/10.1038/nchembio.560

Wang, X., & Wood, T. K. (2016). Cryptic prophages as targets for drug development. *Drug resistance updates : reviews and commentaries in antimicrobial and anticancer chemotherapy*, *27*, 30–38. https://doi.org/10.1016/j.drup.2016.06.001

Webb, J. S., Lau, M., & Kjelleberg, S. (2004). Bacteriophage and phenotypic variation in *Pseudomonas aeruginosa* biofilm development. *Journal of bacteriology*, *186*(23), 8066–8073. https://doi.org/10.1128/JB.186.23.8066-8073.2004

Whipps, C. M., Matthews, J. L., & Kent, M. L. (2008). Distribution and genetic characterization of Mycobacterium chelonae in laboratory zebrafish Danio rerio. *Diseases of aquatic organisms*, *82*(1), 45–54. https://doi.org/10.3354/dao01967

The World Health Organization (2020) *Global Tuberculosis Report*.

Wood T. K. (2016). Combatting bacterial persister cells. *Biotechnology and bioengineering*, *113*(3), 476–483. https://doi.org/10.1002/bit.25721

Wood, T. E., Aksoy, E., & Hachani, A. (2020). From Welfare to Warfare: The Arbitration of Host-Microbiota Interplay by the Type VI Secretion System. *Frontiers in cellular and infection microbiology*, *10*, 587948. https://doi.org/10.3389/fcimb.2020.587948

Wozniak, R. A., & Waldor, M. K. (2009). A toxin-antitoxin system promotes the maintenance of an integrative conjugative element. *PLoS genetics*, *5*(3), e1000439. https://doi.org/10.1371/journal.pgen.1000439

Wu, M., Li, B., Guo, Q., Xu, L., Zou, Y., Zhang, Y., Zhan, M., Xu, B., Ye, M., Yu, F., Zhang, Z., & Chu, H. (2019). Detection and molecular characterisation of amikacin-resistant *Mycobacterium abscessus* isolated from patients with pulmonary disease. *Journal of global antimicrobial resistance*, *19*, 188–191. https://doi.org/10.1016/j.jgar.2019.05.016

Yao, J., Guo, Y., Wang, P., Zeng, Z., Li, B., Tang, K., Liu, X., & Wang, X. (2018). Type II toxin/antitoxin system $ParE_{SO}$ /$CopA_{SO}$ stabilizes prophage CP4So in *Shewanella oneidensis*. *Environmental microbiology*, *20*(3), 1224–1239. https://doi.org/10.1111/1462-2920.14068

Zdobnov, E. M., Tegenfeldt, F., Kuznetsov, D., Waterhouse, R. M., Simão, F. A., Ioannidis, P., Seppey, M., Loetscher, A., & Kriventseva, E. V. (2017). OrthoDB v9.1: cataloging evolutionary and functional annotations for animal, fungal, plant, archaeal, bacterial and viral orthologs. *Nucleic acids research*, *45*(D1), D744–D749. https://doi.org/10.1093/nar/gkw1119

Zhang, D., de Souza, R. F., Anantharaman, V., Iyer, L. M., & Aravind, L. (2012). Polymorphic toxin systems: Comprehensive characterization of trafficking modes, processing, mechanisms of action, immunity and ecology using comparative genomics. *Biology direct*, *7*, 18. https://doi.org/10.1186/1745-6150-7-18

Zimmermann, L., Stephens, A., Nam, S. Z., Rau, D., Kübler, J., Lozajic, M., Gabler, F., Söding, J., Lupas, A. N., & Alva, V. (2018). A Completely Reimplemented MPI Bioinformatics Toolkit with a New HHpred Server at its Core. *Journal of molecular biology*, *430*(15), 2237–2243. https://doi.org/10.1016/j.jmb.2017.12.007

BIOGRAPHY OF THE AUTHOR

Jaycee Cushman was born on June 23rd, 1997, in Farmington, Maine. She grew up in the rural town of Mercer and graduated from Skowhegan Area High School in 2015. Jaycee attended the University of Maine, majoring in microbiology. She competed for the track & field team until 2017 and worked nights at Northern Light Eastern Maine Medical Center from 2017 to 2019. She also volunteered as an undergraduate research assistant in the Molloy Laboratory for three years and was a teaching assistant for the phage genomics course during her senior year. She earned her B.S. in 2019, becoming the first in her family to earn a college degree. She immediately began graduate work for a M.S. in microbiology. Jaycee moved to North Carolina in the spring of 2021 and plans to pursue a career in medicine. She is a candidate for the Master of Science degree in Microbiology from the University of Maine in August 2021.